In compliance with the
Canadian Privacy Legislation
some supporting forms
may have been removed from
this dissertation.

While these forms may be included
in the document page count,
their removal does not represent
any loss of content from the dissertation.

University of Alberta

Regulation of the Na^+/H^+ Exchanger Isoform 1 by Dephosphorylation

by

Angelika J. Misik

A thesis submitted to the Faculty of Graduate Studies and Research in partial fulfillment of the requirements for the degree of Master of Science.

Department of Biochemistry

Edmonton, Alberta

Fall 2003

National Library
of Canada

Acquisitions and
Bibliographic Services

395 Wellington Street
Ottawa ON K1A 0N4
Canada

Bibliothèque nationale
du Canada

Acquisisitons et
services bibliographiques

395, rue Wellington
Ottawa ON K1A 0N4
Canada

Your file Votre référence
ISBN: 0-612-87837-6
Our file Notre référence
ISBN: 0-612-87837-6

The author has granted a non-exclusive licence allowing the National Library of Canada to reproduce, loan, distribute or sell copies of this thesis in microform, paper or electronic formats.

The author retains ownership of the copyright in this thesis. Neither the thesis nor substantial extracts from it may be printed or otherwise reproduced without the author's permission.

L'auteur a accordé une licence non exclusive permettant à la Bibliothèque nationale du Canada de reproduire, prêter, distribuer ou vendre des copies de cette thèse sous la forme de microfiche/film, de reproduction sur papier ou sur format électronique.

L'auteur conserve la propriété du droit d'auteur qui protège cette thèse. Ni la thèse ni des extraits substantiels de celle-ci ne doivent être imprimés ou aturement reproduits sans son autorisation.

Canada

University of Alberta

Library Release Form

Name of Author: **Angelika Jolanta Misik**

Title: **Regulation of the Na^+/H^+ Exchanger Isoform I by Dephosphorylation**

Degree: **Master of Science**

Year this Degree Granted: 2003

Permission is hereby granted to the University of Alberta Library to reproduce single copies of this thesis and to lend or sell such copies for private, scholarly or scientific research purposes only.

The author reserves all other publication, and other rights in association with the copyright in the thesis, and except as herein before provided, nether the thesis nor any substantial portion thereof may be printed or otherwise reproduced in any material form whatever without the author's prior written permission

Sept 29-03

Date

University of Alberta

Faculty of Graduate Studies and Research

The undersigned certify that they have read, and recommend to the Faculty of Graduate Studies and Research for acceptance, a thesis entitled Regulation of the Na^+/H^+ Exchanger Isoform 1 by Dephosphorylation submitted by Angelika Jolanta Misik in partial fulfillment of the requirements for the degree of Master of Science.

Dr. Larry Fliegel

Dr. Charles Holmes

Dr. Marek Michalak

Dr. Christopher Cheeseman

Sept 8/2003
Date

Abstract

Regulation by dephosphorylation of the Na^+/H^+ exchanger isoform 1 (NHE1) was investigated. Treatment of cardiomyocytes with the phosphatase inhibitor okadaic acid, at micromolar concentrations, did not affect the change in pH or steady state pH of the cells. These findings suggested that the okadaic acid sensitive PP2A is unlikely involved in NHE1 regulation *in vivo*. The regulatory C-terminal region of NHE1 was examined using heart cell extracts and purified protein phosphatases, PP1, PP2A and PP2B. The *in vitro* dephosphorylation results revealed that NHE1 is completely dephosphorylated by PP1, partially dephosphorylated by PP2A and not dephosphorylated by PP2B or heart cell extracts. Examination of NHE1 binding with PP1 or PP2B revealed that a weak association occurs between NHE1 and PP1 *in vitro* and *in vivo*. NHE1 does not associate with full length PP2B; however, it does bind an N-terminal fragment of PP2B *in vitro*. Therefore, PP1 is likely the predominant phosphatase involved in NHE1 dephosphorylation. Stable cell lines overexpressing PP1 or Inhibitor-2 (I2) were used to investigate the effect of PP1 on NHE1 activity *in vivo*. The overexpression of PP1 causes a decrease in NHE1 activity but does not affect stimulation of NHE1 by thrombin. The inhibition of PP1 activity in cell lines overexpressing I2 causes NHE1 to be hyperactive and cannot be further stimulated by thrombin. Western blotting with an anti-NHE1 monoclonal antibody was used to measure NHE1 protein levels in cell lines overexpressing PP1 or I2, and in cell lines mock-transfected with an empty vector. It was concluded that NHE1 protein expression is not affected by the overexpression of PP1 or I2.

A loving family has been my greatest source of inner strength

For Patrick, whose continuous motivation and confidence inspired me to achieve my goal

For Mom, Dad, Eve, Kris, Gabrysia and Piotr who encouraged my choices, believed in me and endlessly expressed their pride in my accomplishments

For Rachelle, whose sincere friendship was unsurpassed during trying times

Acknowledgements

First and foremost, I would like to thank Dr. Larry Fliegel for the opportunity to join his research team, his dedicated and patient supervision of this thesis project, for his great efforts in making the working environment enjoyable and for providing me with numerous opportunities that greatly expanded my knowledge and experience in the scientific field.

I owe countless thanks to the members of Dr. Fliegel's laboratory who were always helpful, shared their technical expertise and were delightful to work with: Brenda Brix, Bonnie Bullis, Xiuju Li, Yongsheng Liu, Emily Slepkov and Christine Wiebe.

I would like to thank the members of my thesis committee: Dr. Charles Holmes and Dr. Marek Michalak, for sharing their knowledge and motivating me during this project, and Dr. Chris Cheeseman, who was a pleasure to have as an external examiner for my thesis defense.

I would like to acknowledge Kathleen Perreault who was a dedicated collaborator on this thesis project, shared her technical expertise and knowledge of protein phosphatases.

Table of Contents

Chapter I

A: **Introduction**.....2

1. **Intracellular pH in Mammalian Cells**.....2

2. **The Na^+/H^+ Exchanger Family and Physiological Roles**.....3

3. **Putative Structural Features of NHE1**..... 5

4. **Regulation of NHE1**..... 8
   - 4.1. The N-terminal Domain and Drug Sensitivity of NHE1..... 8
   - 4.2 Regulation of NHE1 Through the C-terminal Domain and its Subdomain.....8
     - 4.2.1 The pH Sensing Domain of NHE1..... 9
     - 4.2.2 Cytosolic Calcium and Regulatory Proteins Mediate NHE1.....10
     - 4.2.3 Cellular ATP, Hormones, Growth factors and Acidosis Regulate NHE1.....13
     - 4.2.4 Direct Phosphorylation Regulates NHE1..... 15

5. **Classification of Protein Phosphatases**..... 20
   - 5.1. Protein Serine/Threonine Phosphatases..... 20

6. **Type-1 Multimeric Protein Phosphatase, PP1**..... 22
   - 6.1. Characteristics of PP1.....22
   - 6.2. Regulation of PP1 by Regulatory Subunits 23
   - 6.3. Interaction of Regulatory Subunits with PP1c..... 23
   - 6.4. Targeting PP1 to the Plasma Membrane by Spinophilin.....25
   - 6.5. Modulation of PP1 Activity by Inhbitor-2.....25

7. **Type-2 Multimeric Phoshatases PP2A and PP2B**.....26
   - 7.1 The β12-13 loop structure of PP2Ac and PP2Bc..... 26
   - 7.2 Regulation and Functions of PP2A.....27
   - 7.3 Regulation and Functions of PP2B.....29

8. **Dephosphorylation of NHE1**..... 30

9. **NHE1 in Disease**..... 32
   - 9.1 Cardiac Hypertrophy.....32
   - 9.2 Ischemia and Reperfusion.....34
   - 9.3 Hypertension.....35
   - 9.4 Diabetes..... 37
   - 9.5 Cancer..... 38

10. **Thesis Objectives**.....41

Chapter II

B: Materials..... 43

C: Methods.....45

1. **Expression and Purification of Proteins**.....45
   - 1.1. The GST-Na^+/H^+ Exchanger Fusion Protein.....45
   - 1.2. The GST-Spinophilin Fusion Protein..... 45
   - 1.3. Protein Phosphatase-1 (PP1γ).....45
   - 1.4. The Catalytic A Subunit of PP2B.....46
   - 1.5. The Catalytic A Subunit of PP2A.....46
   - 1.6. The Inhibitor-2 Protein..... 46

2. ***In Vitro* Phosphorylation and Dephosphorylation of the Regulatory C-terminus of the Na^+/H^+ Exchanger**.....47
   - 2.1 *In Vitro* Phosphorylation of the Na^+/H^+ Exchanger C-terminal Fusion Protein (PCRA).....47
   - 2.2 *In Vitro* Dephosphorylation of the Na^+/H^+ Exchanger C-terminal Fusion Protein (PCRA).....48

3. **Preparation of Heart Cell Extracts**..... 53

4. ***In Vitro* Assay of Physical Interactions of Phosphatases with NHE1**..... 56
   - 4.1 GST Pull-Down Assay..... 56
   - 4.2 Immunoblot Analysis of NHE1 with anti-Phosphatase Antibodies.....57

5. **Immunoprecipitation of NHE1 from Cells Treated or Untreated with Cross-linking Reagents**
   - 5.1 Preparation of Cells for Immunoprecipitation of NHE1.....58
   - 5.2 Treatment of Cells with Cross-linking Reagents..... 59
   - 5.3 Immunoprecipitation of NHE1 from Intact Cells..... 60
   - 5.4 Immunoblot Analysis of NHE1 Following Immunoprecipitation from Untreated Cells.....61
   - 5.5 Immunoblot Analysis of Immunoprecipitated NHE1 with anti-Phosphatase Antibodies.....62

6. **Assay of NHE1 Activity in Rat Heart Cells Following Phosphatase Inhibition with Okadaic Acid..... 62**
6.1 Preparation of Rat Neonatal Myocyte Primary Cultures..... 62
6.2 Measuring Activity of NHE in Primary Myocyte Cultures Treated with Phosphatase inhibitor Okadaic Acid.. 64

7. **Protein Phosphatase-1 and Protein Inhibitor-2 Expression in Mammalian Cells.....65**
7.1 Generating *att*B-PCR Products for Recombination into Gateway Technology-Adapted Vectors..... 65
7.2 Obtaining Concentrated DNA.....67
7.3 Creating Entry and Expression Clones..... 67
7.4 Obtaining Transient and Stable Expression of Proteins in Mammalian Cells..... 75
7.5 Immunoblot Analysis of Stable Protein Expression in Mammalian Cells.....77

8. **Assay of Phosphatase Activity..... 78**
8.1 Phosphatase Activity in Crude Heart Cell Extracts.....78
8.2 Phosphatase Activity in Mammalian Cells.....81

9. **Measurements of Intracellular pH and Buffering Capacity.....86**
9.1 Measuring pH*i* in Cells Transiently Expressing PP1 or PP2B.....86
9.2 Measuring pH*i* in Cells Stably Expressing PP1 or I2.....87
9.3 Measuring Buffering Capacity in Cells Stably Expressing PP1 or I2..... 89

Chapter III

D: Results

1. ***In Vitro* Dephosphorylation of NHE1.....98**
1.1 Dephosphorylation of NHE1 by PP1.....98
1.2 Dephosphorylation of NHE1 by PP2A.....99
1.3 Dephosphorylation of NHE1 by PP2B.....99
1.4 Dephosphorylation of NHE1 by PP1 in the Presence of the Targeting Regulatory Subunit, Spinophilin..... 100
1.5 Dephosphorylation of NHE1 by Heart Extracts..... 101

2. Binding Assays of NHE1 and Proteins Phosphatases..... 102
2.1 Analysis of Phosphatase-NHE1 Binding Assay by Immunoblotting with a Broad Range Phosphatase Antibody..... 102
2.2 Analysis of an NHE1-binding Fragment by Mass Spectrometry..... 104
2.3 Analysis of Phoshatase-NHE1 Binding via Immunoblotting with PP1 or PP2B Specific Antibodies..... 105

3. *In Vivo* Interactions of NHE1 and Protein Phosphatases..... 106
3.1 Immunoblot Analysis Following Immunoprecipitation of NHE1..... 107
3.2 Cross-linking and Immunoprecipitation Analysis of NHE1..... 107

4. The Effects of Phosphatases on NHE1 Activity in Mammalian Cells..... 109
4.1 NHE1 Activity in Neonatal Rat Cardiomyocytes Treated with Okadaic Acid..... 109
4.2 NHE1 Activity in Cells Transiently Overexpressing PP1 or PP2B..... 110
4.3 NHE1 Activity in Cells Stably Overexpressing PP1 or I2..... 111
4.4 Measurement of H^+ Extrusion from Cells Stably Overexpressing PP1 or I2..... 112
4.5 NHE1 Activity Inhibition..... 113

5. NHE1 Expression in Cells Stably Overexpressing PP1 and I2..... 113

6. Measuring Phosphorylase Phosphatase and PP1 Activity..... 114

Chapter IV

E: Discussion..... 165

1. Summary of NHE1 regulation..... 165

2. Dephosphorylation of NHE1..... 165

3. NHE1 Interactions with PP1 or PP2B..... 167

4. NHE1 Activity in the Presence of a Phosphatase Inhibitor, Okadaic Acid.....171

5. NHE1 Activity in Cell Lines Transiently Expressing PP1 or PP2B.....172

6. The Effects of PP1 on NHE1 Activity....., 173

F: Summary and General Conclusions..... 175

G: Future Experiments..... 179

Chapter V

H: References.....182

List of Tables

Table.1. Localization and Physiological Function of Mammalian NHE Family Members..... 4

Table.2. Reactions for Measuring Phosphorylase Phosphatase Activity in Heart Cell Extracts.....80

Table.3. Reactions for Measuring Phosphorylase Phosphatase and PP1 Activity in Cell Lysates..... 83

Table.4. Primers Used in Cloning Experiments..... 91

Table.5. Antibodies Used in Immunoblot Analyses..... 92

Table.6. Recipes for Rat Neonatal Myocyte Culture Solutions.....93

Table.7. Recipes for Acid Load Selection 94

Table.8. Recipes for pH Experiment Solutions.....94

Table.9. Recipes for Cell Lysate Preparation Solutions..... 95

Table.10. Calculation Formulas..... 96

List of Figures

Fig. 1. Schematic of the putative topology of NHE1 and the proposed regulatory mechanisms..... 7

Fig. 2. Phosphorylation and Dephosphorylation of NHE1..... 52

Fig. 3. Preparation of Heart Cell Extracts..... 55

Fig. 4. Restriction maps of entry clone and expression vectors
a. pDONR201..... 72
b. pDEST40 expression clone with PP1 insert 72
c. pDEST40 expression clone with PP2B insert..... 74
d. pDEST40 expression clone with I2 insert.....74

Fig. 5. The Concept of the Phosphorylase *a* Assay for Measuring Phosphatase Activity in Mammalian Cells.....85

Fig. 6. NHE1 dephosphorylation by PP1..... 117

Fig. 7. Dephosphorylation of NHE1 by PP2A in the presence and absence of Mn^{2+}..... 119

Fig. 8. NHE1 dephosphorylation by PP2B..... 121

Fig. 9. NHE1 dephosphorylation by PP1 versus dephosphorylation of NHE1 by PP1 in the presence of spinophilin..... 123

Fig.10. NHE1 dephosphorylation by crude heart cell extracts..... 127

Fig.11. Western blot analysis of PP1 present in NHE1 GST pull-down assays using a broad range phosphatase antibody..... 129

Fig.12. Western blot analysis of PP2B present in NHE1 GST pull-down assays using a broad range phosphatase antibody..... 131

Fig.13. Western blot analysis of PP1 present in NHE1 GST pull-down assays, using a PP1 specific antibody.....133

Fig.14. Western blot analysis of PP2B present in NHE1 GST pull-down assays, using a PP2B specific antibody..... 135

Fig.15. NHE1 immunoprecipitation from AP1-NHE1 and PS127A cells..... 137

Fig.16. Western Blot analysis of phosphatases present in NHE1 immunoprecipitations..... 139

Fig.17. NHE1 activity in neonatal rat myocytes treated with phosphatase inhibitor, okadaic acid..... 141

Fig.18. Western Blot of transient cell lines expressing PP1 and measurement of NHE1 activity..... 143

Fig.19. Western Blot of transient cell lines expressing PP2B and measurement of NHE1 activity..... 145

Fig.20. Western Blot of stable cell lines expressing PP1 and I2..... 147

Fig.21. Typical tracing of NHE1 activity of mammalian cells..... 149

Fig.22. NHE1 activity of cells overexpressing PP1 or I2..... 151

Fig.23. NHE1 activity of cells overexpressing PP1 or I2 stimulated with Thrombin..... 153

Fig.24. H^+ efflux of cells overexpressing PP1 or I2..... 155

Fig.25. NHE1 activity in the presence of the NHE inhibitor Hexamethylene -Amiloride (HMA).....157

Fig.26. NHE1 protein expression in cell lines expressing PP1. 159

Fig.27. NHE1 protein expression in cell lines expressing I2..... 161

Fig.28. Phosphatase activity in heart cell extracts and cells overexpressing I2..... 163

Abbreviations

α_1-AR	Alpha1-adrenoceptor
β-Gal	β-Galactocidase
aa	Amino acids
Ab	Antibody
AKAP 220	A-kinase anchor protein
Amp	Ampicillin
AngII	Angiotensin II
Arg	Arginine
BCECF-AM	2'-7'-bis(2-carboxyethyl)-5(6)-carboxyfluorescein acetoxy methyl ester
BSA	Bovine Serum Albumin
CAII	Carbonic anhydrase II
CaM	Calmodulin
CaMKII	Ca^{2+}/calmodulin-dependent kinase
cAMP	3'5-cyclic adenosine monophosphate
CHO	Chinese hamster ovary
CHP	Calcineurin B homologous protein
CnA	Calcineurin A subunit
CnB	Calcineurin B subunit
CO_2	Carbon dioxide
CsA	Cyclosporin A
Cys	Cysteine
DARPP-32	Dopamine-and cAMP-regulated phosphoprotein, Mr 32,000
DMA	5-(N,N-dimethyl) amiloride
DMSO	Dimethyl sulfoxide
DSP	Dithiobis(succinimidylpropionate)
DSS	Disuccinimidyl suberate
E.coli	Escherichia coli
EIPA	Ethylisopropyl
ERK	Extracellular signal-regulated kinase
ET-1	Endothelin-1
FK506	Tacrolimus
FKBP	FK506 binding protein
GF109203X	PKC inhibitor
GFP	Green fluorescent protein
Gly	Glycine
GSK	Glycogen synthase
GST	Glutathione S-transferase
H+	Proton
HA	Hemagglutinin
HEK293	Human embryonic kidney cells

His	Histidine
HMA	Hexamethylene-amiloride
HOE694	NHE1 inhibitor, cariporide
HPV16	Human papillomavirus type 16
I-1	Inhibitor-1
I-2	Inhibitor-2
IHF	Integration host factor
IL	Interleukin
Int	Integrase
IP_3	Inositol 1,4,5-triphosphate
Kn	Kanamycin
M	Membrane
MAPK	Mitogen-activated protein kinase
MCIP	Modulatory calcineurin-interaction protein
MMb	Myocardial myoblast
Mn^{2+}	Manganese
Mn^{2+}	Manganese
mRNA	Messenger RNA
Na^+	Sodium
NBC	Na^+-HCO_3 cotransporter
NE	Norepinephrine
Nek2	NIMA-related kinase 2
NH4Cl	Ammonium chloride
NHE (#)	Na^+/H^+ exchanger (isoform)
NIK	Nck-interacting kinase
NIPP1	Nuclear inhibitor of protein phosphatase 1
OA	Okadaic acid
OA	Okadaic acid
p38 MAPK	P38 mitogen-activated protein kinase
$p90^{RSK}$	90 kDa ribosomal S6 kinase
PAR	Protease-activated receptor
PBS	Phosphate buffered saline
PCR	Polymerase chain reaction
PCRA	GST fusion-protein of the distal 178 amino acids of NHE1
PD169316	P38 inhibitor
PD98059	MEK (ERK) inhibitor
pH*i*	Intracellular pH
PIP_2	Phosphatidylinositol 4,5-bisphosphate
PKA	Protein kinase A
PKC	Protein kinase C
PKD	Protein kinase D
PMA	Phorbol ester 12-myristate 13-acetate
PP1 c	Protein phosphatase-1 catalytic subunit
PP2A	Protein phosphatase-2A

PP2B	Protein phosphatase-2B (calcineurin)
PP2C	Protein phosphatase-2C
RyR	Ryanodine receptor
Ser	Serine
SHR	Spontaneously hypertensive rats
TBS	Tris buffered saline
TCA	Trichloroacetic acid
Thr	Threonine
TM	Transmembrane
TOPOI	Topoisomerase I
Tyr	Tyrosine
v/w	Volume/weight
VSMC	Vascular smooth muscle cell
Xis	Excisionase

Chapter I

A: Introduction

A: Introduction

1. Intracellular pH in Mammalian Cells

Intracellular pH (pH*i*) influences both cell growth and cell viability. It is tightly controlled in mammalian cells. Both acid extruding and acid loading mechanisms are required to restore and maintain normal steady-state pH*i*. The transport proteins involved in cytoplasmic alkalinization include: NHE (Na^+/H^+ exchanger), NBC (Na^+-HCO_3^- cotransporter), the Na^+-dependent $Cl^-HCO_3^-$ exchanger, the monocarboxylic acid transporter, and the ATP-dependent H^+ pump [1]. The two main proteins involved in acid loading are the Cl^--OH^- exchanger and the anion exchanger. Each transporter contributes to the maintenance of pH*i*; however, their degree of contribution varies among different cell types [1]. For example, at least three different ion transporters are involved in regulating pH*i* in the myocardium: the $Cl^-HCO_3^-$, the Na^+-HCO_3^- and the Na^+/H^+ exchanger [2]. In contrast to the $Cl^-HCO_3^-$, the Na^+-HCO_3^- and the Na^+/H^+ exchanger are activated by intracellular acidification and are the two main mechanisms of acid extrusion in the myocardium [2]. Studies have shown that the Na^+-HCO_3^- only accounts for approximately 38% of the total acid efflux from ventricular myocytes of normal adult rats at pH*i* 6.8 [3, 4]. The Na^+/H^+ exchanger is considered the predominant mechanism for restoring myocardial pH*i* to the neutral range of 7.1 to 7.3 [2].

2. The Na^+/H^+ Exchanger Family and Physiological Roles

To date, eight members of the NHE family of proteins have been identified (NHE1-NHE8) [5-11] in numerous organs and cellular compartments (Table.1). The single, most important physiological role common to all Na^+/H^+ exchanger proteins is the regulation of intracellular pH. In addition, their physiological roles differ from one another and are specific to the environment in which individual isoforms reside. Overall, the amino acid identity among NHE isoforms is diverse, varying from 20-70% [12]. The most widely distributed isoform is the Na^+/H^+ exchanger isoform 1 (NHE1). NHE1 is an integral, plasma membrane protein that catalyzes an electroneutral antiport of Na^+ and H^+ ions, to help maintain or restore normal steady-state intracellular pH of approximately 7.2 [1]. NHE1 is also involved in cell volume regulation, fluid secretion and salt and water absorption across epithelia [13, 14]. In addition, NHE1 plays a key role in cell growth [15-17], differentiation [18, 19] and motility [20-22]. NHE1 is regulated by growth factors that act through phosphorylation and dephosphorylation mechanisms, which shift the activity of the protein making it more active at an alkaline pH [23, 24]. The NHE1 isoform will be the focus in this thesis. The mammalian NHE1 isoforms share a high sequence identity, ranging from 92-100%, in hamster, rat, rabbit, pig and human [25].

Table1: Localization and Physiological Function of Mammalian NHE Family Members [12]

ISOFORM	TISSUE/ ORGANELLAR LOCALIZATION	MEMBRANE LOCATION	FUNCTION	MURINE -/- PHENOTYPE	AMINO ACID IDENTITY TO NHE1
NHE1	Ubiquitous	Plasmalemma (basolateral surface of epithelia)	Cytoplasmic pH & cell volume	Ataxia, seizures, postnatal lethal, diminutive growth	100
NHE2	GI>SkM>>>Kd, Br, Ut, T>>Ht, Lg	Plasmalemma (apical surface of epithelia)	Fluid secretion	↓Viability of gastric parietal cells ↓Parotid gland fluid secretion	46
NHE3	GI>Kd>>>>Br, other epithelia	Plasmalemma (apical surface of epithelia) & Recycling endosomes	Na^+ & HCO_3^- (re)absorption; endosomal acidification	Diarrhea, acidotic, hypotensive	38
NHE4	St>>>>Kd, Br	Plasmalemma (basolateral surface of epithelia)	Cytoplasmic pH & cell volume	?	44
NHE5	Br	Plasmalemma & Recycling edosomes	Endosomal pH?	?	37
NHE6	Ubiquitous	Endosomes	Endosomal pH? Protein sorting?	?	27
NHE7	Ubiquitous	*trans*-Golgi network & endosomes	Organellar pH? Protein sorting?	?	28
NHE8	Ubiquitous	Plasmalemma?	?	?	29

GI, gastrointestinal tract; SkM, skeletal muscle; Kd, kidney; Br, brain; Ut, uterus; T, testis; Ht, heart; Lg, lung, St, stomach

3. Putative Structural Features of NHE1

The innate complications associated with crystallizing membrane proteins have made development of knowledge of NHE1 structure difficult. Hydropathy and substituted-cysteine accessibility analysis have been two commonly used approaches to further elucidate the putative topology of NHE1 [26, 27]. Hydropathy plot analyses have predicted that all NHE proteins exhibit similar membrane topologies (70% overall identity), with 12 predicted, N-terminal, membrane spanning (M) helices (~500 amino acids) and a large C-terminal cytoplasmic domain (~300 amino acids)[26, 27], which shows greater variability among the family members. Analyses of substituted cysteine residues with cysteine-directed biotinylating reagents, have been used to propose the most recently accepted topology model of NHE1 (Fig.1). The new model has confirmed that NHE1 has twelve transmembrane, TM, helices with intact N- and C-termini located intracellularly [27]. In addition Wakabayashi *et al* identified TM segment 10 to be associated with the membrane and suggested that the 2nd and 4th loops of the protein are partially embedded within the membrane and potentially involved in ion translocation across the lipid bilayer [27].

Fig. 1.Schematic of the putative topology of NHE1 and the proposed regulatory mechanisms.

Structural features of NHE1: orange cylinders represent putative membrane-spanning segments 1-12 connected by six extracellular loops (EL1-6) and five intracellular loops (IL1-5); N, N-terminus; C, C-terminus. Factors proposed to regulate NHE1: PIP_2, phosphatidylinositol 4,5-bisphosphate; CHP (isoforms 1, 2), calcineurin homologous protein; CaM, calmodulin; P, phosphorylation sites; $p90^{RSK}$, 90 kDa ribosomal S6 kinase; p38, p38 mitogen activated protein kinase; ERK, extracellular signal-regulated kinase; p160ROCK; NIK, Nck-interacting kinase.

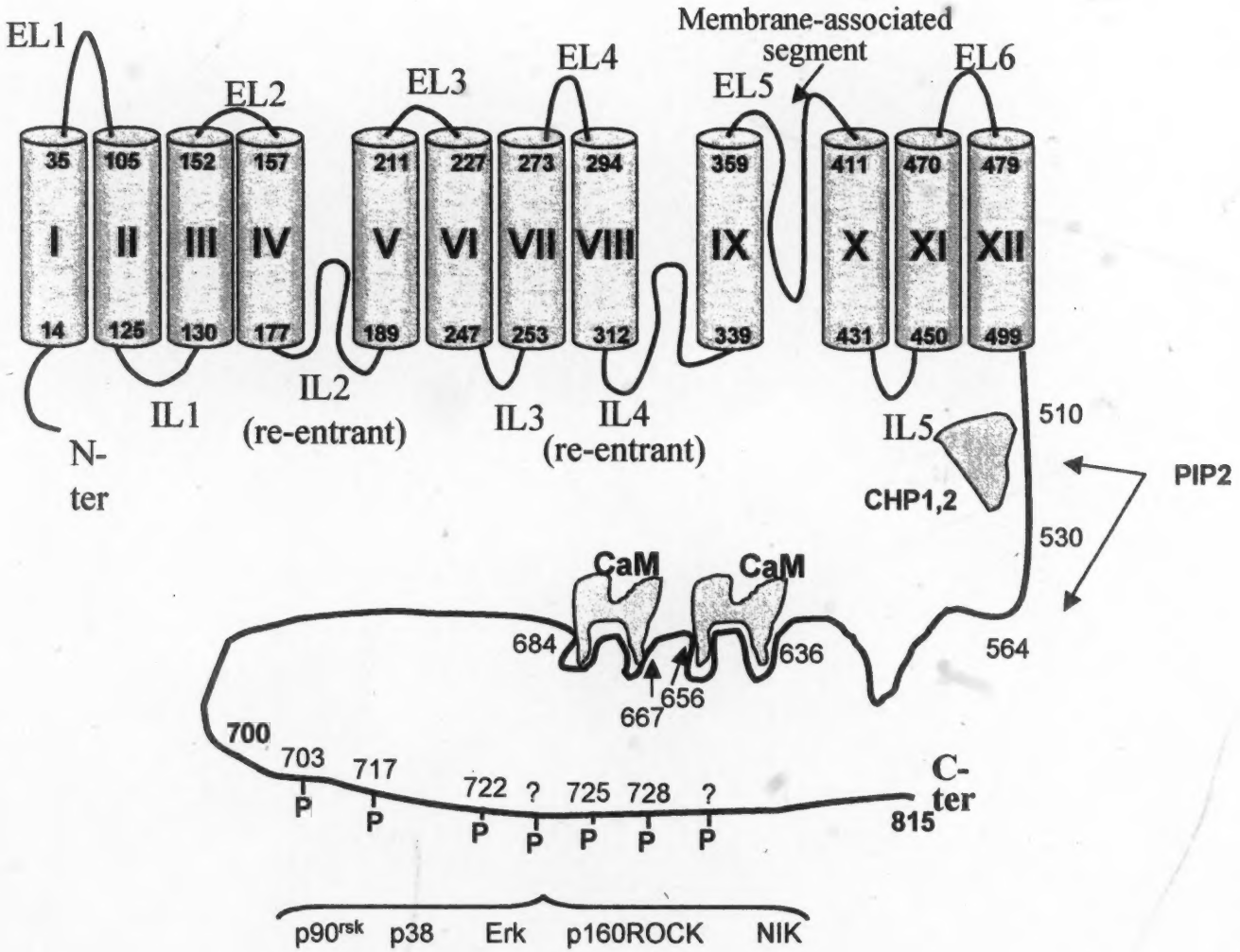
EL1
EL2
EL3
EL4
EL5
Membrane-associated segment
EL6
35
105
152
157
211
227
273
294
359
411
470
479
I
II
III
IV
V
VI
VII
VIII
IX
X
XI
XII
14
125
130
177
189
247
253
312
339
431
450
499
N-ter
IL1
IL2 (re-entrant)
IL3
IL4 (re-entrant)
IL5
CHP1,2
510
530
PIP2
CaM
CaM
684
636
667
656
564
700
703
717
722
?
725
728
?
815
C-ter
P
p90rsk
p38
Erk
p160ROCK
NIK

4. Regulation of NHE1

4.1. *The N-terminal Domain and Drug Sensitivity of NHE1*

Biochemical and mutational analyses has produced evidence that the TM domain catalyzes Na^+/H^+ exchange [28] and is responsible for drug recognition [26, 29, 30] [31]. The Na^+/H^+ exchangers are targets for inhibition by the diuretic compound amiloride and its analogues, and by novel benzoyl guanidinium compounds such as HOE694 (cariporide) [26]. The NHE affinity for these inhibitors varies among isoforms, with the following order of sensitivity: NHE1 $\geq$ NHE2 > NHE5 > NHE3 [26]. Not only does the NHE1 isoform show the highest amiloride sensitivity it is the primary subtype found in the mammalian cardiac cell, [32, 33], which has lead to therapeutic exploitation of these inhibitors for treatment of cardiac ischemia and reperfusion injuries [26].

4.2. *Regulation of NHE1 Through the C-terminal Domain and its Subdomains*

The cytoplasmic domain of NHE1 is essential for regulation of the protein. Removal of the entire NHE1 cytosolic tail causes an acidic shift of pH*i* dependence of basal exchange activity and the disappearance of growth factor-induced cytoplasmic alkalinization [28]. The cytoplasmic domain of NHE1 is over 300 amino acids in length and has been divided into at least four distinct functional subdomains that are involved in regulation [27]. These include pH*i* sensitivity, regulation of the exchanger by cytosolic calcium (Ca^{2+}) and binding proteins, cellular ATP and protein phosphorylation [34].

4.2.1. *The pH Sensing Domain of NHE1*

Maintenance of intracellular pH in cells is a remarkably dynamic process involving plasma membrane Na^+/H^+ exchangers, which extrude H^+ against the concentration gradient driven by the downhill entry of Na^+ [35]. Twenty years ago, experiments with brush border membrane vesicles demonstrated the existence of a pH sensing or modifying site in a Na^+/H^+ exchanger protein, representative of the Na^+/H^+ exchangers found in other tissues [35]. Evidence demonstrates that the H^+ modifier and H^+ transport sites of NHE1 are different. When the pH sensor site is occupied by a H^+, the NHE1 protein becomes active, allowing recovery of cells from acidosis. In contrast, when a H^+ dissociates from this site, exchange activity is halted, preventing cells from alkalosis. This protonation/deprotonation reaction can be regulated by fluctuations of H^+ affinity for the modifier site, which can be accomplished by numerous extrinsic stimuli [36]. Extreme intracellular acidification (<p*Hi* 6.2) also showed attenuation of Na^+ efflux. Currently it is presumed that this inhibition occurs as a result of competition between intracellular H^+ and Na^+ at the transport site [36]. These observations suggest that the pH sensor of Na^+/H^+ exchange has key physiological roles and its functional mechanisms are strictly regulated and complex.

Studies on NHE1 have suggested that both the N-terminal and C-terminal domains are involved in pH sensing [36]; however, to date only the involvement of the cytoplasmic domain has been conclusive [27, 37-39]. Deletion mutants of the C-terminal cytoplasmic domain expressed in the exchanger-deficient Chinese hamster lung fibroblast cell line (PS120), clearly demonstrated that the C-terminal tail of NHE1 is a critical participant in the regulation of pH sensing [27, 39]. Recently,

Wakabayashi *et al* has suggested that two glycine residues, Gly^{455} and Gly^{456} of TM11 and Arg^{440} of the fifth intracellular loop of NHE1, are involved in pH sensing regulation [40]. Mutations of these residues have demonstrated shifts in pH*i* dependence of the basal exchange activity either to an alkaline or acidic side [40]. Furthermore, the substitution of Gly^{455} with more bulky residues resulted in a greater alkaline shift, suggesting that small residues in this position are required for normal pH*i* sensitivity [40].

4.2.2. *Cytosolic Calcium and Regulatory Proteins Mediate NHE1*

Calcium is an essential intracellular signaling molecule, often referred to as a second messenger. Elevation of the level of intracellular calcium stimulates protein-protein interactions leading to rapid alterations in cellular function [37]. One example of this mechanism is the interaction between NHE1 and calmodulin (CaM).

Calmodulin is a 17 kDa protein with a near ubiquitous distribution. It contains four Ca^{2+} binding sites that contribute to dramatic conformational changes of the protein when occupied by the cation [41]. Bertrand *et al* [37] provided evidence of the interaction between CaM and the cytoplasmic tail of NHE1. The results were obtained by measurements of dansyl-calmodulin fluorescence in the presence of the NHE1 cytoplasmic domain fusion protein, and by incubating CaM with fusion proteins containing different parts of the C-terminal of NHE1 [37]. The latter experiments also confirmed that the NHE1 cytoplasmic domain contains two CaM binding sites between amino acids (aa) 637-656 and 656-700, and that this protein-protein interaction is Ca^{2+}-dependent [37]. Further analysis of both binding sites

demonstrated different affinities for CaM, the region between aa 656-691 displaying a significantly higher affinity. Different mutations were created in the high affinity CaM-binding region, subsequently utilized in expression studies using the exchanger deficient, PS120 cell line. These studies showed that single point mutations in the high affinity CaM binding region did not abolish NHE1 activity in response to growth factor (α-thrombin) or osmotic stress; however, the data indicated that CaM binding to this region is required for the complete activation of NHE1 in response to external stimuli [37]. In contrast, the deletion or charge reversal mutations in the CaM high-affinity binding site constitutively activated the exchanger. This significantly reduced thrombin stimulation of NHE1 [38].

Two calcineurin B homologous proteins CHP1 and 2 also interact with the cytoplasmic tail of NHE1 and contribute to the Ca^{2+} regulation of the exchanger [12]; however, their individual interactions with NHE1 are not Ca^{2+} dependent [42]. CHP1 is a ubiquitously expressed protein that contains four EF-hand Ca^{2+} binding motifs and shares 65% homology with the calcineurin B subunit [43]. Exploitation of various methods including *in vitro* binding assays, Western blot analysis, co-immunoprecipitation and co-localization of GFP-tagged CHP1 with NHE isoforms 1-3, have demonstrated that CHP1 binds to the juxtamembrane domain of these exchangers particularly between amino acids 510-530 of NHE1 [42]. Deletion of the CHP1-binding region from the cytoplasmic domain of NHE1-3 has demonstrated a reduction in Na^+/H^+ exchanger activity to 5-10% of the wild type exchanger activity. CHP binding is required for optimal NHE1 activity [42].

CHP2 shares 61% amino acid identity with CHP1; however, it demonstrates a much lower level of expression in most human tissues. A high level of expression of CHP2 has been demonstrated almost exclusively in cells that have become malignant [44]. Co-expression studies and pull-down assays of both calcineurin homologous proteins with NHE1 revealed a competitive relationship between CHP1 and CHP2 for the same binding site on the C-terminal tail of Na^+/H^+ exchanger isoforms 1-3 [44]. Investigations of the binding efficiencies of CHP1 and CHP2 with NHE1 suggested a 5-fold stronger bond between CHP2 and NHE1 [44]. Under normal conditions both CHP1 and CHP2 enhanced NHE1 activity when coexpressed and demonstrated similar roles in cell growth. A distinct effect of these proteins on NHE1 was observed when serum was depleted [44]. Cells expressing CHP2-NHE1 were significantly more resistant, retaining viability at 60% after 10 days of serum starvation, while cells expressing CHP1-NHE1 were more sensitive and lost viability within this time frame. These results demonstrated a physiological importance of the CHP2 interaction with NHE1, a protein-protein combination that can protect cells from death resulting from serum deprivation [44].

Tescalcin is a newly discovered calcium binding protein that is homologous to CHP and calmodulin. It has tissue specific expression and is strongly expressed in the myocardium [45]. Coprecipitation and immunofluorescence experiments demonstrated that tescalcin binds directly to the distal 182 amino acids of NHE1, an interaction that is enhanced by calcium [46]. Competition studies have shown that tescalcin does not compete with calmodulin for its binding site on NHE1 [46]. Furthermore, expression of tescalcin *in vivo* caused nearly a 50% decrease in NHE

activity. The inhibition was more pronounced in the presence of serum and it was dependent on the presence of an intact C-terminal 182 amino acids of the NHE [46].

Finally, a recent study has demonstrated that the protein carbonic anhydrase II (CAII) binds to the cytoplasmic tail and regulates activity of the NHE. Carbonic anhydrase catalyzes the hydration of CO_2 to produce HCO_3 and H^+. The interaction between NHE1 and CAII occurs both *in vitro* and *in vivo* [47]. Chinese hamster ovary cells coexpressing NHE1 and CAII demonstrated a higher H^+ transport rate compared with cells expressing NHE1 alone. This effect was reduced in the presence of the CAII inhibitor, acetazolamide. The activity of NHE1 was affected through direct interaction with CAII at the C-terminal region and the binding was increased by phosphorylation of NHE1 [47]. It should be noted however that CAII is only present transiently during development in the myocyte so it is unlikely to play a major regulatory role in the myocardium [48].

4.2.3. *Cellular ATP, Hormones, Growth factors and Acidosis Regulate NHE1*

Subdomain I of the cytoplasmic tail of NHE1, which contains the CHP binding site, also contains two binding motifs at aa 509-516 and 552-560 for phosphatidylinositol 4,5-bisphosphate (PIP_2) [49]. Like other polyphosphoinositides, PIP_2 is a ubiquitous constituent of animal plasma membranes, found to exert regulatory effects on the activity of several ion transporters such as K^+ channels [50, 51] and Na^+/Ca^{2+} antiporters [50]. Aharonovitz *et al* demonstrated that reduction of PIP_2 or depletion of ATP, which reduces PIP_2, inhibits the exchange activity of NHE1 [49]. The association of PIP_2 with NHE1 may account for a substantial portion of

ATP-dependence of NHE1 [49], while other ATP-dependent regulatory factors remain to be identified.

Numerous hormones and growth factors are responsible for indirect regulation of NHE1: aldosterone [52], thyroid hormone [53, 54], epidermal growth factor [55], endothelin, angiotensin II, epinephrine, thrombin, [56] and adenosine [57]. Several mechanisms of regulation involve receptor-mediated pathways, for example thrombin. Thrombin is an effector protease involved in coagulation that can also function like a hormone to regulate cellular behavior [58]. Thrombin signaling cascades are partially regulated by a family of G protein-coupled protease-activated receptors (PARs) of which four members, PAR1-4, have been characterized [58]. With respect to the cardiac myocyte, in adult rat ventricular myocytes it has been shown that thrombin and a synthetic thrombin receptor activating peptide SFLLRN activate sarcolemmal NHE activity [59]. Although thrombin receptors PAR2 and PAR3 have been cloned and shown to be present in the myocardium [60, 61], stimulation of NHE activity is believed to occur, at least partially, *via* PAR1 [59]. PAR1 activation by thrombin is irreversible and occurs when its N-terminal exodomain is cleaved, revealing a new receptor amino terminus [58]. Other thrombin receptors, which have proposed additional avenues for activation of NHE by thrombin have not been conclusively investigated.

Environmental stimuli also affect the level of expression of NHE1. Eukaryotic cells produce acid through a number of metabolic mechanisms. To cope with an increased acid load, the kidney and several renal cell lines increase their level of NHE1 [62-65]. As a result of ischaemia, chronic acidosis causes an increase in the

activity of NHE1 in isolated cardiomyocytes. In isolated perfused hearts and in myocytes ischaemia elevates NHE1 mRNA levels [66, 67].

4.2.4. *Direct Phosphorylation Regulates NHE1*

It has been demonstrated that the Na^+/H^+ exchanger is a phosphoprotein and that its level of phosphorylation is increased in mitogen-stimulated cells [68-71]. Stimulation of the antiporter by mitogens and phorbol esters is associated with the activation of protein kinases [72]. Phosphorylation of NHE1 leads to a shift in the pH*i* sensitivity of the modifier site, accounting for activation of exchange activity and cytosolic alkalinization [40, 72]. Phosphorylation of the Na^+/H^+ exchanger stimulates activity in the myocardium and other tissues. In response to growth factors, phosphorylation of NHE1 occurs in the distal 178 amino acids of the cytoplasmic domain [73-75]; however, it only accounts for approximately 50% of the NHE1 activation [76]. The current list of putative NHE1 kinases includes: Ca^{2+}/calmodulin-dependent kinase II (CaMKII) [77], extracellular signal-regulated kinase (ERK) [70], p160ROCK [78], the 90 kDa ribosomal S6 kinase ($p90^{RSK}$) [79], p38 mitogen-activated protein kinase (p38 MAPK) [80] and Nck-interacting kinase (NIK) [23]. Further evidence demonstrates that regulation of NHE1 occurs via the PKC and PKD pathways and the PKA pathway, although the latter is cell specific [25].

Mitogen-activated protein kinase (MAPK) directly phosphorylates the C-terminus of NHE1. Fractions from rabbit skeletal muscle containing ERK1/2, phosphorylated the NHE1 C-terminus, while immunodepletion of the kinase diminished this phosphorylation [70]. When Chinese hamster ovary cells were

transfected with an inducible MAPK dominant-negative mutant, there was a reduction in serum-stimulated alkalinization in the cells, demonstrating the involvement of ERK1/2 in agonist-induced activation of NHE1 [70]. More recent studies utilizing isolated cardiomyocytes demonstrated that MAPK regulates NHE1 in the myocardium [73]. In addition, it was shown that the role of ERK1/2 may be enhanced with ischaemia and reperfusion of the myocardium [81]. Recently, it was showed that the ERK pathway activates the sarcolemmal NHE through a novel mechanism that is mediated by intracellular acidosis. Inhibition of the acidosis-induced activation of ERK resulted in inhibition of the sarcolemmal NHE activity [82].

The 90 kDa ribosomal S6 kinase, $p90^{RSK}$, is dependent on activation by ERK-mediated phosphorylation [83, 84]. Indirect ERK-mediated stimulation of NHE1 has been demonstrated to occur through $p90^{RSK}$ by phosphorylation of the Ser 703 residue in the C-terminus of NHE1 [76, 79]. More recently $p90^{RSK}$ was identified as a myocardial kinase involved in NHE1 phosphorylation [73]. Studies of neonatal rat cardiomyocyte extracts stimulated with endothelin or serum demonstrated a higher level of phosphorylation of a GST fusion protein composed of the distal 178 amino acids of NHE1 [73]. Fluorometric experiments demonstrated stimulation of steady-state intracellular pH by ET-1 and serum, which was abolished upon the introduction of a MEK inhibitor, PD98059, confirming that the phosphorylation of NHE1 was in fact initiated through the MAPK signal transduction pathway [73]. In addition, $p90^{RSK}$ has shown to phosphorylate NHE1 in vascular smooth muscle cells when stimulated with angiotensin II (AngII) [85].

An increase in intracellular pH is an early sign of dysfunctional interleukin or cytokine receptor signaling, which leads to cell death. This mechanism of alkalinization was examined using two cytokine-dependent cell lines: D1, thymocytes dependent on interleukin-7 (IL-7); and FL5.12A, a pro-B-cell line dependent on interleukin-3 (IL3) [80]. The membrane ion transporters investigated included: Na^+/K^+ ATPase, the Na^+-dependent and independent anion exchangers and the Na^+/H^+ exchanger [80]. This study produced convincing evidence that another member of the MAPK kinase family, p38 MAPK, phosphorylates NHE1 in these cell types [80]. Based on sodium dependence, the requirement of a sodium gradient, and the effect of NHE inhibitors, the Na^+/H^+ exchanger was identified as the predominant pH regulatory protein responsible for cell alkalinization following cytokine withdrawal [80]. In this study, NHE1 phosphorylation was examined in interleukin-dependent and independent cell lines with the p38 kinase inhibitor PD169316. The results showed significant inhibition of NHE1 phosphorylation in the presence of PD169316 following IL-3 withdrawal [80]. Evidence of p38 directly phosphorylating NHE1 came from in gel kinase assays and mutational analyses of NHE-GST fusion proteins, followed by mass spectrometry. Four p38 *in vitro* phosphorylation targets were identified in NHE1 including: Thr 717, Ser 722, Ser 725 and Ser 728 [80]. This study greatly contributed to our present knowledge of NHE1 phosphorylation.

Protein kinase C (PKC) pathways are activated by phorbol esters such as 12-myristate 13-acetate (PMA), and are known to stimulate NHE1 activity [25]. In addition, down-regulation of PKC and inhibitors of PKC pathways such as staurosporine have been shown to block aldosterone-induced activation of NHE1

[52]. Recent studies of sarcolemmal NHE regulation have shown that increased NHE activity can be caused by activation of α_1-adrenoceptors (α_1-ARs). These receptors are activated by mechanisms involving both PKC and ERK pathways that when blocked by specific pathway inhibitors (GF109203X or PD98059 respectively) NHE activity cannot be stimulated [86]. PKC is involved in Na^+/H^+ exchanger regulation by phosphorylation; however, direct phosphorylation of NHE1 by PKC has not been demonstrated. In addition, it has been shown that PKC is involved in phosphorylation of protein kinase D (PKD) [87]. Like PKC, the PKD pathway is stimulated by phorbol esters [88, 89]. PKD does contribute to regulation of the NHE but likely does not directly phosphorylate the protein [90].

Na^+/H^+ exchange activity can also be regulated by the protein kinase A (PKA) pathway even though NHE1 does not contain any classical consensus sites for PKA association. Unlike PKC, MAPK or $p90^{RSK}$, PKA activation of NHE1 seems to be cell specific. For example, in PS120 (NHE1-deficient) cells, which have a functional PKA pathway, the expression of human and rabbit NHE1 does not show any response to cyclic AMP [91] [91] analogs [92, 93]. When human NHE1 is stably expressed in opossum kidney cells, activity of the exchanger is inhibited after PKA or PKC activation [94]. In contrast, studies of NHE1 in murine macrophages [95], primary rat hepatocytes [96], rat osteoblastic UMR-106 cells [97] or AP1-NHE1 cells [98] showed that NHE activity can be stimulated with cAMP. Clearly the cAMP/PKA regulation of NHE activity is largely influenced by cellular milieu.

Other kinases that regulate NHE1 are p160 ROCK, NIK and CaMKII. p160ROCK plays a key role in cytoskeleton organization, particularly in focal

adhesion assembly and actin stress fibres induced by the Rho family of small GTPases [78]. p160ROCK-induced stress fibre formation in fibroblasts was inhibited when NHE1 activity was attenuated with ethylisopropyl (EIPA), an NHE inhibitor [78]. Similar to *in vitro* experiment results, expression of an activated p160ROCK in fibroblasts caused stimulation of NHE1 [78]. Recently, a novel serine/threonine kinase, NIK has been added to the list of NHE1 regulatory kinases. Mutational experiments have indicated that NIK binds directly to NHE1 between amino acids 538 and 638 [23], which also corresponds to the CHP binding region [43]. Interaction of NIK with NHE1 was investigated in human embryonic kidney cells (HEK293) and fibroblasts transiently overexpressing NIK. The results demonstrated that overexpression of NIK caused an increase in the exchanger activity and steady-state pH*i* in both cell types [23]. Ca^{2+}/calmodulin-dependent protein kinase II (CaMKII) was also shown to phosphorylate NHE1 in a Ca^{2+}/CaM dependent manner *in vitro*. Further examinations determined that NHE1 has three consensus sequences for CaMKII and that CaMKII and calmodulin can affect NHE1 activity *in vivo* [99].

Phosphorylation of NHE1 is mediated by a growing number of kinases and has provided scientists with many avenues to investigate diverse NHE1 functions. To date, intracellular Ca^{2+}, regulatory proteins, ATP, hormones, growth factors and protein kinases account for the majority of NHE1 activation. However, early studies have demonstrated that the phosphatase inhibitor, okadaic acid, causes intracellular alkalinization. Sodium dependence and inhibition studies of Na^+/H^+ antiport suggested that this alkalinization occurs via the Na^+/H^+ exchanger. It is therefore possible that NHE1 can also be activated and regulated by the inhibition of

phosphatases [72]; however, the roles of phosphatases in NHE1 regulation by dephosphorylation have not been characterized.

This is the first report outlining the investigations of the effects of PP1 on NHE1 *in vivo* and dephosphorylation of NHE1 by PP2A and PP2B. It is therefore important to briefly outline the characteristics of these phosphatases and the major factors involved in their regulation.

5. Classification of Protein Phosphatases

The process of protein phosphorylation is mediated by protein kinases, whereas dephosphorylation is mediated by protein phosphatases. Of the 500 protein kinases encoded by the human genome, approximately 2/3 are serine/threonine kinases (ser/thr). Approximately 150 members of the protein phosphatases are distributed among four distinct families; however only about 40 are ser/thr phosphatases [100]. The ratio of ser/thr kinases to ser/thr phosphatases is also high in *Drosophila,* approximately 6:1 [101].

5.1. *Protein Serine/Threonine Phosphatases*

Based on a general structure, ser/thr protein phosphatases are classified into two major groups: multimeric and monomeric. Multimeric protein phosphatases are composed of two components: a catalytic subunit and a regulatory subunit [102]. The catalytic subunits are responsible for associations with substrates, toxins and protein inhibitors and for the removal of phosphates from other proteins. The regulatory subunits mediate substrate specificity and intracellular localization of the multimeric

phosphatases [102]. Protein phosphatase 1, 2A and 2B are representative members of multimeric phosphatases and belong to the same gene family [103]. The monomeric protein phosphatases lack the regulatory subunit. Their catalytic subunits alone are considered sufficient to catalyze dephosphorylation reactions and determine substrate specificity of the proteins [104]. A representative member of monomeric phosphatases is PP2C, a magnesium dependent phosphatase [104]. Distinct amino acid sequences in the catalytic core, crystal structure and inhibition studies have provided evidence that PP2C is in a different gene family than multimeric phosphatases [102]. As a result PP2C was not investigated in this study and this report focuses on the involvement of multimeric protein phosphatases in NHE1 dephosphorylation.

In humans, seven members of the multimeric, ser/thr protein phosphatase family have been identified. These include protein phosphatase-1 (PP1), PP2A, PP4, PP6, PP2B (calcineurin), PP5 and PP7 [100, 105]. Three of the most characterized members are PP1, PP2A and PP2B. These three phosphatase proteins share 40-50% sequence identity among their catalytic subunits; however, are highly variable in their regulatory subunits [106, 107].

6. Type-1 Multimeric Protein Phosphatase, PP1

6.1 *Characteristics of PP1*

Type-1 ser/thr protein phosphatases are expressed in all eukaryotic cells and have been implicated in numerous physiological processes such as carbohydrate and lipid metabolism, protein synthesis and gene transcription [108, 109]. Five mammalian PP1c genes identified have been termed PP1β, PP1α, PP1α_2, PP1γ_1 and PP1γ_2, the latter four arising through alternative splicing [100, 110-113]. All PP1c isoforms share 90% sequence identity; however highly variable regulatory subunits, with which the catalytic subunits interact, mediate the diversity of PP1 function [100].

To gain a greater understanding of PP1 function many studies have focused on site-directed mutagenesis of the PP1 catalytic subunit expressed in *E.coli* [100] and structure-function studies of PP1 in Sf9 insect cells using the baculovirus expression system [114]. It is necessary to note that recombinant PP1 in these two expression systems differs in several important properties. First, recombinant PP1 in *E.coli* is inactive in the absence of Mn^{2+}; therefore, the presence of Mn^{2+} in growth media and purification buffers is essential in expression and purification of *E.coli* PP1. Second, *E.coli* PP1 is able to dephosphorylate phospho-tyrosine-containing substrates and *para*-nitrophenyl phosphate. Third, *E.coli* PP1 is relatively insensitive to inhibition by phospho-inhibitor-1 and its homolog phospho-DARPP-32 (dopamine- and cAMP-regulated phosphoprotein, M_r 32,000). Finally, recombinant PP1 in *E.coli* is insensitive to regulation by several targeting subunits [114]. With respect to these four properties, PP1 expressed in insect cells functions in a reverse manner. The recombinant PP1 produced in insect cells exhibits properties very similar to those of

native PP1; therefore many structure-function studies of PP1 have been performed using the baculovirus expression system [114].

6.2. *Regulation of PP1 by Regulatory Subunits*

To date, nearly 50 established or putative mammalian regulatory subunits of PP1c have been characterized. The regulatory subunits of PP1c can be divided into two distinct categories: targeting subunits and modulating subunits. Targeting subunits direct PP1c to specific subcellular locations such as: glycogen particles, myofibrils, nucleus, ribosomes, plasma membrane, actin cytoskeleton, sarcoplasmic reticulum, centrosomes, mitochondrial membrane and the cytosol [100]. Modulating subunits lack targeting ability; however, they regulate substrate specificity of the catalytic subunit and include members such as chaperones, inhibitor and activator proteins. Most regulatory subunits of PP1 do not share high sequence homology unless they are isoforms [100]. The vast number of regulatory subunits account for the diverse functions of PP1 involved in: glycogen metabolism, smooth muscle relaxation, skeletal muscle contraction, pre-mRNA splicing, cell cycle regulation, protein synthesis, nuclear envelope reassembly, synapse and dendritic morphology, co-ordination of PKA and PP1 signalling, chloride ion transport and centrosome separation [100].

6.3. *Interaction of Regulatory Subunits with PP1c*

A conserved PP1c-binding motif, RVxF, was initially identified in studies of the glycogen-targeting subunits, G_M and G_L, and the myosin-targeting subunit M_{110}

[115]. Later studies indicated that the binding motif varies, (R/K)(V/I)xF, in PP1c association with regulatory subunits other than G_M and G_L [116]. Valine and phenylalanine are essential residues in this motif as their mutation has been shown obliterate PP1 interaction with several subunits including: spinophilin [117], NIPP1, Nek2 and AKAP 220 [100, 118-121]. Through emerging studies on mammalian or yeast regulatory subunits, variants of this motif have been identified, therefore the current consensus sequence established for the PP1c-binding motif is (R/K)x_1(V/I)x_2(F/W), where x_1 may be absent or any residue excluding large hydrophobic residues and x_2 may be any amino acid excluding large hydrophobic residues [100].

Further studies of the G_M, glycogen-targeting subunit lead to the discovery of a hydrophobic groove near the c-terminus of PP1c that contains amino acids Ile169, Leu243, Phe257, Leu289-Cys291 and Phe293. These amino acids are important in the interactions with valine and phenylalanine residues in peptides containing the RVxF motif [116]. The hydrophobic groove is isolated from the active site, which is responsible for binding to substrates and the phosphorylated residues of inhibitor proteins [100]. The active site is partially shielded by a flexible β12-13 loop structure, which is thought to undergo conformational changes. This loop contains a highly conserved Tyr272 residue close to the active site, that is a critical determinant of PP1 sensitivity to several toxins including microcystin, okadaic acid, and calyculin A [122-126]. Alterations of the β12-13 loop have also been shown to affect the binding of inhibitor-1 (I-1) and inhibitor-2 (I-2) [125, 127].

6.4. *Targeting PP1 to the Plasma Membrane by Spinophilin*

Several PP1 binding proteins have been shown to target the phosphatase to the plasma membrane or actin skeleton, one of them is spinophilin [100]. Spinophilin is an 817 amino acid protein that is expressed in many tissues but enriched in the brain. Early reports show that spinophilin is an F-actin binding protein [128] and a PP1 interacting protein [129]. *In vitro* binding assays, expression studies and co-localization of the membrane bound dopamine receptor (D2) with spinophilin, have facilitated the characterization of spinophilin as a linker protein that brings intracellular signaling molecules, such as PP1, into close proximity with the plasma membrane [130]. In spinophilin, the RVxF motif determines the binding to PP1c, whereas a domain upstream from the PP1c-binding motif regulates the activity of PP1c [117].

6.5. *Modulation of PP1 Activity by Inhibitor-2*

Protein phosphatase-1 activity is modulated by interaction with heat-stable inhibitor proteins including I-1, DARPP-32 and inhibitor-2 (I2). I2 has two key roles in the regulation of PP1: it inhibits free cytosolic PP1 and it controls an inactivation/activation cycle of PP1 [131]. Unlike I-1 and DARPP-32, I2 is not phosphorylated when it interacts with PP1c [100]. An unphosphorylated I2 forms a complex with PP1c and changes its conformation to an inactive state [100, 132]. Conversion of PP1c to an active form in the complex can be induced by I2 phosphorylation on Thr72 by GSK3 (glycogen synthase kinase 3) [133, 134]. I2 can

interact with denatured PP1c and promotes refolding of the enzyme to restore its activity [135].

As previously mentioned, biochemical characteristics of recombinant PP1c are different from those of native PP1c [132]; however, it has been shown that incubation of PP1c with I2 and subsequent reactivation by GSK3 allows the recombinant enzyme to behave more like native PP1c [135, 136]. Studies investigating I2 ability to fold newly synthesized or denature PP1c into is correct conformation have strongly suggested that I-2 acts as a molecular chaperone for PP1c [132]. Furthermore, I2 can be phosphorylated by CKII (casein kinase II) on three serine residues (Ser-86, Ser-120 and Ser-121). CKII phosphorylation does not alter I2 activity, but facilitates phosphorylation by GSK3α [137]. Despite the importance of the RVxF motif, which does exist in I-2, mutagenesis experiments have shown several sites in the inhibitor interacting with PP1c [100, 138]. I2 has been shown to bind to a negatively charged region close to the RVxF-binding groove of PP1c [139]. The N-terminal domain of I2 is involved in inhibition, while other regions control PP1c inactivation and reactivation [138].

7. Type-2 Multimeric Phosphatases PP2A and PP2B

7.1. *The β12-13 loop structure of PP2Ac and PP2Bc*

Similar to PP1, the Type-2 phosphatase proteins PP2A and PP2B also contain a β12-13 loop structure that is important for inhibitory mechanisms of these ser/thr phosphatases [127]. The Tyr272 residue in β12-13 loop of PP1, shown to be

important in the interaction of the enzyme with toxins, is also highly conserved in PP2A and PP2B; however its function has remained inconclusive in Type-2 phosphatases [114]. Studies on the yeast PP2B catalytic subunit showed that mutating Thr350 in its β12-13 loop structure to either lysine or arginine reduced PP2B sensitivity to inhibition by the immunosuppressive drug cyclosporin [140]. Analogous research on the PP2A catalytic subunit demonstrated that Cys269 in the predicted β12-13 loop participates in an interaction with fostriecin (FOS), a structurally novel antitumor antibiotic, which promotes inhibition of PP2A [141].

7.2. *Regulation and Functions of PP2A*

Protein phosphatase 2A is a dimer composed of a catalytic subunit (PP2Acα or β) and a regulatory A subunit, also termed PR65 based on its molecular weight of 65 kDa. A third regulatory B subunit can associate with the core structure, for which four different families have been identified and termed: B, B', B" and B"' [142]. The two isoforms of PP2Ac share 97% amino acid identity and are ubiquitously expressed; however, significantly higher levels of expression of PP2Ac, predominantly the α-isoform, are found in the brain and heart compared to other tissues [143]. The regulatory A subunit is tightly associated with PP2Ac and allows binding of various regulatory B subunits in a mutually exclusive manner [144]. In mammals, each of the B families, of associating regulatory subunits, contains several gene products. Some isoforms are highly expressed in the heart, skeletal muscle, and the brain, while others have a wide tissue distribution. Although there are only two catalytic subunits of PP2A, nearly 75 different combinatorial associations can occur

with the A and B/B'/B"/B'" regulatory subunits [142], leading to diverse PP2A functions.

PP2A is directly regulated by phosphorylation and methylation. *In vitro*, inactivation of PP2Ac can occur upon the phosphorylation of a conserved Tyr307 residue by tyrosine kinases $pp60^{v\text{-}src}$ and $pp56^{lck}$, the epidermal growth factor and insulin receptors. In intact cells phosphorylation of PP2A can be enhanced by cell transformation and growth factors causing the phosphatase to become inactive [145]. Studies have suggested that PP2A can re-activate itself in an autodephosphorylation reaction under normal conditions [142]. The PP2Ac has a $T^{304}PDYFL^{309}$ motif in the c-terminus, which contains the conserved Tyr307 and a recognition site for carboxymethylation by a specific carboxyl methyltransferase [146]. Methylation occurs on the Leu309 residue of the carboxy group and is reversible *in vivo* in the presence of a specific methylesterase [147]. Studies have demonstrated conflicting data with respect to the effect of PP2A methylation on its catalytic activity, some suggesting that the phosphatase activity increases under these conditions; however these results have not been replicated [142].

Other factors involved in the regulation of PP2A activity are, the second messenger ceramide and inhibitor proteins. Ceramide is an important second signal molecule that regulates diverse signaling pathways involving apoptosis, cell senescence, the cell cycle, and differentiation [148]. Ceramide has been found to specifically activate mitochondrial PP2A in leukaemia cell lines, resulting in dephosphorylation of an anti-apoptotic protein, Bcl2 [149]. Two specific, non-competitive and heat-stable proteins, I_1^{PP2A} and I_2^{PP2A}, have been shown to inhibit

PP2A at nanomolar concentrations. In the presence of Mn^{2+} these inhibitor proteins modulated the activities of PP1 and PP2A against certain substrates in opposite directions, significantly activating PP1c and completely inhibiting PP2A [150]. These results suggested a novel role for I_1^{PP2A} and I_2^{PP2A} in the co-ordination of PP1 and PP2A activities in cells [150]. These distinct PP2A modulating factors increase the diversity of PP2A function in: cell cycle mechanisms, cell transformation, signal transduction, translation, apoptosis and stress responses [142].

7.3. *Regulation and Functions of PP2B*

The Ca^{2+}/calmodulin-dependent protein phosphatase, calcineurin is composed of calcineurin A (CnA), a catalytic subunit, and calcineurin B (CnB), a regulatory subunit. Calcineurin A contains binding domains for calcineurin B and calmodulin as well as an autoinhibitory region [151]. Micromolar Ca^{2+} changes within the cell stimulate Ca^{2+} binding to CnB directly or as a Ca^{2+}/CaM complex with CnA. This mechanism causes a displacement of the autoinhibitory domain allowing access for substrates to interact with the catalytic domain [152, 153]. Calcineurin is also regulated by MCIP (modulatory calcineurin-interaction proteins)[154]. MCIP proteins contain a conserved stretch of 31 amino acids including phosphoamino acid residues that are substrates for calcineurin and bind directly to CnA [155, 156].

Calcineurin signaling is inhibited by several mechanisms including those induced by the calcineurin B homologous protein (CHP) [157] and A238L, which is a viral-encoded protein that inhibits calcineurin in infected macrophages [158]. Other proteins that have been shown to target calcineurin to the ryanodine and IP_3 receptors

include immunophillins, or FK506 binding proteins (FKBP), FKBP12 and FKBP12.6 [159, 160]. FKBP and cyclophilin A are important immunophillins involved in calcineurin binding to immunosuppressive drugs FK506 and cyclosporin A (CsA), which are involved in calcineurin inhibition [153, 161]. In addition, these immunosuppressive drugs have been demonstrated to disrupt calcineurin interactions with MCIP, suggesting that the drug/immunophilin complexes compete with MCIP for binding sites on calcineurin [154, 162]. These distinct calcineurin modulating factors control calcineurin signaling in a vast number of complex, cellular processes including: T-cell activation, synaptic plasticity and apoptosis of neurons, development, hypertrophy as well as gene regulation in skeletal and cardiac muscle [163-165].

8. Dephosphorylation of NHE1

Protein phosphatases are responsible for the dephosphorylation of proteins. The regulation of phosphatases has been mostly studied using phosphatase inhibitors. Early studies by Takai *et al* demonstrated inhibition of PP1 and PP2A activity by a naturally occurring phosphatase inhibitor, okadaic acid [166]. Okadaic acid is a polyether derivative of a fatty acid that has different efficacies towards the different phosphatase isoforms [167]. It has an IC_{50} of 0.1-0.2 nM for PP2A *in vitro*, an IC_{50} of 10-20 nM for PP1 *in vitro* and it inhibits PP1 at micromolar concentrations *in vivo*, while at these concentrations it does not inhibit PP2B [107]. Thus, studies using low μM concentrations of okadaic acid and showing significant effects are usually said to

have demonstrated that either PP2A or PP1 are the phosphatase of interest, while PP2B is not affected by these concentrations of inhibitors [71, 72, 167-171].

Studies on the regulation of the NHE by protein phosphatases are few and are mostly indirect, involving the use of phosphatase inhibitors to modify activity of the protein. In platelets, rat thymic lymphocytes, human bladder carcinoma cells and in Chinese hamster lung fibroblasts NHE is tightly regulated by phosphorylation and dephosphorylation. Okadaic acid could directly increase phosphorylation and activity of the NHE in these cell lines [71, 72, 168, 169]. Okadaic acid has also been reported to increase the activity of ERK1/2 and NHE1 in human red blood cells and PD98059 (the MEK inhibitor) blocked this effect. This further indicates that NHE1 regulation occurs through the ERK pathway, and that okadaic acid sensitive phosphatases are involved [171]. Okadaic acid can activate NHE in human blood lymphocytes [170] and another ser/thr phosphatase inhibitor, calyculin A, can activate NHE1 in Ehrlich ascites tumor cells [172]. The trout βNHE protein is related to NHE1 in mammals and is also regulated by an okadaic acid sensitive mechanism. It was suggested that PP1 was the phosphatase regulating βNHE [173-175]. However, it should be noted that trout and mammalian Na^+/H^+ exchangers are regulated by different stimulatory pathways [174, 175].

Only one study has examined NHE1 regulation by phosphorylation more directly. It has been previously demonstrated that serine residue 703 plays a key role in NHE1 function. The mutation of serine 703 to alanine was shown to prevent stimulation of NHE1 by serum [79]. Recently, the 14-3-3, phosphoserine binding protein [176] was shown to bind to phosphorylated serine 703 of NHE1. The binding

of 14-3-3 prevented *in vitro* dephosphophorylation of NHE1 by PP1 [177]. Although it was suggested that PP1 plays a role in NHE1 regulation, the effect of PP1 and other phosphatases on NHE1 *in vivo* or in the myocardium have not been investigated.

9. NHE1 in Disease

The theoretical framework behind NHE1 regulation is important for the implementation of novel therapies. The Na^+/H^+ exchanger plays a pivotal role in several disease states of the myocardium and also in diabetes and cancer. Current statistics released by Heath Canada indicate that the leading cause of death in Canada is cardiovascular or heart disease. Underlying and potent factors that contribute to this disease are: high blood pressure (hypertension); high blood cholesterol; obesity and diabetes [178].

9.1. *Cardiac Hypertrophy*

Cardiac hypertrophy is an increase in cardiac cell size without cell division. It can be induced by a mechanical load, such as cell-stretch, humoral factors including: angiotensin II [179], endothelin (ET)-1, and α_1-adrenergic agonists or peptide growth factors such as norepinephrine (NE), which is a potent growth factor for cardiac myocytes [180, 181]. Protein kinase pathways are primary targets for these external stimulatory agents. During mechanical stress in cardiac myocytes these external stimuli activate several protein kinase cascades such as PKC, Raf-1 kinase, MAPK, ERK and $p90^{RSK}$ [182]. In response to humoral factors tyrosine kinase and S6 kinase are activated in addition to MAPK and PKC [183].

It is important to note that sodium ions are also mediators of cell hypertrophy [184]. An increased concentration of sodium in cell culture medium causes hypertrophy in neonatal rat myocardial myoblasts (MMbs) and vascular smooth muscle cells (VSMCs) [185]. Observations were made of increased cell diameter, cell volume and protein content in both cell types, as well as measurements of cell protein turnover and cell proliferation. These findings established that the cell hypertrophy resulted from an increase in the rate of cellular protein synthesis and a decrease in the rate of cellular protein degradation. Upon returning the hypertrophied cells to normal sodium medium the condition was completely reversed within two days [185]. Further experiments suggested that Na^+ influx induces hypertrophic response in myocytes through the activation of the PKC cascade [186].

Briefly as described earlier, factors known to induce cardiac hypertrophy such as ET-1, AngII and the $\alpha_1$adrenoceptor can stimulate NHE1 [186]. Most of the studies suggesting that the Na^+/H^+ exchanger contributes to signaling pathways leading to cardiac hypertrophy have involved the use of NHE inhibitors. In cardiomyocytes the NHE inhibitor HOE694 suppressed intracellular alkalinization induced by the α-adrenoceptor agonist phenylephrine (PE), ET-1 and PMA [186]. NHE inhibition by HOE694 also blocked stretch-induced hypertrophy in neonatal cardiac myocytes [181]. In the four-week postinfarcted rat myocardium NHE1 inhibition by amiloride reduced myocardial fiber size, which can lead to a hypertrophic response and congestive heart failure [184]. Together these studies suggest that NHE1 is an effective contributor to cardiac hypertrophy.

9.2. *Ischemia and Reperfusion*

The Na^+/H^+ antiporter also contributes to myocardial injury produced by ischemia and reperfusion. The contribution of the NHE in ischemia and reperfusion has been elegantly described in the sarcolemma, as a complex process involving two other sarcolemmal transport proteins, the Na^+/K^+ pump and the Na^+/Ca^{2+} exchanger [187]. Under normal physiologic conditions Na^+ is extruded from the cell predominantly by the Na^+/K^+ pump, while NHE remains inactive and the Na^+/Ca^{2+} exchange protein favors Ca^{2+} efflux from the cell [187]. Inadequate blood supply in a portion of the heart muscle can lead to an ischemic condition. This condition causes an inactivation of the Na^+/K^+ pump and shifts the intracellular pH towards an acidic environment, known to activate NHE [66]. Together, these two factors cause a rise in intracellular Na^+ that reverses the Na^+/Ca^{2+} exchanger, resulting in Na^+ efflux in exchange for Ca^{2+} influx [187]. Accumulation of intracellular Ca^{2+}, which progresses during reperfusion, leads to detrimental effects within the myocardium causing ventricular arrhythmias, contractile dysfunction and cell death [188].

To interrupt the damaging process of ischemia and reperfusion, many studies have examined NHE inhibition and its ability to protect the myocardium from further damage [187, 188]. Initial studies used amiloride, which is an inhibitor that can suppress a number of NHE isoforms and other transport pathways. Amiloride demonstrated beneficial effects on recovery of myocardial function following ischemia and reperfusion; however it has a low specificity for the NHE. Additional concerns arose suggesting that amiloride was toxic and it was required during early ischemia to exert advantageous effects, otherwise it was ineffective [189-191]. These

findings lead to the development of a selective NHE inhibitor, cariporide (HOE694), which does not inhibit other transport pathways at concentrations that inhibit the NHE [192] and exerts a high level of specificity for the NHE1 isoform [193]. The antiarrhythmic potential effects of cariporide were compared with that of a calcium antagonist or beta-blocker, an angiotensin-converting enzyme (ACE) inhibitor and a class I antiarrhythmic agent. Of all these, cariporide demonstrated superior beneficial effects against ventricular premature beats, ventricular fibrillation and ventricular tachycardia. The beta-blocker was only more effective against ventricular fibrillation or tachycardia, while the class I agent was only effective against ventricular tachycardia. The calcium antagonist and ACE were ineffective against any of the ischemic arrythmias [192].

The effects of cariporide on intracellular ion concentrations support the theory that inhibition of NHE helps to lessen the disruption of sodium and calcium homeostasis during periods of ischemia [187, 194]. Selective NHE1 inhibition has been shown to reduce myocardial damage due to ischemia and reperfusion and could potentially reduce ischemia-related arrhythmias, contractile dysfunction and tissue necrosis [187, 192, 195], however best results using HOE694 still remain most effective when the drug is administered before or during early stages of ischemia [187, 196].

9.3. *Hypertension*

Increased NHE1 activity has been reported in hypertensive rats and in patients with essential hypertension. Spontaneously hypertensive rats (SHR) display an

elevated Na^+/H^+ exchange is platelets, lymphocytes, neurophils, erythrocytes, mesangial cells, kidney epithelial cells, isolated segments of arteries vascular smooth muscle cells (VSMC) and striated muscle cells [197]. Similarly 45% of patients with essential hypertension possessed increased Na^+/H^+ exchange in erythrocytes, platelets, lymphocytes and immortalized lymphoblasts [197]. In fact, a great portion of hypertension research suggests that numerous ion transporters display alterations in their activities including: Na^+-K^+-Cl^- cotransporters and amiloride-senstivite Na^+ channels in kidney function, the Na^+/K^+ pump and Na^+/Ca^{2+} exchanger in vascular smooth muscle function and Ca^{2+}-activated K^+ channels [197].

During further studies to elucidate the molecular mechanisms underlying the pathogenesis of hypertension, with respect to NHE1 surprising results surfaced, showing no mutations in the coding region of NHE1 cDNA obtained by reverse transcription of mRNA from VSMC of SHR [198]. Other findings demonstrated a 2.2-fold increase in the phosphorylation state of NHE1 in SHR myocytes, compared to normal myocytes, potentially leading to the increased NHE activity of these cells [199]. A more specific discovery demonstrated that a 90 kDa kinase that phosphorylates NHE1 ($p90^{RSK}$) is 1.8-fold higher in activity in SHR VSMC compared to normal rat VSMC [200]. Alterations associated with the cascade of $p90^{RSK}$ may be vital in determining additional information underlying the pathology of hypertension.

To test the hypothesis that increased Na^+/H^+ exchange causes hypertension Kuro-o M., *et al* produced transgenic mice overexpressing NHE1 and analyzed their blood pressure and their metabolism of Na^+ [201]. Surprisingly

immunohistochemical studies detected the transgene only in cell membranes of renal tubular cells and epithelial cells of the stomach, intestine and glomerulus. Compared to controls, the transgenic mice showed a significant decrease in urinary pH and excretion of water, Na^+, K^+ and Cl^-. Systolic blood pressure was only elevated in transgenic mice after 4-5 weeks of chronic salt loading, and then was normalized after 8 weeks of high salt diet [201]. The authors suggested that the overexpression of NHE1 in renal tubules was the cause of Na^+ retention and salt-sensitive blood pressure elevation; however, the reestablishment of normal blood pressure after eight weeks suggested in involvement of other compensatory mechanisms [201]. Although NHE1 activity is clearly involved in some aspects of this disease, these particular studies were not conclusive in the role of NHE1 in hypertension.

9.4. *Diabetes*

The 2003 Health Canada statistics show that over 2.25 million Canadians are estimated to have diabetes and about 1/3 of the adults are unaware of their condition (www.statscan). Diabetes mellitus is a significant metabolic disease, which is categorized into two forms, Type 1 and Type 2. Type 1 diabetes is an immunological disease resulting from an acute failure to produce insulin. Patients require life-long insulin treatment [202]. Type 2 diabetes is a complex metabolic disorder resulting from an initial decline of insulin responsiveness followed by loss of beta cell function and decreasing insulin secretion [202, 203]. Type 2 diabetes is associated with dietary factors and obesity.

Several groups have investigated the role of NHE in diabetes using different model systems including: blood-borne cells [204]; cultured vascular smooth muscle cells (VSMCs) [205]; and the streptozotocin-induced diabetic rats [206]. In the streptozotocin-induced diabetic rats activation of NHE in the vascular smooth muscle resulted in the development of vascular hypertrophy. The involvement of NHE was confirmed by the administration of cariporide to the rats, which prevented the development of vascular hypertrophy [206]. Studies on luminal membranes of the proximal tubule of diabetic rats, demonstrated that increased growth was due to an elevation of NHE activity [207]. In addition, subsequent to noticeable signs of vascular hypertrophy, an elevated NHE activity was observed in mesenteric arteries of diabetic rats within 1 week of onset of diabetes [208]. The level of NHE1 expression was also shown to be elevated in a diabetic state [205, 206]. Together, these groups have suggested that NHE activity may be an important early mechanism of response to diabetes.

9.5. *Cancer*

The second most common cause of death in Canada is cancer. According to the National Cancer Institute in Canada approximately 140,000 new cases of cancer and 67,000 deaths from cancer will occur in 2003. Currently the most frequently diagnosed cancers in women are breast, lung and colorectal cancers, while for men are prostate, lung and colorectal cancers. Men outnumber women for both cases and deaths, by 4% for incidence and 13% for mortality (www.cancer.ca).

Tumors originate from numerous genetic alterations leading to the loss of normal cellular growth control. A common phenotype to all tumor cells is cellular alkalinization, which is believed to be a consequence of NHE1 stimulation [209]. Early studies showed that cells deficient in the Na^+/H^+ exchanger do not induce tumor formation or show severe abnormalities in tumor growth when implanted in immuno-deprived mice [210]. To study the involvement of NHE in malignant transformations an experimental model was developed by infecting mouse fibroblasts (NIH3T3 cells) with a wild type E7 oncoprotein of the human papillomavirus type 16 (HPV16), which induces tumorigenic transformations in these cells. Control cells were infected with a HPV16 E7 mutant unable to induce transformations. Steady-state intracellular pH was elevated in the wild type protein, while the mutant protein did not induce alkalinization [209]. Treatment of the cells with an amiloride analog 5-(N,N-dimethyl) amiloride (DMA), an NHE1 inhibitor, suppressed the alkalinization induced by the wild type protein without decreasing E7 protein expression [209]. To determine if this alkalinization occurred in early stages of transformation a recombinant retrovirus was constructed. The retrovirus contained the HPV16 E7 gene, which was under the control of an inducible promoter, negatively regulated by tetracycline, meaning that recombinant HPV16 E7 could only be detected in the absence of tetracycline from the culture medium. NIH3T3 cells were infected with the recombinant retrovirus and E7-regulated transformations were induced 24 hours before measuring steady-state pH*i*. Intracellular pH in these cells was significantly elevated with E7-induced transformation. These effects were abolished in the presence of two NHE1 inhibitors, DMA or HOE694 [209], the latter being a highly

specific NHE1 inhibitor. Further experiments supported these results by demonstrating that the rate of proton extrusion was significantly quicker in cells with E7-induced transformations, an effect not due to a change in NHE1 expression as verified with Western blotting analysis [209].

Recently, a drug against a broad spectrum of cancers, has been conclusively linked to NHE1 [211]. In human breast cancer cells (MDA-MB-435) paclitaxel had a dose-dependent inhibitory effect on NHE activity; however, did not change NHE1 protein expression [211]. Previous studies have shown that paclitaxel alters activity and the phosphorylation state of MAP kinases ERK, JNK and SAPK [212-214]. Paclitaxel-induced apoptosis studied in three different breast cancer cell lines (MDA-MB-435) caused inhibition of PKA or p38, which in turn reversed the paclitaxel-dependent inhibition of NHE activity. In contrast, stimulation of PKA or p38 caused an increase in the paclitaxel inhibitory effect on NHE activity [211]. Paclitaxel-dependent apoptosis was also investigated in the presence of NHE1 inhibitor, DMA. Incubation of breast cancer cells with DMA or paclitaxel alone caused an insignificant increase in apoptosis; however, when combined (0.5-6 nM paclitaxel + 2 μM DMA) a dramatic increase in apoptosis was observed [211]. These studies have defined the pivotal role of NHE1 in breast cancer.

10. Thesis Objectives

The first objective of my thesis was to study the *in vitro* dephosphorylation of the C-terminus of NHE1 by PP1, PP2A and PP2B. This system investigated the following questions:

1) Does PP1, PP2A or PP2B dephosphorylate the Na^+/H^+ exchanger *in vitro*?
1) Do PP1 and PP2B physically interact with the cytoplasmic tail of NHE1?

The second goal of my thesis was to elucidate the role of protein phosphatases in regulation of NHE1 *in vivo* in intact cells. This involved the use of the phosphatase inhibitor okadaic acid and the production of stable cell lines expressing protein phosphatase-1 and Inhibitor-2. The second objective investigated the following questions:

1) Is NHE1 activity regulated by phosphatases *in vivo*?
1) Does PP1 affect hormonal stimulation of NHE1 *in vivo*?
3) Does PP1 inhibition affect the activity of NHE1 *in vivo?*

Chapter II

B: Materials

C: Methods

B. Materials

The plasmids containing cDNA of the phosphatase PP1 (pCW-HPP1γ) and Inhibitor-2 (pET3a-Inhibitor2) were supplied by Dr. Charles Holmes (University of Alberta, Edmonton, Alberta). Dr. Eric Olson (The University of Texas Southwestern Medical Center, Dallas, Texas) provided the plasmid (pcDL-SRα296) used as a source of Calcineurin. The plasmid (pGEX5X2-spino 100-767) provided by Dr. Sharon Milgram (University of North Carolina, Durham, North Carolina) was used as a source of spinophilin. The Gateway Cloning and expression vectors (pDONR201, pDEST40) were purchased from Gibco BRL. Restriction enzymes were obtained from Gibco BRL or New England Biolabs. MWG Biotech, Inc. and Qiagen generated oligonucleotides for DNA sequencing and PCR primers. PWO polymerase was purchased form Boehringer Mannheim and Topoisomerase I was purchased from Invitrogen Life Technologies. All other PCR reagents were obtained from Gibco BRL, including dNTPs, and PCR buffer. Other commercial kits were also used: the Bio-Rad DC Protein Assay kit for protein quantification and the QiaQuick PCR Purification kit for purification of PCR products.

AP1 cells were a generous gift from Sergio Grinstein (University of Toronto, Toronto, Ontario). CHO cells were purchased from American Type Culture Collection. AP1a221 cells are AP1 cells overexpressing the human sequence of NHE1, which were created in Dr. Larry Fliegel's laboratory (University of Alberta, Edmonton, Alberta)[215]. AP1a221 cells will be referred to as AP1-NHE1 cells in this report. The University of Alberta Health Sciences Laboratory Animal Services provided 5-6 day old, Harlan Sprague-Dawley rats used for generating neonatal

primary culture cardiac myocytes. The cell culture media αMEM, was purchased from Sigma Aldrich, while several media supplements such as HEPES, L-glutamine, gentamicin, fetal bovine serum, antibiotic penicillin/streptamycin and the selection reagent geneticin were purchased from Gibco BRL. The transfection reagent Lipofectamine 2000 was purchased from Invitrogen Life Technologies, Inc. and Opti-MEM transfection media was purchased from Gibco BRL. Cross-linking reagents used to treat cells prior to a number of immunoprecipitation experiments, disuccinimidyl suberate (DSS) and dithiobis(succinimidylpropionate) (DSP) were purchased from Pierce Biotechnology. Micro glass coverslips (11x22 mm), used for cell culture and fluorometric experiments were purchased from Thomas Scientific.

Some antibodies for immunoblotting were purchased from Santa Cruz Biotechnology, Inc. (anti-PP1 polyclonal antibody, anti-PP2B-A polyclonal antibody), Invitrogen Life Technologies (anti-V5 epitope antibody), and Chemicon International, Inc. (anti-NHE1 monoclonal antibody). The anti-PP1 monoclonal and anti-PP2A polyclonal antibodies were a kind gift from Dr. Mary Pato (University of Saskatchewan, Saskatoon, Saskatchewan) and the anti-βgal-NHE1 polyclonal antibody was developed in the laboratory of Dr. Larry Fliegel (University of Alberta, Edmonton, Alberta) [216].

For fluorometric experiments such as measuring intracellular pH, the fluorescent probe 2'-7'-bis(2-carboxyethyl)-5(6)-carboxyfluorescein acetoxy methyl ester (BCECF-AM), was purchased from Molecular Probes, Sigma and Alexis Corporation. Thrombin (T-4648) and nigericin were purchased from Sigma.

C. Methods

1. Expression and Purification of Proteins

1.1. *The GST-Na^+/H^+ Exchanger Fusion Protein*

The carboxyl-terminal 178-amino acid sequence of the rabbit cardiac Na^+/H^+ exchanger was expressed as described previously [70, 73] as a fusion protein with GST (and named PCRA or PCR178) using the plasmid pGEX-3X [70]. The *Escherichia coli* TOPP 2 strain was induced with 1 mM isopropylthio-D-galactoside. PCRA was purified via glutathione-sepharose 4B affinity chromatography as described earlier [70, 73].

1.2. *The GST-Spinophilin Fusion Protein*

The cDNA fragment encoding spinophilin (amino acids 100-767) was excised from pPC86.clone7 as a *Sal*I-*Not*I fragment and subcloned into pGEX5X2 (Amersham Pharmacia Biotech) [130]. The plasmid, pGEX5X2.spinophilin (100-767), was transfected into the *E. coli* TOPP 2 strain allowing expression of spinophilin as a glutathione *S*-transferase (GST) fusion protein. This protein was subsequently purified using glutathione-sepharose 4B affinity chromatography [70].

1.3. *Protein Phosphatase-1 (PP1γ)*

The catalytic subunit of recombinant PP1γ was subcloned into the pCW vector and expressed in the *E. coli* DH5α strain, in the laboratory of Dr. Charles Holmes (University of Alberta, Edmonton, Alberta). This allowed expression of the human

PP1 protein in *E.coli*, which was subsequently purified using heparin affinity, Mono Q and Superdex-75 gel filtration chromatography [135, 217].

1.4. *The Catalytic A Subunit of PP2B*

The catalytic A subunit of rat calcineurin was subcloned into the pET-21a(+) vector and expressed in the *E.coli* HMS174(DE3) strain, in the laboratory of Dr. Charles Holmes. The for purifying this protein was modified from that previously described [218]. The modification involved the addition of a Toyopearl HW65 column used after calmodulin-Sepharose affinity and before using gel filtration chromatography to purify the protein (unpublished).

1.5. *The Catalytic A Subunit of PP2A*

The catalytic subunit of PP2A was purified from bovine cardiac muscle as previously described [219]. PP2Ac was purified using the DEAE sepharose column, the Poly (L-lysine) sepharose affinity column, the Superdex 75 column and the Mono Q anion exchange column [217, 219].

1.6. *The Inhibitor-2 Protein*

The cDNA of human Inhibitor-2 (I2) was subcloned into the pET3a vector and expressed in the *E. coli* BL21(DE3) strain, in the laboratory of Dr. Charles Holmes. This protein was purified using the Q-sepharose and Mono-Q columns, as described previously [220].

2. *In Vitro* Phosphorylation and Dephosphorylation of the Regulatory C-terminus of the Na^+/H^+ Exchanger

2.1 *In Vitro Phosphorylation of the Na^+/H^+ Exchanger C-terminal Fusion Protein (PCRA)*

The C-terminal Na^+/H^+ exchanger fusion protein (PCRA) was phosphorylated *in vitro* to subsequently determine which purified protein phosphatase had the ability to remove phosphates from the protein. Phosphorylation of PCRA was performed as previously described [73] and it is summarized in Fig. 2. The standard reaction conditions for phosphorylation of heart extract fractions contained 10 µg of PCRA, 8 µg of heart extract, 12.5 mM MOPS at pH 7.0, 8.5 mM magnesium chloride, 0.5 mM EGTA, 500 µM ATP, and 1 µl of 10 µCi/µl [γ-^{32}P]ATP (3000 Ci/mmol). Dithiothreitol (2 mM) was freshly prepared for each reaction. The protein phosphatase inhibitors okadaic acid (6 µM) and sodium fluoride (0.24 mM) were added to halt endogenous phosphatase activity towards PCRA. The total volume of each reaction was 25 µl. In control heart extracts were omitted. Samples were incubated at 30°C for 90 minutes and the reaction was terminated by the addition of SDS loading buffer [73]. The proteins were separated on 10% SDS gels, dried, and exposed for autoradiography. When phosphorylated, a radio-labeled phosphate-PCRA protein band of approximately 44 kDa [70] was visible, while the control, unphosphorylated protein was not visible on autoradiograms.

2.1. *In Vitro Dephosphorylation of the Na^+/H^+ Exchanger C-terminal Fusion Protein (PCRA)*

Purified protein phosphatase-1 (PP1), calcineurin A (PP2B-A), protein phosphatase 2A (PP2A), as well as crude heart cell extracts were used to dephosphorylate the Na^+/H^+ exchanger C-terminus. To determine the action of individual phosphatases or heart cell extracts on the PCRA fusion protein, PCRA was phosphorylated as previously described [73]; however, termination of the reaction by addition of SDS loading buffer was delayed until the dephosphorylation reaction was completed. This procedure is summarized in Fig. 2. For each dephosphorylation reaction a 12.5 µl aliquot of the cocktail containing phosphorylated fusion protein was mixed with glutathione sepharose beads and shaken lightly for 15 minutes at room temperature. Once the fusion protein was bound to the glutathione beads, the supernatant was removed, the beads were washed 2-3 times with 1x phosphate buffer saline solution. The phosphorylated PCRA protein bound to the beads was made to a volume of 25 µl with standard dephosphorylation cocktail. The dephosphorylation cocktail varied with the phosphatases used and a source of specific ions was required for optimal activity of each individual phosphatase.

The standard dephosphorylation cocktail contained 12.5 mM MOPS at pH 7.0, freshly prepared 2 mM dithiothreitol, and 8.5 mM magnesium chloride. EGTA is a chelating reagent and was for that reason eliminated from these reactions to allow calcium to remain in solution. This allowed divalent cations to be available to optimize dephosphorylation reaction conditions, which is especially important in the presence of calcineurin, a calcium dependent phosphatase. In addition to these

components, either 10 μg of purified phosphatase or 8.0 μg of crude heart cell extracts was added to each reaction. When PP1 was the phosphatase used in the reaction, 5 mM manganese chloride was added as a source of Mn^{2+} ions essential for recombinant PP1 activity [221]. In other experiments the degree of dephosphorylation of PCRA by PP1 was tested in the presence of spinophilin. Spinophilin is one of many regulatory subunits of PP1 which can target PP1 to the plasma membrane and cytoskeleton [100, 130]. For these experiments a 5 μg supplement of purified spinophilin was added to the standard PP1 dephosphorylation reaction. The requirement of essential ions for optimal function of PP2A is uncertain, and as a result dephosphorylation experiments involving PP2A were performed in the presence and absence of 5 mM Mn^{2+}. Finally, to ensure that calcineurin A was active, 10 mM calcium chloride was added as a source of Ca^{2+} ions [151] and EGTA was omitted. The dephosphorylating ability of calcineurin A was tested in the presence or absence of 5 μg purified calmodulin protein, which binds to the regulatory region of calcineurin A and activates calcineurin [151]. The total volume of each reaction was 25 μl. Control dephosphorylation samples had no added phosphatases.

Samples were incubated at room temperature lightly shaking for 90 minutes. The reaction was terminated by the addition of SDS loading buffer. Proteins were separated on a 10% SDS-PAGE gel, dried, and exposed for autoradiography. Image Gauge (Bio-Rad) software was used to quantify protein bands of both Coommasie blue stained samples initially separated by SDS-PAGE, as well as the appropriate protein bands identified by autoradiography from the same SDS-PAGE gel. The

stoichiometry of dephosphorylation was determined by calculating the ratio of [^{32}P] incorporated into the protein bands/total protein in the bands.

Fig. 2. Phosphorylation and Dephosphorylation of NHE1
A summary of the method used to phosphorylate and dephosphorylate the C-terminus of NHE1. The NHE1 protein used was a GST-fusion protein composed of the distal 178-amino acid sequence of the rabbit cardiac Na^+/H^+ exchanger (GST-NHE1, also known as PCRA). GST beads, glutathione sepharose beads; P, phosphorylation. This procedure is detailed in the methods sections 2.1-2.2.

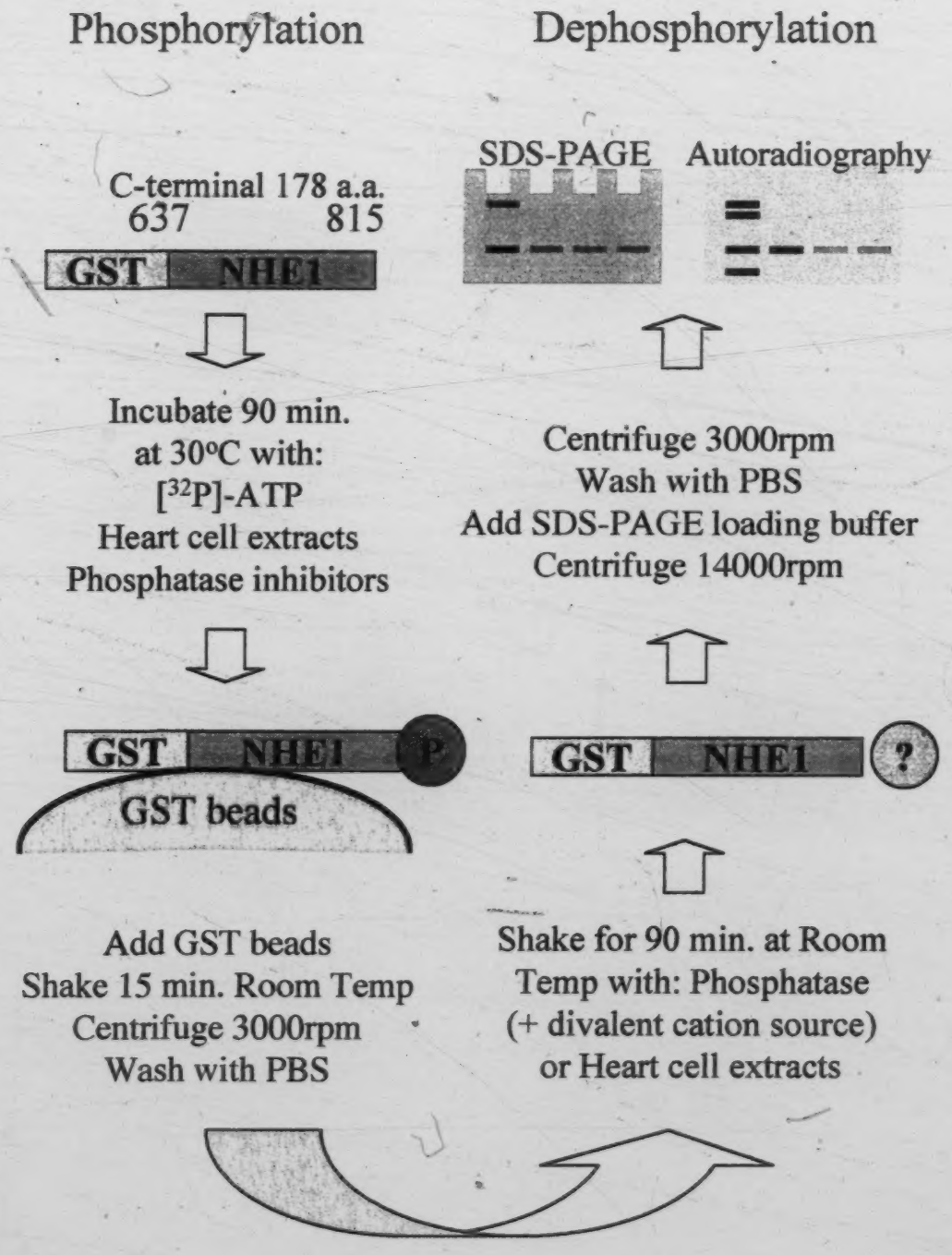
Phosphorylation
Dephosphorylation
SDS-PAGE
Autoradiography
C-terminal 178 a.a.
637
815
GST
NHE1
Incubate 90 min.
at 30°C with:
[32P]-ATP
Heart cell extracts
Phosphatase inhibitors
Centrifuge 3000rpm
Wash with PBS
Add SDS-PAGE loading buffer
Centrifuge 14000rpm
GST
NHE1
P
GST beads
GST
NHE1
?
Add GST beads
Shake 15 min. Room Temp
Centrifuge 3000rpm
Wash with PBS
Shake for 90 min. at Room
Temp with: Phosphatase
(+ divalent cation source)
or Heart cell extracts

3. Preparation of Heart Cell Extracts

Rat heart cell extracts that were employed in *in vitro* dephosphorylation studies were obtained as previously described [73]. Animals were sacrificed by using carbon dioxide, as accepted by the University of Alberta Animal Welfare Committee. As summarized in Fig. 3, hearts were removed from two untreated, adult, Harlan Sprague-Dawley rats and placed in cold saline solution. The atria, blood vessels and connective tissue were separated from the ventricles using a scalpel blade and discarded. The remaining ventricles were weighed prior to being cut into fine pieces with a scalpel blade and transferred to a falcon tube. The heart tissue was homogenized at a high setting with a Polytron homogenizer two times for 30 seconds in 2.5 %(v/w) of extraction buffer. The extraction buffer contained: 10 mM sodium phosphate; 60 mM glycerophosphate; 1 mM dithiothreitol; 15 mM EGTA; 15 mM magnesium chloride pH 7.5; 10 mM phenylmethylsulfonyl fluoride in methanol; 1 mM benzamidine hydrochloride in ethanol, and a protease inhibitor mixture [73, 222]. The homogenized heart tissue was placed on ice for 1 minute and sonicated for 30 seconds at 4°C. The sonicated tissue was transferred to a cold 30 ml oakridge tube and centrifuged at 6,000 rpm at 4°C for 1 hour. The supernatant was transferred to a new tube and centrifuged a second time at 10,000 rpm at 4°C for 1 hour. The crude heart cell extracts were aliquoted into chilled eppendorf tubes and stored at –80°C until further use.

Fig. 3. Preparation of Heart Cell Extracts
A summary of the method used to prepare heart cell extracts from adult, Harlan Sprague-Dawley rats. This procedure is detailed in the methods section 3.

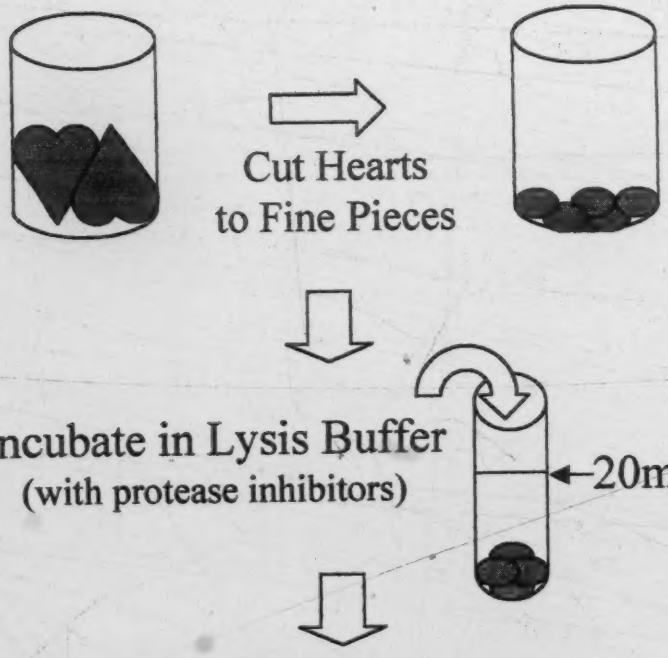
Cut Hearts
to Fine Pieces
Incubate in Lysis Buffer
(with protease inhibitors)
20ml
Homogenize 30 sec.
Sonicate 30 sec.
Centrifuge
6,000rpm
1hr
+
10,000rpm
1hr
Aliquot Supernatant
Store at -80°C

4. *In vitro* Assay of Physical Interactions of Phosphatases with NHE1

4.1. *GST Pull-Down Assay*

GST pull-down experiments were performed using purified PP1 or PP2B and PCRA to examine physical interactions between protein phosphatases PP1, PP2B and the cytoplasmic tail of the Na^+/H^+ exchanger. Each GST pull-down experiment contained: 20 μg of PCRA (GST-fusion protein), 10 μg of phosphatase either PP1 or PP2B, and 0.1% BSA to stabilize the enzyme activity. PCRA was replaced with an equal concentration of purified GST in control experiments. To ensure optimal phosphatase activity, the experiments containing PP1 were supplemented with 1 mM $MnCl_2$ as a source of Mn^{2+} ions, while assays containing PP2B were supplemented with 5 mM $CaCl_2$, a source of Ca^{2+} ions. In addition, experiments investigating PP2B binding were performed in the presence of 5 μg and 10 μg of purified CaM. Protein concentrations of purified PCRA, PP1, PP2B, CaM and GST were carefully determined using the Bio-Rad DC Protein Assay kit to ensure a controlled amount of each protein was used in various reaction combinations.

Fifteen microliters of glutathione-sepharose beads was added to each reaction to immobilize the PCRA protein. The reactions were incubated at 37°C for 90 minutes with light shaking. Next, proteins were solubilized from the glutathione beads with 1x SDS PAGE loading buffer and centrifuged at 14000 rpm for 2 minutes at room temperature. Proteins in the final supernatant were separated on a 10% SDS gel, and transferred to a nitrocellulose membrane for 1.5 hours at 200 mV. The membrane was subsequently incubated overnight at 4°C in 10% milk/TBS.

4.2. *Immunoblot Analysis of NHE1 with anti-Phosphatase Antibodies*

Three different primary antibodies were used for detection of PP1 or PP2B interactions with the NHE1 C-terminus. PP1(FL-18):sc-443 (Santa Cruz Biotech Inc.) is an affinity-purified rabbit polyclonal antibody raised against a polyhistidine fusion protein with sequences corresponding to the full length catalytic subunit of human PP1. This antibody also reacts with the catalytic subunits of PP2A, PP2B and PPX of mouse, rat and human origin and was termed the general phosphatase antibody. Other antibodies used were more specific in detecting PP1 and PP2B. The first was an anti-PP1α monoclonal antibody raised against the catalytic subunit of PP1, a generous gift from Dr. Mary Pato (University of Saskatchewan, Saskatoon, Saskatchewan). The second, PP2B-A(H-209):sc-9070 (Santa Cruz Biotech Inc.) was a rabbit polyclonal antibody raised against a recombinant protein corresponding to amino acids that mapped the carboxy terminus of human PP2B catalytic subunit Aα. This antibody also reacts with all PP2B-A isoforms of mouse, rat and human origin.

For the immunological reaction, the membrane was incubated with an appropriate phosphatase antibody in 1% milk/TBS (1/2000 dilution) for two hours at room temperature. The membrane was washed 4 times for 15 minutes with 1xTBS followed by incubation with a secondary antibody in 1% milk/TBS (1/2000 dilution) for 1.5 hours at room temperature. The secondary antibodies (BioCan) used were goat anti-mouse antibody if the primary antibody was a mouse monoclonal antibody, or goat anti-rabbit antibody if the primary antibody was a rabbit polyclonal. Following incubation with the secondary antibody, the membrane was washed with

1xTBS four times for 15 minutes. Finally, the Amersham Enhanced Chemiluminescence detection system was used to visualize immunoreactivity.

5. Immunoprecipitation of NHE1 from Cells Treated or Untreated with Cross-linking Reagents

5.1. *Preparation of Cells for Immunoprecipitation of NHE1*

The two cell lines employed in NHE1 immunoprecipitation studies were PS127A, a Chinese hamster lung fibroblast line, and AP1-NHE1, a Chinese hamster ovary cell line. Although both of these cell lines overexpress human NHE1, only the AP1-NHE1 cells express NHE1 that contains a hemagglutinin (HA) epitope tag [215]. Unlike AP1-NHE1 cells the PS127A cell line requires an acid selection treatment to ensure overexpression of NHE1. Acid selection was performed on cells grown to 60% confluency. Cells were washed with 1xPBS before being immersed in 10 ml of isotonic NH_4Cl medium (recipe described in Table 7) and incubated for 30 minutes at 37°C. A nominally CO_2-free atmosphere was used to ensure inactivation of the anion exchanger in cells. Following the incubation, cells were promptly washed twice with 10 ml of isotonic Na^+-saline solution to remove extracellular NH_4^+. The cells were incubated in Na^+-saline medium for one hour at 37°C again in a CO_2-free atmosphere, after which the Na^+-saline medium was replaced with normal culture medium. This procedure was repeated 3-5 times over a 1-2 week period.

Cell lysates from PS127A and AP1-NHE1 cells were prepared by incubating cells in 300 µl RIPA lysis buffer lacking detergents (recipe detailed in Table 9) on dry ice for 1 minute before allowing them to thaw on ice. Once the cells thawed, they

were scraped with a cell scraper (Fisher) for two minutes and transferred to an eppendorff tube. The cells were centrifuged at 14000 rpm for 15 minutes at 4°C. The supernatant was discarded while the pellet, containing the Na^+/H^+ exchanger, was resuspended in 1 ml of RIPA lysis buffer containing detergent and sonicated for 20 seconds. Centrifugation was repeated at 14000 rpm for 1 hour at 4°C [47]. Finally, approximately 1 ml of the supernatant was collected and frozen in liquid nitrogen for later use in immunoprecipitation studies.

5.2. *Treatment of Cells with Cross-linking Reagents*

Cross-linking prior to immunoprecipitation of NHE1 from cells was an alternative method performed to determine whether PP1 or PP2B could physically interact with NHE1. The AP1-NHE1 cell line was exclusively utilized in cross-linking studies. The cells were treated with N-hydroxysuccinimide-ester cross-linkers DSS (disuccinimidyl suberate) or DSP [dithiobis(succinimidylopropionate)] (Pierce) to determine if PP1 or PP2B could be linked to NHE1 by these covalent bond-forming reagents. The preparation of the cross-linking reagents and subsequent treatment of cells was performed according to the manufacturers instructions (Pierce). Both water insoluble cross-linkers were dissolved in dimethyl sulfoxide (DMSO) immediately before the experiment because their hydrolysis occurs within hours causing loss of activity. Cells growing in T-75 flasks were washed with 1xPBS (Gibco BRL) twice and incubated with 2 mM DSS or DSP for 30 minutes at room temperature. The reaction was quenched with 20 mM Tris-HCl, pH 7.5 for 15

minutes. Cell lysates of AP1-NHE1 treated with cross-linking reagents were made as detailed above.

5.3. *Immunoprecipitation of NHE1 from Intact Cells*

Regardless of whether cross-linking reagents were employed, cell lysates utilized in immunoprecipitation of NHE1 were carefully thawed on ice and 100 µl of lysate was retained for a positive control. To minimize non-specific binding, 20 µl of Protein A sepharose beads (Sigma) and 50 µl of BSA (Sigma) were added to 1 ml of cell lysate for 30 min while slowly rotating. The sample was centrifuged at 4°C and 7000 rpm for 5 minutes to remove the beads. The supernatant was transferred to a tube containing 30 µl of rabbit polyclonal anti-NHE1 antibody made against the β-Gal-NHE [216], and was again gently rotated for 3 hours. Meanwhile, in a different eppendorf tube, 150 µl of Protein A sepharose beads were pretreated with 1 ml of RIPA lysis buffer containing detergents, and slowly rotated at 4°C for 1 hour. The pretreated beads were centrifuged, combined with the lysate-antibody solution and incubated overnight continuously rocking at 4°C. The following day the beads were washed 3 times with RIPA lysis buffer containing detergents. Next, the beads were resuspended in 40 µl of 4x SDS-PAGE loading buffer and initially incubated at 37°C for 15 min followed by a second 15 minute incubation at 60°C. A 10 µl aliquot of the final sample was used to separate the proteins on a 10% SDS-PAGE gel, and subsequently transferred to a nitrocellulose membrane for 1.5 hours at 200 mV. In preparation for the immunological reaction, the nitrocellulose membrane was incubated overnight at 4°C in 10% milk/TBS.

5.4 *Immunoblot Analysis of NHE1 Following Immunoprecipitation from Untreated Cells*

To examine successful immunoprecipitation of NHE1 from PS127A cells the membrane initially blocked overnight in 10% milk/TBS was washed with 1xTBS three times for 5 minutes and incubated with a mouse monoclonal primary antibody against NHE1 (Chemicon) in 1xTBS (1/2000 dilution) overnight at 4°C. The next day the membrane was washed three times with 1xTBS followed by incubation with a goat anti- mouse antibody (BioCan) in 1% milk/TBS (1/2000 dilution) for 1 hour at room temperature. Finally, the membrane was washed with 1xTBS for 1 hour prior to using the Amersham Enhanced Chemiluminescence reaction to visualize immunoreactivity.

To ascertain if successful immunoprecipitation of NHE1 occurred from AP1-NHE1 cells, the membrane was incubated with a mouse monoclonal primary antibody against the HA epitope tag for 2.0 hours at room temperature. The membrane was washed 4 times for 15 minutes with 1xTBS followed by incubation with a goat anti-mouse antibody for 1.5 hours at room temperature, as indicated in Table 5. After incubation with the secondary antibody, the membrane was washed in 1xTBS four times for 15 minutes, and the Amersham Enhanced Chemiluminescence reaction was again utilized to visualize immunoreactivity.

5.5 *Immunoblot Analysis of Immunoprecipitated NHE1 with anti-Phosphatase Antibodies*

To determine whether PP1 or PP2B were naturally bound to NHE1 in either cell line or successfully cross-linked with NHE1 in the AP1-NHE1 cell line, the nitrocellulose membrane, previously probed for successful immunoprecipitation of NHE1, was stripped by incubation in a 0.2M glycine-HCl solution pH 2.8 for 30 minutes at room temperature. Next, the membrane was washed for 15 minutes with distilled water and then with 1xTBS while gently rocking at room temperature. Finally, the membrane was re-blocked with 10% milk/TBS overnight continuously rocking at 4°C. The following day the membrane was incubated with a primary antibody to determine if the phosphatase of interest was bound or cross-linked to NHE1. The primary antibodies included a polyclonal anti-PP1α, a monoclonal anti-PP1, or a polyclonal anti-calcineurin A. The antibodies and nitrocellulose membrane treatment were previously described in the methods section 4.2.

6. Assay of NHE1 Activity in Rat Heart Cells Following Phosphatase Inhibition with Okadaic Acid

6.1. *Preparation of Rat Neonatal Myocyte Primary Cultures*

Rat neonatal myocyte primary cultures were prepared as previously described [73]. Following euthanasia by decapitation, as accepted by the University of Alberta Animal Welfare Committee, hearts were removed from 5-6 day old rats, and placed in 10 ml of Solution I (recipes for Solutions I-V are given in Table 6). The atria,

blood vessels and connective tissue were separated from the ventricles using a scalpel blade and discarded. The ventricles were transferred to a new dish and were minced with a scalpel blade while remaining moistened in Solution I. Next, the tissue was transferred to a flask containing 20 ml of Solution II and incubated at 37°C continuously stirring for 20 minutes. Once the tissue fragments settled to the bottom of the flask, the liquid portion was removed and placed in a tube containing 20 ml of Solution III. Fifteen milliliters of fresh Solution II was added to the remaining tissue in the flask for a second 20 minute incubation at 37°C. This was followed by removal of the liquid from the flask and neutralizing it with and equal volume of Solution III in a new tube. This procedure was repeated two more times.

Isolated myocytes in Solution II and Solution III were filtered using a nylon 70 μm Falcon cell strainer (Becton Dickinson Labware #0312980). The filtrate was centrifuged at 1200 rpm in a clinical centrifuge for 10 minutes and the supernatant was discarded. The remaining pellet was resuspended in 15 ml of Solution IV supplemented with 15% fetal bovine serum. Next, the myocytes were placed in a T-75 Corning flask and incubated at 37°C for 30 minutes. During the incubation fibroblasts, endothelial cells and smooth muscle cells quickly attach to the flask while myocytes remain in suspension. The suspended myocytes were removed and aliquoted onto 11x22 mm glass coverslips, placed in 35 mm dishes containing 2 ml of Solution V. The following day the myocytes were extensively washed with PBS ABC solution after which they continued to be cultured in fresh Solution V for 3-4 days.

6.2 *Measuring Activity of NHE in Primary Myocyte Cultures Treated with Phosphatase Inhibitor Okadaic Acid*

Myocytes grown on glass coverslips were serum starved in Solution IV overnight prior to physiological experiments. The acetoxy methyl ester of 2'-7'-bis(2-carboxyethyl)-5(6)-carboxyfluorescein (BCECF-AM), a widely used, membrane-permeant, fluorescent indicator was used to measure pH*i* as described earlier [66, 70, 73]. Measurements were performed on a Shimadzu RF5000 using excitation wavelengths of 452 and 503 nm and an emission wavelength of 524 nm. These wavelengths were chosen because they coincide with excitation ratio of BCECF-AM [73] that are pH independent and dependent. The ratio of emissions at 524 nm gives a measurement of pH*i* that is independent of dye concentrations [19].

Once myocytes were 90% confluent each glass coverslip was placed in Na^+-containing buffer (recipes for all pH measurement buffers are detailed in Table 8) immediately prior to the addition of 0.7-1.0 µl of BCECF-AM. The fluorescent dye was monitored within the myocytes until at a sufficient level to continue further pH measurements. BCECF-AM loading was kept constant for each coverslip. Intracellular pH measurements began in Na^+-containing buffer until a steady pH*i* level was recorded, approximately 2 minutes. Next, the myocytes were acid loaded with an ammonium chloride prepulse (40mM for 3 minutes), followed by a transfer into Na^+-free buffer for less than 30 seconds. The myocytes were again transferred into fresh Na^+-containing buffer, pH 7.3 with 8 µM okadaic acid and monitored until recovery to a stable resting pH*i* was observed. Data from the first 20 seconds of recovery was used to determine the rate of recovery (ΔpH/min) of the myocytes.

Control experiments used an equal volume of dimethyl sulfoxide (DMSO) was added, the reagent used to dissolve the okadaic acid.

To measure steady state pH the myocytes were not acid loaded. Once loaded with BCECF-AM, the coverslip was placed in Na^+-containing buffer for 1-2 minutes, then 8 μM okadaic acid was introduced into the buffer and activity was monitored for 10 minutes. In control experiments, okadaic acid was substituted with DMSO.

7. Protein Phosphatase 1 and Protein Inhibitor-2 Expression in Mammalian Cells

7.1 Generating attB-PCR Products for Recombination into Gateway Technology-Adapted Vectors

Polymerase chain reaction (PCR) was used to amplify *att*B-PCR products for PP1, PP2B or Inhibitor-2. These products were designed for transfer of the genes between pDONR201 and pDEST40 vectors in the Gateway Cloning System (Invitrogen Life Technologies). Forward and reverse primers (Table 4) were created to produce PP1, PP2B or Inhibitor-2 genes all flanked by *att*B recombination sequences (Invitrogen Life Technologies). The forward primers also contained a repetitive Shine-Dalgarno sequence and a Kozak consensus sequence, to provide optimal conditions for translation of the gene. To allow for future use of the V5-epitope and Hisidine (His) tags in the analysis of protein expression, the reverse primers were designed without a stop codon, which was found in the vector after the V5 epitope.

Immediately before combining PCR reaction components the template DNA was denatured for 10 min at 65°C. The 50 µl PCR reactions were prepared on ice and contained: 200 µM deoxynucleoside triphosphates (dNTPs), 7.5 µl of 10 µM downstream primer, 7.5 µl of 10 µM of upstream primer, 5 µl of template DNA (0.1-0.75 µg final DNA concentration), 19.5 µl of sterile dH_2O, 5 µl of 10x PCR buffer with 2.0 mM $MgSO_4$, providing optimal conditions for PWO polymerase activity. PWO DNA polymerase 0.5 µl was the last component added to the reactions to avoid degradation of template and primer DNA.

The PCR products were obtained using the following step-down PCR protocol [223]. One cycle at 94°C for 10' was required to denature proteinase activity in the crude DNA preparations prior to adding PWO polymerase.

1. Three cycles at 94°C for 1'; 69°C for 2' and 72°C for 1.5'
2. Three cycles at 94°C for 1'; 66°C for 2' and 72°C for 1.5'
3. Three cycles at 94°C for 1'; 63°C for 2' and 72°C for 1.5'
4. Three cycles at 94°C for 1'; 60°C for 2' and 72°C for 1.5'
5. Three cycles at 94°C for 1'; 57°C for 2' and 72°C for 1.5'
6. Three cycles at 94°C for 1'; 55°C for 2' and 72°C for 1.5'
7. Ten cycles at 94°C for 1'; 55°C for 2' and 72°C for 1.5'
8. One cycle at 72°C for 7'

A 5 µl sample of each PCR product was combined with 6x loading dye, and analyzed on a 0.8% agarose gel under ultraviolet light. The specific *att*B-PCR products were identified according to size, approximately 1045 base pairs for *att*B-PP1, 1287 base pairs for *att*B-PP2B and 691 base pairs for *att*B-Inhibitor-2.

7.2. *Obtaining Concentrated DNA*

To achieve a higher percentage of positive clones following transformation of DH5α bacterial cells, PCR products were sterilized using the PEG/$MgCl_2$ procedure, according to the Gateway Cloning Technology instructions. In microfuge tubes the PCR products were diluted 4-fold with TE buffer (10 mM Tris-HCl at pH 7.5, and 1 mM EDTA). The 30% PEG/$MgCl_2$ solution, provided in the Gateway Cloning kit, was added to the PCR dilution at one half the volume of the PCR dilution. The final concentration of the PEG/$MgCl_2$ solution was 10% PEG and 10 mM $MgCl_2$. The mixture was mixed thoroughly with a vortex and centrifuged for 15 at 14000 rpm. The supernatant was carefully removed and a nearly translucent pellet was resuspended in TE buffer to >10 ng/µl. The sterilized DNA was analyzed on an 0.8% agarose gel under ultraviolet light. Ultimately, some DNA was lost during the purification and the concentration of DNA was determined using a spectrophotometer and measuring absorbance at 260 nm.

7.3. *Creating Entry and Expression Clones*

Using the *att*B-PCR products, three plasmids were constructed to generate mammalian cells that overexpressed either human PP1 (Fig. 4b pDEST40-PP1), a constitutively active form of Calcineurin (Fig. 4c pDEST40-PP2B) or Inhibitor-2 (Fig. 4d pDEST40-I2). The Gateway Cloning Technology kit was used to generate the constructs for protein expression. The donor vector (Fig.4a pDONR201) was used to make entry clones. The inserts were transferred into the destination vector

(pDEST40) creating the new expression clones. These were ultimately employed in the transfection of mammalian cells. Other components included in the kit were reaction buffers, Proteinase K, a broad-spectrum serine protease, and Clonase Enzyme mixtures. The BP and LR Clonase Enzyme mixtures were used to transfer the PCR product into pDONR201 and pDEST40, respectively, according to the Gateway Technology manual. The BP and LR Clonase Enzyme mixtures contained the protein integrase (Int), encoded by the lambda (λ) genome and the integration host factor (IHF), an *E.coli*-encoded protein. The BP reaction mediated the recombination of *att*B and *att*P sites creating an entry clone. The LR Clonase solution contained an additional λ recombination protein, excisionase (Xis), which together these proteins mediated the transfer of the gene into pDEST40, creating a new expression clone (Invitrogen Life Technologies).

The 20 µl BP reaction prepared on ice contained: 4 µl of BP reaction buffer, 5 µl of *att*B-PCR DNA (≥10 ng/µl), 150 ng/µl pDONR201, 5 µl of TE buffer and the final component added was 4 µl of the BP Clonase Enzyme mixture. The reaction was mixed by briefly vortexing twice and incubated at 25°C for 1 hour. Two µl of Proteinase K solution was added to the reaction and incubated for 10 min at 37°C to terminate the BP reaction. One µl of the BP reaction was transformed into DH5α competent cells by electroporation. Cells were then cultured in S.O.C. medium for 1 hour and selected by growing on LB plates containing 50 µg/ml kanamycin, since the pDONR201 vector contained a kanamycin (Kn) resistance gene. Clones that grew on the LB-Kn plates contained the *att*B-PCR genes recombined in the pDONR201 vector. To confirm the identity of the genes the BP reaction was digested with

restriction enzymes appropriately chosen depending of the gene being investigated. The pDONR-PP1 containing clones were digested with PstI and NcoI restriction enzymes simultaneously. Similarly, clones containing pDONR-PP2B were digested with KpnI and XbaI, while those containing pDONR-I2 were digested with a NcoI restriction endonuclease. All digestion reactions contained: 5 µl of a small DNA preparation (miniprep), 1 µl of each restriction enzyme, 2 µl of an appropriate restriction enzyme buffer to ensure efficient cleavage, 0.1% BSA to stabilize enzymatic activity and distilled water to make up the reaction volume to total 20 µl. The digest reactions were incubated at 37°C for 3 hours and analyzed on an ethidium bromide stained, 0.8% agarose gel under ultraviolet light. When it was confirmed that the entry clones contained the gene of interest in the pDONR vector, the LR reaction was performed to transfer the gene to a pDEST40 expression vector.

The 20 µl LR reaction was assembled on ice and contained: 1 µl of Topoisomerase I (TOPOI) to relax supercoiled DNA, 4 µl of LR reaction buffer, 2 µl of the Entry Clone (100-300 ng/20 µl reaction), 300 ng/20 µl reaction of pDEST40 vector, 8 µl of TE buffer and finally 4 µl of LR Clonase Enzyme mix. The reaction was mixed briefly by vortexing and incubated for 60 minutes at 25°C. Next, 2 µl of Proteinase K solution was added and the reaction was incubated at 37°C for 10 minutes. To ascertain if successful recombination of each gene occurred into the pDEST40 vector, 1 µl of the LR reaction was used to transform electrocompetent DH5α cells by electroporation. The cells were then cultured in S.O.C. medium for 1 hour at 37°C and grown on LB plates containing 100 µg/ml ampicillin, to select for the pDEST40 vector containing an ampicillin resistance gene. The confirmation of

the correct gene was again achieved using restriction endonucleases, digesting clones containing pDEST40-PP1 with NcoI, pDEST40-I2 with PstI and pDEST40-PP2B with KpnI and XbaI.

Fig. 4a. Restriction map of pDONR201 entry clone vector.
The pDONR201 was used for subcloning of cDNA of protein phosphatases and I2. The pDONR201 vector contains two *att*P sites that allow for recombination between PCR products that contain *att*B sites. ccdB, a native gene in pDONR201 vector that is lethal to *E.coli* and is replaced by the PCR product; Kn^r, Kanamycin resistance gene; Cm^r, chloramphenicol resistance gene; ori, origin for expression; T-T2, *rrn*B transcription termination sequences.

Fig. 4b. Restriction map of pDEST40 expression clone with PP1 insert.
The pDEST40 was used for subcloning of cDNA of protein phosphatases and I2. pDEST40 contains: CMV, human cytomegalovirus immediate-early promoter; *att*R recombination sites; Neo^r, neomycin resistance gene; Ap^r, ampicillin resistance gene; ori, origin for expression; SV40, early promoter; V5 epitope tag; His tag; BGH, bovine growth hormone polyadenylation sequence. The location of the human PP1γ insert is indicated by horizontal lines.

A

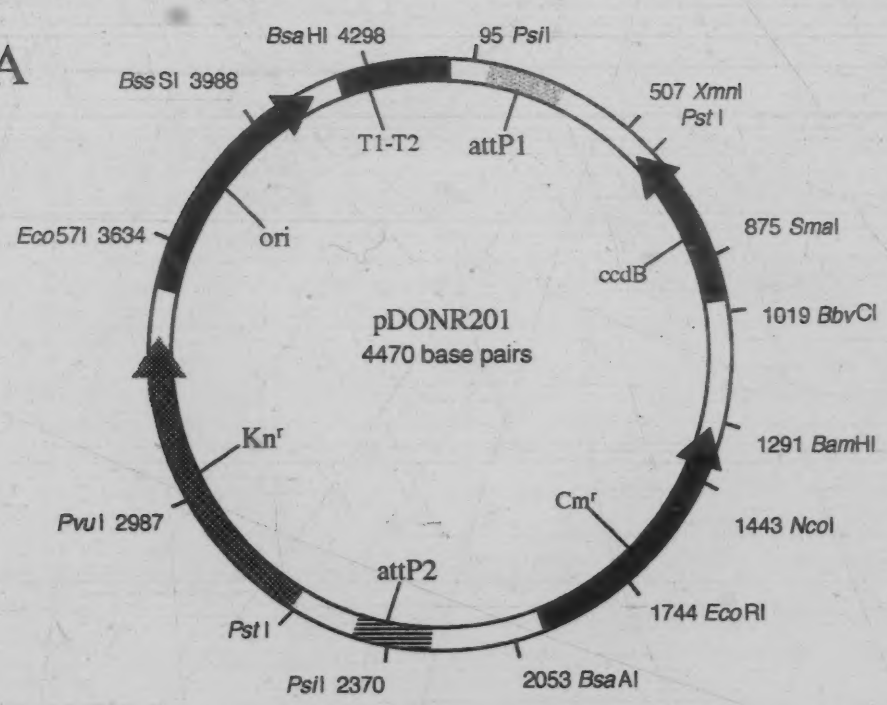
BsaHI 4298
95 PsiI
Bss SI 3988
507 XmnI
PstI
T1-T2
attP1
Eco571 3634
ori
875 SmaI
ccdB
pDONR201
4470 base pairs
1019 BbvCI
Kn^r
1291 BamHI
Cm^r
PvuI 2987
1443 NcoI
attP2
1744 EcoRI
PstI
PsiI 2370
2053 BsaAI

B

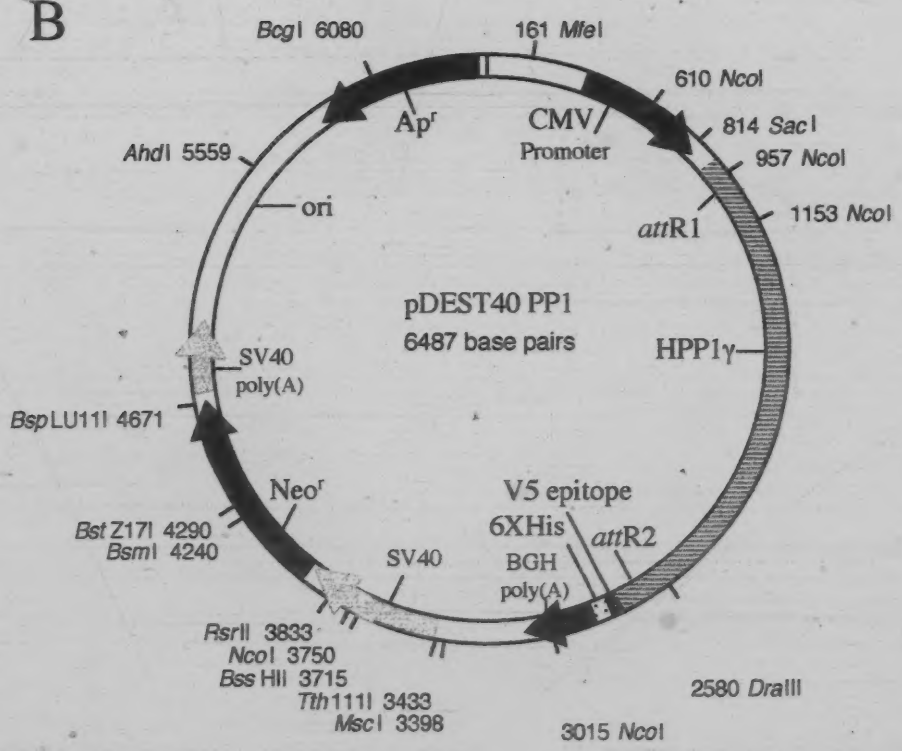
Bcgl 6080
161 MfeI
610 NcoI
Ap^r
CMV
Promoter
814 SacI
AhdI 5559
957 NcoI
ori
attR1
1153 NcoI
pDEST40 PP1
6487 base pairs
HPP1γ
SV40
poly(A)
BspLU11I 4671
Neo^r
V5 epitope
6XHis
attR2
Bst Z17I 4290
BsmI 4240
SV40
BGH
poly(A)
RsrII 3833
NcoI 3750
BssHII 3715
Tth111I 3433
MscI 3398
2580 DraIII
3015 NcoI

Fig. 4c. Restriction map of pDEST40 expression clone with PP2B insert.
The pDEST40 was used for subcloning of cDNA of protein phosphatases and I2. pDEST40 contains: CMV, human cytomegalovirus immediate-early promoter; *att*R recombination sites; Neo^r, neomycin resistance gene; Ap^r, ampicillin resistance gene; ori, origin for expression; SV40, early promoter; V5 epitope tag; His tag; BGH, bovine growth hormone polyadenylation sequence. The location of the human PP2B insert is indicated by the dotted area.

Fig. 4d. Restriction map of pDEST40 expression clone with I2 insert.
The pDEST40 was used for subcloning of cDNA of protein phosphatases and I2. pDEST40 contains: CMV, human cytomegalovirus immediate-early promoter; *att*R recombination sites; Neo^r, neomycin resistance gene; Ap^r, ampicillin resistance gene; ori, origin for expression; SV40, early promoter; V5 epitope tag; His tag; BGH, bovine growth hormone polyadenylation sequence. The location of the human I2 insert is indicated the checkered area.

C

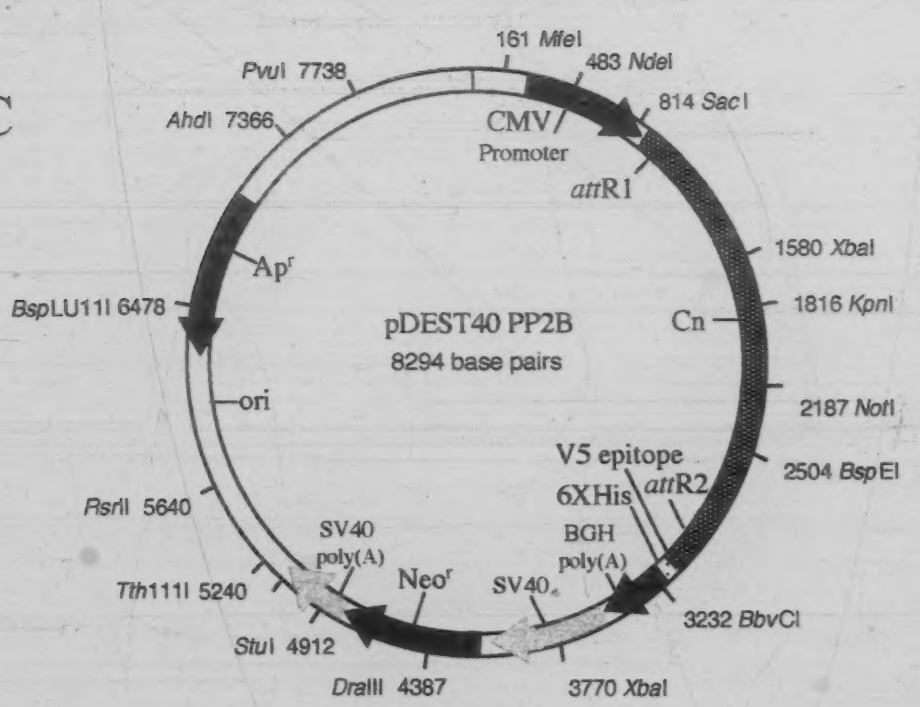
161 MfeI
483 NdeI
814 SacI
CMV/
Promoter
attR1
1580 XbaI
1816 KpnI
Cn
2187 NotI
2504 BspEI
V5 epitope
6XHis
attR2
BGH
poly(A)
SV40
3232 BbvCI
3770 XbaI
SV40
poly(A)
Neor
SV40
DraIII 4387
StuI 4912
Tth111I 5240
RsrII 5640
ori
BspLU11I 6478
Apr
PvuI 7738
AhdI 7366
pDEST40 PP2B
8294 base pairs

D

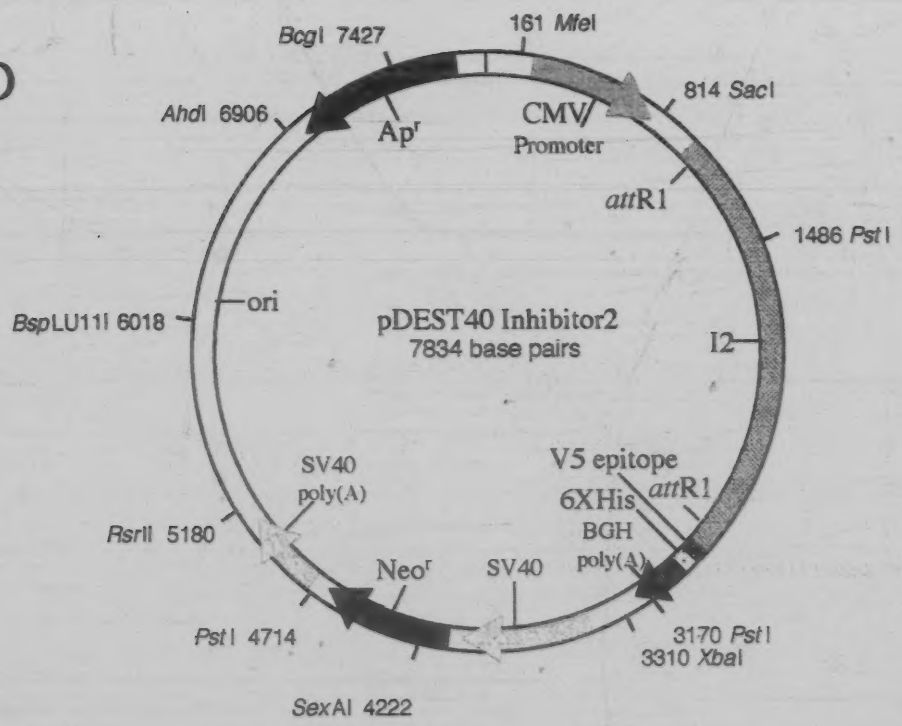
161 MfeI
814 SacI
CMV/
Promoter
attR1
1486 PstI
I2
V5 epitope
6XHis
attR1
BGH
poly(A)
SV40
3170 PstI
3310 XbaI
SexAI 4222
PstI 4714
Neor
SV40
poly(A)
RsrII 5180
ori
BspLU11I 6018
Apr
BcgI 7427
AhdI 6906
pDEST40 Inhibitor2
7834 base pairs

7.4. *Obtaining Transient and Stable Expression of Proteins in Mammalian Cells*

CHO cells that were 90% confluent were trypsinized and resuspended in 5 ml of growth medium. The cells were then centrifuged at 1200 rpm for 3 minutes and the medium was discarded. The pellet of cells was resuspended in 1 ml of fresh medium and a 20X dilution of the cells was obtained. The cells were counted using a Bright-line Hemocytometer, a cell counting chamber (Sigma), to determine the total number of cells present in 1ml. The volume required to obtain the desired number of cells was calculated by dividing the number of cells sought by the number of cells counted. Cells were counted and plated at 4.0×10^5 cells per 35 mm Petri dish for stable transfections or 1.0×10^6 cells per 60 mm Petri dish for transient transfections. The cells were cultured overnight at 37°C and 5% CO_2 in normal growth medium containing serum but lacking antibiotics.

The pDEST40 vector was used for cloning and expression experiments in mammalian cells. The three expression clones were constructed as previously outlined in methods section 7.3 to yield expression of human PP1γ, I2 and a constitutively active form of calcineurin, in Chinese hamster ovary cells. An empty pDEST40 plasmid was utilized for mock transfections of the same cells and included in analysis as a control. In addition, a β-Galactosidase expressing plasmid was used to confirm successful transfection of the Chinese hamster ovary cells.

The required amount of sterile DNA was diluted in Opti-MEM medium (Sigma), 500 µl per 10 µg of DNA or 250 µl per 4 µg of DNA. In addition, Opti-MEM was used to dilute the LF2000 Transfection Reagent (Invitrogen Life Technologies). A 500 µl volume of medium per 20 µl of reagent was used for each 60

mm Petri dish and 250 µl of medium was used to dilute 8 µl of reagent for each 35 mm Petri dish. The diluted reagent was mixed and incubated at room temperature for no longer than 5 minutes. The diluted DNA and reagent were combined and incubated at room temperature for 20 minutes, allowing DNA-reagent complexes to form. An appropriate volume of the complexes was added to each Petri dish, 1000 µl to a 600 mm dish and 500 µl to a 35 mm dish followed by gentle swirling of the dish. To establish a transient expression of the protein, the cells were incubated in a controlled environment at 37°C and 5% CO_2 for 24 hours.

The efficiency of the transfection was then monitored by transfecting a 35 mm dish of cells with a β-Galactosidase expression plasmid. The cells were fixed with 0.2% glutaraldehyde/PBS for 5 minutes at room temperature and washed twice with 1xPBS. Immediately following the washes, the cells were incubated with a staining solution containing X-Gal substrate for 2 hours at 37°C and 5% CO_2. The staining solution was replaced with 70% glycerol prior to visualizing the cells by microscopy. The cells that were transfected with the β-Galactosidase expression plasmid appeared blue. The efficiency of the transfection was calculated by dividing the number of blue cells by the total number of cells in the dish.

To achieve stable expression of the proteins, cells were passaged at a 1:10 and 1:100 dilutions into fresh growth medium enriched with antibiotics 24 hours after the transfection. The medium was changed daily for 3 days and supplemented with 800 µg/ml of Geneticin, a selection reagent allowing cells containing the pDEST40 expression construct, with the neomycin resistance gene to proliferate. The frequency of changing the media was decreased to every other day and the Geneticin

concentration was gradually reduced to 400 µg/ml. The colonies of amplified cells were then isolated into individual dishes. The isolated colonies were transferred into larger dishes as required and growth was maintained in 400 µg/ml Geneticin.

7.5. *Immunoblot Analysis of Stable Protein Expression in Mammalian Cells*

The level of PP1 and I2 protein expression in stably transfected Chinese hamster ovary cells was examined using samples of cell lysates from numerous colonies of each cell line. Cells were grown in 60 mm Petri dishes under normal culture conditions. Once cells reached 90% confluence the medium was removed and cells were washed with cold 1xPBS. Dishes were incubated on ice for 3 minutes in 100 µl of RIPA lysis buffer containing detergents (Table 9). Cells were scraped with a disposable scraper (Fisher) and transferred into an eppendorf microfuge tube. The cell lysates were centrifuged for 5 minutes x 14000 rpm at 4°C. The supernatant was retained and the proteins were separated on a 10% SDS-PAGE gel, followed by transfer to a nitrocellulose membrane at 300 mA for 1 hour.

The nitrocellulose membrane was gently rocked for 1 hour at room temperature in 10 ml of 5% milk/PBS augmented with 0.05% Tween. The blocking solution was washed twice with 20 ml PBS-Tween for 5 minutes. Next, the membrane was incubated for 2 hours at room temperature or overnight at 4°C, with a monoclonal anti-V5 antibody diluted 1:5000 in 5% milk/PBS/0.05% Tween. This antibody was used to probe for the protein of interest tagged with a V5-epitope. Following a wash with 20 ml of PBS-Tween twice for 5 minutes, the membrane was incubated with a goat anti-mouse secondary antibody (1:2000 dilution in 1%

milk/TBS) for 1.5 hours gently rocking at room temperature. Finally, the membrane was washed with 1xTBS, four times for 15 minutes prior to development with the Amersham Enhanced Chemiluminescence reaction.

8. Assay of Phosphatase Activity

The phosphorylase *a* assay is a procedure used to determine phosphorylase phosphatase activity in a given sample. This radioactive assay uses [^{32}P]-phosphorylase *a* as a substrate (Fig. 5) for the catalytic subunits of PP1 or PP2A. The phosphorylase *a* substrate was prepared by Kathleen Perreault in Dr. Charles Holmes' laboratory (University of Alberta, Edmonton, Alberta) as described earlier [224]. The phosphorylase *a* assay was performed as previously described [224] using two distinct sample preparations, first testing phosphatase activity in crude heart cell extracts, and second in cell lysates prepared from cells overexpressing PP1 or Inhibitor-2.

8.1. *Phosphatase Activity in Crude Heart Cell Extracts*

The phosphorylase *a* assay was used to determine if any phosphorylase phosphatase activity was present in rat heart cell extracts as they were employed in the dephosphorylation of PCRA experiments previously described in the methods section 2.2. Immediately prior to performing the assay, 100 µl [^{32}P]-phosphorylase *a* was resuspended in 240 µl of Solution A containing: 50 mM Tris HCl, 0.1 mM EDTA at pH 7.0, 0.2% beta-mercaptoethanol and 1 mg/ml Bovine Serum Albumin (BSA). The BSA was added to facilitate complete precipitation of the substrate. In

addition, the substrate was supplemented with 60 µl of caffeine (11.25 mM) resulting in a final concentration of 3.75 mM caffeine in each 30 µl reaction, and each solution was mixed well by inverting. Caffeine binds to phosphorylase *a* and is included because it prevents inhibition and contamination of phosphorylase *a* or the phosphatase. It increases phosphorylase activity 2-3 fold, and it allows phosphorylase *a* to be stored in ice without crystallizing [224].

Several assay tubes were prepared in advance to monitor different reaction mechanisms as detailed in Table 2. Experimental tubes received equal amounts of both enzyme and radioactive substrate, and revealed the amount of [^{32}P] released by the enzyme without any inhibitors present in the reaction. In addition to the contents present in experimental tubes, control tubes contained okadaic acid to inhibit phosphorylase phosphatase activity (IC_{50} PP1= 20 nM and IC_{50} PP2A = 2 nM) [107]. As a result, the difference between experimental samples and the controls revealed specifically phosphorylase phosphatase activity present in the samples, eliminating the possibility that the measured activity was due to the presence of other phosphatases. Total tubes were used to represent the total amount of radioactivity added to each reaction. The blank tubes, consisting of the substrate mixed and incubated with buffer alone, were necessary to monitor the level of [^{32}P] released from the substrate in the absence of any phosphatase enzyme.

Table 2: Reactions assembled for measuring phosphorylase phosphatase activity in heart cell extracts.

Contents of Tubes	Experimental Tubes	Control Tubes	Blank Tubes	Total Tubes (1 ml scintillation fluid)
Experimental Sample (Enzyme)	10 µl (crude rat heart cell extracts)	10 µl (crude rat heart cell extracts)	-	-
Enzyme Inhibitor	-	1 µl O.A. standard	-	-
^{32}-P Phos *a* (Radioactive substrate)	10 µl	10 µl	10 µl	10 µl
Solution A	10 µl	9 µl	20 µl	-
Total Volume	30 µl	30 µl	30 µl	1010 µl

The experimental samples, controls and blanks were briefly centrifuged to ensure that all of the contents were concentrated at the bottom of each tube, and were incubated at 30°C for 10 minutes. One blank and control tube was placed at the beginning and end of all the samples. Two total tubes, labeled 1 and 2 were filled with 1 ml of scintillation fluid and remained on ice throughout the duration of the experiment. Following 10 minutes pre-incubation of samples at 30°C, 10 µl of substrate was added to the first total tube. Next, 10 µl of substrate was added to each sample including blanks, at 20 second intervals between each sample. In this manner each reaction continued for exactly the same period of time, 10 minute pre-incubation of enzyme followed by 10 minutes incubation with substrate. Once the substrate was added to all of the samples, 10 µl of substrate was added to the second total tube. Once the first sample reached a 10 min incubation period with the substrate, 200 µl of 20% cold trichloroacetic acid (TCA) was added and mixed in each tube at 20 second intervals and the tubes were immediately placed on ice. This was necessary to stop

the reaction mechanism and to ensure precipitation of the substrate protein. When the last reaction was stopped all samples remained on ice for an additional 2 minutes.

Next, sample and blank tubes were centrifuged at 14000 rpm for 3 minutes and 200 µl of the supernatant was transferred to labeled tubes containing 1 ml of scintillation fluid. Care was taken so as to ensure that the pellet at the bottom of each sample was not disturbed. The pellet represented the sedimented substrate bound to the enzyme and its disruption would cause a high increase of radioactivity, incorrectly representing radioactivity initially released in the sample. Tubes still containing the pellet were discarded. The total tubes and tubes containing sample in scintillation fluid were mixed by inversion, and the inorganic [^{32}P] was counted in a Wallac 1209, Rackbeta Liquid Scintillation Counter. Calculations of phosphatase activity are explained in Table 10.

8.2. *Phosphatase Activity in Mammalian Cells*

The phosphorylase *a* assay was also used to determine the level of active PP1 in Chinese hamster ovary cells expressing PP1 or I2. For these phosphorylase *a* assays, cell lysates were prepared as follows. Cells were grown in 60 mm petri dishes to 90% confluency. Cells were washed several times with 1xTBS containing the following protease inhibitors: aprotinin (0.5 µg/µl), leupeptin (1.0 µg/µl), pepstatin (1.0 µg/µl) and phenylmethanesulfonyl fluoride (PMSF) 1 mM. Cells were replenished with 100 µl of harvesting buffer (50mM Tris-HCl, 1mM EDTA) and detached from the dish surface with a disposable cell scraper. The harvesting buffer containing the cells was removed from the culture dish into a 1 ml microfuge vial,

followed by a final rinse of the dish with 50 µl of harvesting buffer to obtain any remaining cellular protein. The cells were centrifuged at 14000 rpm for 5 minutes at 4°C in eppendorff microfuge tubes. The supernatant was transferred to a separate vial. Fresh harvesting buffer (50 µl) was added to the pellet that contained the protein, and using a 50 µl Hamilton syringe, the pellet was dispersed to make a homogenous solution. Ten microliter samples of the initial supernatant and the dispersed pellet were obtained for protein determination with the Bio-Rad Protein Quantification kit, while the remaining sample was frozen in liquid nitrogen for further use in phosphorylase *a* assays.

Various assay tubes were prepared to monitor different reaction mechanisms, as outlined in Table 3. Experimental and control tubes received 5 µg of the total protein present in cell lysates. In addition, 10 µl of radioactive substrate was added, which revealed the amount of [^{32}P] released by the enzyme without any inhibitors present in the reaction. As summarized in Fig. 5, the experimental tubes represented the total phosphorylase phosphatase activity (PP1 and PP2A) in cells. The control tubes also contained purified I2, which inhibits PP1 activity but not PP2A. The difference between experimental samples and the controls represented PP2A activity present in the cells. Consequently, the difference between the PP2A activity and the total phosphorylase phosphatase activity represented PP1 activity in the cells. To ensure that the purified I2 protein was fully active, a sample of purified PP1 was included in the assay, both in the presence and absence of I2, the latter being a control and revealing the initial PP1 activity.

Total tubes and blank tubes were also included in the experiment. The remainder of the phosphorylase *a* assay was performed as described in methods section 8.1.

Table 3: Reactions for measuring Phosphorylase Phosphatase and PP1 activity in cell lysates.

Contents of Tubes	**Experimental Tubes**	**Experimental Control Tubes**	**Testing I-2 activity Tube**	**Testing PP1 activity Tube**	**Blank Tubes**	**Total Tubes (1 ml scintillation fluid)**
Experimental Sample (Enzyme)	5 µg total protein (cell lysates)	5 µg total protein (cell lysates)	1 µg Purified PP1	1 µg Purified PP1	-	-
Enzyme Inhibitor	-	1 µl (29nM) purified Inhibitor2	1 µl (29nM) purified Inhibitor2	-	-	-
[^{32}P] Phos *a* (Radioactive substrate)	10 µl	10 µl	10 µl	10 µl	10 µl	10 µl
Solution A	µl (dependent on cell lysate volume)	µl (dependent on cell lysate volume)	µl (dependent on PP1 volume)	µl (dependent on PP1 volume)	20 µl	-
Total Volume	30 µl	30 µl	30 µl	30 µl	30 µl	1010 µl

Fig. 5. The Concept of the Phosphorylase *a* Assay for Measuring Phosphatase Activity in Mammalian Cells

Cell lysates from cells expressing I2 and control mock-transfected cells were prepared as detailed in the methods section 8.2. Phos. kinase, phosphorylase kinase; PP1, protein phosphatase-1; PP2A, protein phosphatase-2A; I2, inhibitor-2; P, phosphate; TCA, trichloroacetic acid; cpm, counts per minute. This procedure is detailed in the methods section 8.0-8.2.

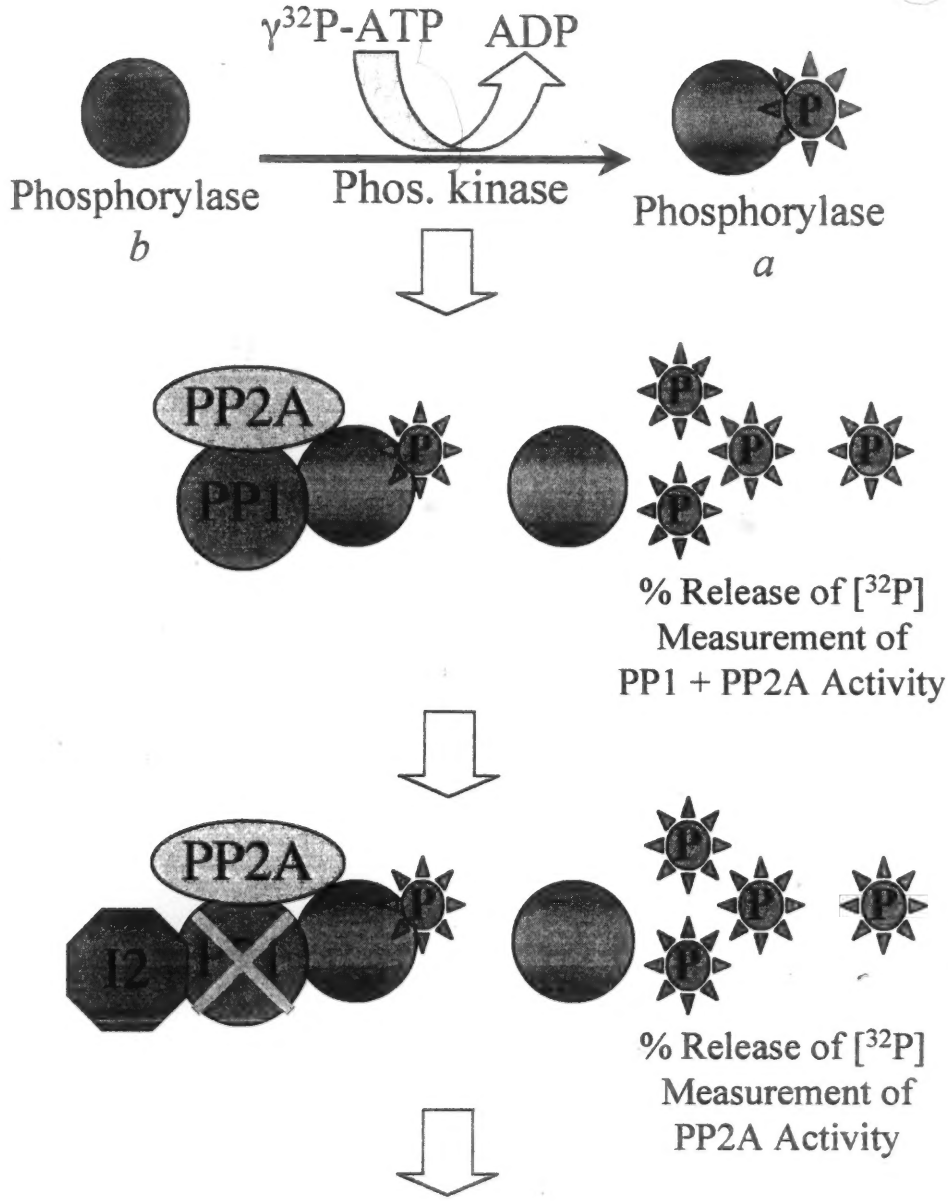
γ32P-ATP
ADP
Phosphorylase
b
Phos. kinase
Phosphorylase
a
PP2A
PP1
% Release of [32P]
Measurement of
PP1 + PP2A Activity
PP2A
I2
% Release of [32P]
Measurement of
PP2A Activity
TCA ppt protein, centrifuge,
Measure cpm in supernatant

9. Measurements of Intracellular pH and Buffering Capacity

9.1. *Measuring pHi in Cells Transiently Expressing PP1 or PP2B*

Chinese hamster ovary cells transiently expressing PP1 or PP2B were assayed after 24 hours of initial transfection. The average transfection efficiency of CHO cells was 57.5% during PP1 transfections and 57% during PP2B transfections. The Na^+/H^+ exchanger activity was tested in both cell lines by measuring intracellular pH (pH*i*) using a Shimadzu RF5000 Fluorometer. The cells were grown and transfected on glass coverslips. For pH measurements cells were in Na^+-containing buffer (Table 8) and treated with 1 µl of a pH sensitive, fluorescent dye, BCECF-AM, for 2-4 minutes as described earlier [73]. The preset excitation wavelengths on the Shimadzu RF5000 were 452 and 503 nm with an emission wavelength of 524 nm.

Intracellular pH was measured following an acid load using 40 mM NH_4Cl in Na^+-containing buffer (pH 7.3) for 3 minutes, followed by briefly placing the cells into an NH_4Cl and Na^+-free buffer (pH 7.3) for approximately 20-30 seconds. Cells were quickly returned to a Na^+-containing buffer for 3 minutes to determine their ability to recover from the acid load [73]. Fluorescence ratios were converted to intracellular pH values using a calibration curve. The pH*i* values at zero and 20 seconds of the recovery period were subsequently utilized to calculate the rate of recovery from the acid load. The final units were ΔpH/min and the detailed formula is shown in Table 10.

Some transiently transfected cells remained in each petri dish, from which the glass coverslips were removed for assays. These were used to prepare RIPA lysates and verify the level of expression of PP1 and PP2B by Western Blot analysis. The

protein concentration of each lysate was determined using the Bio-Rad DC Protein Assay kit, and 100 μg of total protein from each petri dish was separated on a 10% SDS-PAGE gel, followed by transfer to a nitrocellulose membrane. The membrane was blocked overnight with 10% milk/TBS and subsequently probed with a monoclonal anti-PP1 (1:2000 in 1% milk/TBS) or a polyclonal anti-PP2B-A antibody (1:2000 in 1% milk/TBS). Details of antibodies used are briefed in Table 5. The results were visualized with autoradiography.

9.2. *Measuring pHi in Cells Stably Expressing PP1 or I2*

To test whether PP1 activity affected the performance of the Na^+/H^+ exchanger *in vivo,* two separate approaches were used. Stable cell lines of Chinese hamster ovary cells were made expressing either PP1 or I2. The expression of PP1 protein was expected to cause more PP1 activity in cells. In contrast, the expression of I2 was expected to reduce PP1 activity, compared to an endogenous level of PP1 activity tested in mock-transfected CHO cells.

The Na^+/H^+ exchanger activity was tested in both cell lines by measuring pH*i* using excitation wavelengths of 452 and 503 nm with an emission wavelength at 524 nm in a Photon Technology Institute, DeltaScan Flurometer. The cells were grown on glass coverslips in αMEM culture medium. One night before performing fluorometric experiments, the medium was replaced with αMEM culture media containing reduced serum (0.5%). The accuracy of data collected using the DeltaScan fluorometer was superior to that of the Shimadzu RF5000; however, it required a higher level of dye to be present in the cells. Consequently, the cells were preincubated with BCECF-AM

(40 μg/μl) in serum-free culture medium, for 45 minutes at 37°C. This was done in serum-free medium to eliminate possible breakdown of the fluorescent compound in the presence of serum.

Intracellular pH and the recovery of cells from an acid load was measured in an identical manner as described in experiments performed using the Shimadzu RF5000, on cells transiently overexpressing PP1 and PP2B. An imperative difference in the assays performed using the DeltaScan fluorometer was that every coverslip underwent a three-point calibration following the recovery of cells from an acid challenge, as follows. After recovery in Na^+-containing buffer for 3 minutes, fluorescence ratios were converted to pH*i* by treating each coverslip with 10 μM nigericin (Sigma) in calibration buffer (Table 8) at pH 8.0, pH 7.0 and 6.0. This allowed for a standard curve to be obtained. The standard curve was used to calculate the rate of recovery from an acid load with final units in pH/min.

Analogous to the protocol described above, other experiments performed on the stable cell lines overexpressing PP1 or I2 were aimed at testing whether the Na^+/H^+ exchanger could be stimulated with Thrombin [225, 226] when PP1 or I2 were expressed. After ammonium chloride induced acidosis, the hormone was introduced into Na^+-containing buffer (2 units/ml) for 3 minutes. Following this incubation, the rate of recovery from an acid load was measured. This procedure was repeated in the presence of 10 μM Hexamethylene-amiloride (HMA), a specific NHE inhibitor [99], to ascertain that the results being obtained were due to the activity of NHE1.

9.3. *Measuring Buffering Capacity in Cells Stably Expressing PP1 and I2*

The buffering capacity of stable cell lines was measured to ensure that the changes in pH*i* that were observed, were due to the changes in Na^+/H^+ exchanger activity and not due to changes in buffering capacity of the cells. To measure buffering capacity, cells grown on glass coverslips were preincubated with BCECF-AM (40 μg/μl) for 45 minutes at 37°C. Each coverslip was placed in Na^+-containing buffer until a signal was observed. The coverslip was than transferred to a cuvet with 25 mM NH_4Cl in Na^+-containing buffer for one minute. This was repeated, transferring the coverslip into different cuvets, each decreasing in NH_4Cl concentration by 5 mM until the final 1 minute incubation was performed in the absence of NH_4Cl. This series of transfers was followed by a three-point calibration of each coverslip in calibration buffers at pH 8.0, 7.0 and 6.0 as detailed in earlier experiments. The ratios were converted to pH values and the average pH for every 1 minute incubation was recorded for individual coverslips. Furthermore, an average pH for each NH_4Cl concentration was obtained after the experiment was repeated eight times for each cell line.

Proton efflux, the true movement of H^+ from the cells, was calculated using the buffering capacity and the rate of change in pH*i*. First, the buffering capacity was measured and a standard curve was obtained, which generated an equation of the line as follows:

$$y = mx + b \qquad (m = \text{slope}; b = \text{y-intercept})$$

The calculated rate of recovery from an acid load and the pH at 10 seconds of recovery (mid point pH) was obtained from pH*i* measurements described in the methods section 9.2. The buffering capacity of the cells was calculated as follows:

Formula for Calculating the Buffering Capacity and H^+ Efflux

Buffering Capacity = m (mid point pH) + b

The proton efflux by NHE1 was calculated as follows:

H^+ Efflux = Buffering Capacity x Rate of recovery from acid load

Table 4: Primers Used in Cloning Experiments	
Primer Name	**Primer Sequence**
Gateway PP1 forward primer	5' GGGGACAAGTTTGTACAAAAAAGCAGGCTTAGAAGGAGATAGAACC atggcggatttagataaactcaacatcg 3'
Gateway PP1 reverse primer	5' GGGGACCACTTTGTACAAGAAAGCTGGGT atttctttgcttgctttgtgatcatacc 3'
Gateway I-2 forward primer	5' GGGGACAAGTTTGTACAAAAAAGCAGGCTTAGAAGGAGATAGAACC atggcggcctcgacggcctcgcaccgg 3'
Gateway I-2 reverse primer	5' GGGGACCACTTTGTACAAGAAAGCTGGGTT tgaacttcgtaatttgttttgctgttgg 3'
Gateway PP2B forward primer	5' GGGGACAAGTTTGTACAAAAAAGCAGGCTTAGAAGGAGATAGAACC atgtccgagcccaaggcgattgatcc 3'
Gateway PP2B reverse primer	5' GGGGACCACTTTGTACAAGAAAGCTGGGTC ctacttgtttctgatgacttccttc 3'
NOTE:	Upper case = *att*B1 sequence including SD and kozak consensus sequences. Lower case = gene of interest sequence

Table 5: Antibodies Used in Immunoblot Analyses				
Antibody Name	**Dilution/Solution**	**Experiment**	**Incubation Period**	**Source**
anti-PP1α rabbit polyclonal	1:2000/1% milk in TBS	Western Blot	2 hours	Santa Cruz Biotechnology Inc.
anti-PP1 mouse monoclonal	1:2000/1% milk in TBS	Western Blot	2 hours	Dr. Mary Pato University of Saskatchewan
anti-PP2B-A rabbit polyclonal	1:2000/1% milk in TBS	Western Blot	2 hours	Santa Cruz Biotechnology Inc.
anti-V5 epitope mouse monoclonal	1:5000/5% milk in PBS/0.05% Tween	Western Blot	2 hours or overnight	Invitrogen Life Technologies
anti-NHE1 mouse monoclonal	1:2000/TBS	Western Blot	overnight	Chemicon International, Inc.
anti-β-Gal NHE rabbit polyclonal	N/A	Immunoprecipitation	3 hours	Dr. Larry Fliegel University of Alberta
anti-HA mouse monoclonal	1:2000/1% milk in TBS	Western Blot	2 hours	Boehringer Mannheim
goat anti-mouse	1:2000/1% milk in TBS	Western Blot	1.5 hours	BioCan
goat anti-rabbit	1:2000/1% milk in TBS	Western Blot	1.5 hours	BioCan

Table 6: Recipes for Rat Neonatal Myocyte Culture Solutions	
Solution	**Contents**
Solution I	20 mM HEPES and 1% penicillin/streptomycin in 1xHBSS (Hanks Buffered Salt Solution)
Solution II	0.1% collagenase, 1% penicillin/streptomycin and 20 mM HEPES in 1xHBSS
Solution III	20% fetal bovine serum (FBS) and 1% penicillin/streptomycin in 1xHBSS
Solution IV	DMEM F12 (Gibco) media pH 7.3 supplemented with: 2.438 g/l $NaHCO_3$ 10 g/l BSA 0.25 g/l Fetuin (Sigma, F-2379) 2.5 mg/l Transferrine 1% Penicillin/streptomycin 5 µg/l Insulin 5 µg/l Transferrin 10 ng/ml Selenium 80 µg/l $CaCl_2$ 20 µg/l L-ascorbic acid 1x MEM-Nonessential amino acids (Sigma A-4403) 1x Vitamin 100x (Gibco) 2 ml/l BSA-palmitate (see recipe below)
Solution V	DMEM F12 (Gibco) media pH 7.3 supplemented with: 2.438 g/l $NaHCO_3$ 10% Fetal bovine serum 30 mM HEPES 10 µg/ml Transferrin 10 µg/ml Insulin 1% Penicillin/streptomycin 50 mM Bromodeoxyuridine 5 µg/ml Linoleic acid 2 mg/ml BSA 1x MEM-Nonessential amino acids (Sigma A-4403) 1x Vitamin 100x (Gibco) 10 ng/ml Selenium 3 mM Pyruvic acid 100 µM ascorbic acid
BSA-palmitate	1.2 g BSA per 20 ml of water (6% BSA) in dialysis bag. The BSA was dialyzed overnight at 4°C in PBS enriched with 10 mM EDTA and 1.4 g of palmitate dissolved in 95% ethanol.
Solution PBS-ABC	136 mM NaCl 2.7 mM KCl 15.7 mM $Na_2HPO.7H_2O$ 250 mg/L KH_2PO4 0.90 mM $CaCl_2.2H_2O$ 1.0 mM $MgCl_2.6H_2O$

Table 7: Recipes for Acid Load Selection Cell Culture Experiment	
Solution	**Contents**
NH_4^+ saline medium (Na^+ free)	50 mM NH_4Cl 70 mM Choline Chloride 5 mM KCl 1 mM $MgCl_2$ 2 mM $CaCl_2$ 5 mM D-glucose 20 mM HEPES Adjust pH to 7.4 using HCl and KOH.
Na^+ saline medium	120 mM NaCl 5 mM KCl 1 mM $MgCl_2$ 2 mM $CaCl_2$ 5 mM D-glucose 20 mM HEPES Adjust pH to 7.4 using HCl and KOH.

Table 8: Recipes for pH Experiment Solutions	
Solution	**Contents**
Normal Na^+ containing buffer	135 mM NaCl 5 mM KCl 1.8 mM $CaCl_2$ 1.0 mM $MgSO_4$ 5.5 mM Glucose 10 mM Hepes pH solution to 7.4 with HCl or KOH
Na^+ free buffer	135 mM N-Methyl Glucamine 5 mM KCl 1.8 mM $CaCl_2$ 1.0 mM $MgSO_4$ 5.5 mM Glucose 10 mM Hepes pH solution to 7.4 with HCl or KOH
Calibration buffer	135 mM N-Methyl Glucamine 135 mM KCl 1.8 mM $CaCl_2$ 1.0 mM $MgSO_4$ 5.5 mM Glucose 10 mM Hepes pH solution to 8.0, 7.0, 6.0 with HCl or KOH add 10μM Nigericin

Table 9: Recipes for Cell Lysate Preparation Solutions		
Solution	**Contents**	
Ripa Lysis Buffer NO Detergents for Immunoprecipitation	150 mM	NaCl
	80 mM	NaF
	50 mM	Tris-HCl pH 8.0
	5 mM	EDTA
	1 mM	EGTA
	5 mM	NaPyrophosphate
	1 mM	NaOrthovanadate
	1 mM	PMSF
	1 mM	Benzamidine
	1 µl/ml	Protease inhibitor cocktail
Ripa Lysis Buffer with Detergents for Immunoprecipitation	In addition to the above contents:	
	1.0% (v/v)	NP-40 (IGEPAL A-630)
	0.5% (w/v)	deoxycholate
	0.1% (w/v)	SDS
Ripa Lysis Buffer for Western Blot	50 mM	Tris pH 7.4
	150 mM	NaCl
	1.0% (v/v)	NP-40 (IGEPAL A-630)
	0.5% (w/v)	sodium deoxycholate
	0.1% (v/v)	Triton X-100
	1 mM	EGTA
	1 mM	PMSF
	1 mM	Benzamidine
	1 µl/ml	Protease inhibitor cocktail
Cell Lysate Harvest Buffer for Phosphorylase *a* Assay	50 mM	Tris HCl
	1mM	EDTA

Table 10: Calculation Formulas	
Experiment	**Formula/Calculations**
Phosphorylase Phosphatase Activity in Heart Cell Extracts	% [^{32}P] release = $\frac{\text{sample – blank (ave)}}{\text{total (ave) – blank (ave)}}$ x 1.15* • calculations performed for samples with and without okadaic acid present • difference in results between the two samples represented % [^{32}P] release due to phosphorylase phosphatase activity (PP1 and PP2A combined).
Phosphorylase Phosphatase Activity in Mammalian Cells (CHO overexpressing PP1 or I-2)	CALCULATION A % [^{32}P] release = $\frac{\text{sample – blank (ave)}}{\text{total (ave) – blank (ave)}}$ x 1.15 • calculations performed for samples without Inhibitor 2
Protein Phosphatase 2A Activity Activity in Mammalian Cells (CHO overexpressing PP1 or I-2)	CALCULATION B % [^{32}P] release = $\frac{\text{sample – blank (ave)}}{\text{total (ave) – blank (ave)}}$ x 1.15 • calculations performed for samples with Inhibitor 2
Protein Phosphatase 1 Activity in Mammalian Cells (CHO overexpressing PP1 or I-2)	Calculations A - B = PP1 activity in cells
Rate of Recovery from an Acid Load	BCECF-AM at zero sec of recovery and 20 sec of recovery, converted to pH units using a standard curve obtained during calibration (pH @ 20 sec – pH @ 0 sec) x 3 = ΔpH/min
Buffering Capacity in Mammalian Cells (CHO overexpressing PP1 or I-2)	From buffering capacity results, obtained a standard curve potting buffering capacity VS mid pH, producing an equation of the line: y = mx+ b Further experiments: obtained rate of recovery and pH value at 10 sec of the recovery (using unstimulated cells) Solve the equation of the line: Buffering Capacity = m (10s pH) + b
H^+ Efflux in Mammalian Cells (CHO overexpressing PP1 or I-2)	H^+ Efflux = Buffering Capacity x Rate of recovery from acid load (unstimulated cells)

* Once TCA was added to the sample the total volume was 230 µl: however only 200 µl of the supernatant was used to count radioactivity. The 1.15 value represents 230 µl/200 µl.

Chapter III

D: Results

D. Results

1. *In Vitro* Dephosphorylation of NHE1

A GST-178 C-terminal amino acid, Na^+/H^+ exchanger, fusion protein named PCRA [70, 73], was employed in *in vitro* dephosphorylation experiments. The dephosphorylation of NHE1 was investigated using three purified protein phosphatases, PP1, PP2A and PP2B as well as crude heart cell extracts. First, the NHE1 C-terminal, GST fusion protein was phosphorylated [73] using crude heart cell extracts in combination with ATP, [γ^{32}P]-ATP and the phosphatase inhibitors okadaic acid and sodium fluoride. The phosphorylated PCRA protein was incubated with each purified phosphatase, PP1, PP2B or PP2A under the appropriate conditions required to maintain their activity. Recombinant PP1 requires a source of Mn^{2+} ions to remain active [114] as a result a key component in the dephosphorylation reaction involving PP1 was 5 mM $MnCl_2$. A source of Ca^{2+} ions was added to the dephosphorylation reactions involving PP2B, which were done in the presence or absence of CaM. Both Ca^{2+} and CaM optimize the activity of this phosphatase [151].

1.1 *Dephosphorylation of NHE1 by PP1*

The results of NHE1 dephosphorylation were observed using autoradiography and quantified using the Image Gauge (Bio-Rad) software. The phosphorylation of PCRA was confirmed by autoradiography and ninety minutes was allowed for PP1, PP2A or PP2B to remove the phosphate from NHE1. Incubation of PCRA with PP1 abolished the radioactive phosphate signal (Fig.6a DP PP1/Mn^{2+}). In control dephosphorylation reactions the radioactive phosphate signal was apparent (Fig.6a

DP Ctrl). The Coomassie blue stained SDS-PAGE gel (Fig.6b) showed that relatively equal amounts of PCRA were eluted from the glutathione beads and analyzed. A quantitative analysis of these experiments using the ratio of [^{32}P]:protein confirmed that PP1 removed almost all of the [^{32}P] from the protein (Fig.6c). These results clearly indicate that PP1 can completely dephosphorylate NHE1.

1.2 *Dephosphorylation of NHE1 by PP2A*

Dephosphorylation of NHE1 by PP2A was done in the presence or absence of Mn^{2+}. A quantitative analysis of the [^{32}P]:protein ratios revealed a significant dephosphorylation of NHE1 by PP2A in the presence or absence of Mn^{2+} (Fig.7c). In both cases, PP2A reduced the [^{32}P] signal (Fig.7a DP PP2A); however, in the absence of Mn^{2+} (Fig.7a DP PP2A -Mn^{2+}) the signal was significantly decreased from that observed in the presence of Mn^{2+} (Fig.7a DP PP2A +Mn^{2+}). This result quantified in Fig.7c. Equal amounts of protein were analyzed in each experiment as indicated by the Coomassie stained SDS-PAGE gel (Fig.7b). Dephosphorylation of NHE1 in the presence of PP2A was not as great as that in the presence of PP1. Dephosphorylation of NHE1 by PP1 is significantly more complete than by PP2A, as demonstrated in Fig.7a (DP PP1) and quantified in Fig.7c.

1.3 *Dephosphorylation of NHE1 by PP2B*

Active purified PP2B was tested for its ability to dephosphorylate the cytosolic domain of NHE1. Incubation of phosphorylated PCRA with PP2B in the presence of Ca^{2+} and CaM did not change the intensity of the radioactive phosphate

signal (Fig.8a DP PP2B/Ca^{2+}/CaM). The [^{32}P] signal was comparable to that observed in the dephosphorylation control reaction (Fig.8a DP Ctrl), which lacked PP2B/Ca^{2+}/CaM. The phosphorylation of PCRA was confirmed by a strong [^{32}P] signal observed on the autoradiogram (Fig.8a P). Identical results were observed in the absence of CaM (data not shown). The Coomassie blue stained SDS-PAGE gel confirmed that PCRA was present in equal amounts in each reaction (Fig.8b). A quantitative analysis of the [^{32}P]:protein ratios revealed that PP2B did not dephosphorylate NHE1 significantly in the presence of Ca^{2+} and CaM (Fig.8c). Together the *in vitro* dephosphorylation experiments indicate that PP1 or PP2A can both dephosphorylate NHE1, with the dephosphorylation by PP1 being more complete than that by PP2A.

1.4 *Dephosphorylation of NHE1 by PP1 in the Presence of the Targeting Regulatory Subunit, Spinophilin.*

In other *in vitro* dephosphorylation experiments, the degree of dephosphorylation of NHE1 by PP1 was examined in the presence of spinophilin, a protein known to target PP1 to the plasma membrane and actin cytoskeleton [130]. Fifteen minutes was allowed for the dephosphorylation of PCRA in the presence of PP1, Mn^{2+} and spinophilin. Control dephosphorylation reactions were deficient in spinophilin and PP1. In addition, dephosphorylation experiments were simultaneously performed in the presence of PP1 and Mn^{2+}, and in the absence of spinophilin. The radioactive phosphate signals observed on the autoradiogram were almost completely abolished in the presence of PP1 (Fig.9a DP PP1/Mn^{2+}). Control dephosphorylation

reactions in the absence of PP1 demonstrated a strong [^{32}P] signal (Fig.9a DP Ctrl). The Coomassie blue stained SDS-PAGE gel indicated relatively equal amounts of PCRA present in each reaction (Fig.9b). Under identical experimental conditions and autoradiographic exposure time, the [^{32}P] signal observed in reactions supplemented with spinophilin was stronger (Fig.9c DP PP1/Mn^{2+}/spinophilin) than that observed in the presence of PP1 alone (Fig.9a DP PP1/Mn^{2+}), even though identical amounts of protein were analyzed (Fig.9d). A quantitative analysis of the [^{32}P]:protein ratios indicated that PP1 significantly dephosphorylated NHE1 in the presence of spinophilin; however, the degree of the dephosphorylation was reduced by 6% (Fig.9e).

1.5 *Dephosphorylation of NHE1 by Heart Extracts*

Finally, *in vitro* dephosphorylation of NHE1 was examined using crude heart cell extracts. Phosphorylation of the C-terminal NHE1 fusion protein was confirmed by a strong [^{32}P] signal viewed by autoradiography (Fig.10a P). Equal amounts of protein were analyzed (Fig.10b) and the dephosphorylation signal in the presence of heart cell extracts (Fig.10a DP Heart Cell Extracts) was not significantly different from that observed in the dephosphorylation control, deficient in heart cell extracts (Fig.10a DP Ctrl). Fig.10c illustrates a quantitative analysis of the [^{32}P]:protein ratios.

2. Binding Assays of NHE1 and Protein Phosphatases

To investigate physical interactions of the C-terminal with PP1 and PP2B, the NHE1 fusion protein, PCRA was employed in GST pull-down experiments. Four reaction combinations were prepared: the first contained PCRA, PP1 and Mn^{2+}; the second reaction contained PCRA, PP2B, Ca^{2+} and CaM. The third and fourth reactions served as controls and contained the same components as combinations 1 and 2, except PCRA was substituted with an equal concentration of GST. Reactions were incubated with glutathione sepharose beads at 37°C, lightly shaking, to immobilize PCRA. The reactions were terminated by pelleting the beads and any attached complexes, as described in the methods section 4.1. For Western Blot analysis of the pellets, three different primary antibodies were used. These included: a monoclonal antibody raised against PP1α, a polyclonal antibody against PP2B or a polyclonal broad range phosphatase antibody able to detect the catalytic subunits of PP1, PP2A, PP2B and PPX of mouse, rat and human origin. Results of the GST pull-down experiments were examined using the Amersham Enhanced Chemiluminecence Assay.

2.1 *Analysis of Phosphatase-NHE1 Binding Assay by Immunoblotting with a Broad Range Phosphatase Antibody*

The analysis of PP1-NHE1 binding assays using the broad range phosphatase antibody is depicted in Fig.11. A control reaction (GST-PP1) showed negligible binding of PP1 to the GST purified protein. This is indicated by a faint, 37 kDa protein band (Fig.11a lanes 3,4). Experiments examining an interaction between PP1

and PCRA showed binding of PP1 to PCRA, indicated by an identical 37 kDa protein band (Fig.11a lanes 5,6). Protein bands of this size were absent from negative control samples of PCRA (Fig.11a lane 2) and GST alone (Fig.11a lane1). The immunoblot results were quantified using the Image Gauge Bio-Rad software and are summarized in Fig.11b. The binding of PP1 to PCRA was significantly greater than to GST alone. These GST pull-down experiments of PCRA in the presence of PP1 suggest that, PP1 can bind to the C-terminus of the Na^+/H^+ exchanger.

The size of the full length calcineurin (PP2B) protein is approximately 59-61 kDa. A sample of purified calcineurin protein (Fig.12a lane 5) was used as a positive control, required to identify the location of the calcineurin protein band in the GST pull-down experiments and to confirm immunoreactivity of the antibody. This sample contained full length calcineurin of approximately 60 kDa in size (Fig.12a, top arrow) and a fairly visible 31 kDa fragment of calcineurin (Fig.12a, bottom arrow) also recognized by the broad range phosphatase antibody. Several other protein bands were visible on the immunoblot due to the lack of specificity of the antibody, possibly due to its ability to recognize various types of phosphatases. A positive control for NHE1 was also included in the SDS-PAGE gel (Fig.12a, lane 4). The control reaction (GST-PP2B) did not demonstrate binding of PP2B to GST (Fig.12a lane 1). It did not contain significant amounts of the 60 kDa calcineurin band. Similarly, the 60 kDa protein band was not observed in two individual experimental samples (Fig.12a lanes 2,3) where PP2B and PCRA were used together in a GST pull-down reaction. These results suggested that the full length calcineurin protein is not able to bind with the C-terminus of NHE1. Interestingly, the C-terminal fusion protein of NHE1 showed

strong binding to the 31 kDa fragment of calcineurin (Fig.12a lanes 2,3, bottom arrow). This fragment did not bind to the GST purified protein (Fig.12a lane 1). The intensity of the 31 kDa protein band visualized on the autoradiogram (Fig.12a lanes 2,3) was compared to that of the control GST pull-down experiment (Fig.12a lane 1) and quantified using Image Gauge (Fig.12b). These results suggested that the C-terminus of NHE1 could bind a fragment of calcineurin.

2.2 *Analysis of an NHE1-binding Fragment by Mass Spectrometry*

The identity of the 31 kDa protein band was investigated using mass spectrometry, to confirm whether it was a fragment of calcineurin or a contaminant that copurified with calcineurin. A sample of purified calcineurin protein (10 μg total protein) used in GST pull-down experiments was separated on a 10% SDS-PAGE gel and stained with Coomassie blue. The 31 kDa protein band was excised from the gel and submitted to the Institute for Biomolecular Design (IBD) for sequencing. The results of the mass spectrometry identified the 31 kDa protein as a fragment of calcineurin located in the N-terminal region of the protein sequence between amino acids 32 and 43 (Fig.12c, bold black sequence). The results confirmed that the 31 kDa protein was an N-terminal fragment of calcineurin that can bind to the C-terminus of NHE1.

2.2 *Analysis of Phosphatase-NHE1 Binding via Immunoblotting with PP1 or PP2B Specific Antibodies*

Two other antibodies were utilized in the Western Blot analysis of PCRA-PP1 or PCRA-PP2B, GST pull-down experiments. First, a monoclonal antibody raised against the PP1α isoform was used to specifically detect PP1 interaction with the C-terminus of NHE1. Negative controls, GST protein (Fig.13a. lane 1) PCRA (Fig.13a. lane 2), and a positive control of purified PP1 (Fig.13a. lane 8), were included in the SDS-PAGE gel. The resulting immunoblot clearly showed that PP1 bound to PCRA (Fig.13a. lanes 5-7) and bound to GST alone (Fig.13a. lanes 3,4). The binding of PP1 to PCRA (Fig.13b. NHE1 PP1) was not significantly greater than to GST alone (Fig.13b. GST PP1). These GST pull-down results suggest that PP1 lacks the ability to bind to the C-terminus of NHE1.

Finally, to further observe the interactions of full length PP2B protein with the NHE1 C-terminal fusion protein, a polyclonal antibody raised against amino acids 312-521 of PP2B was used. The anti-PP2B reacts with the C-terminus of PP2B therefore the N-terminus of PP2B was not detected. Controls, GST protein (Fig.14a. lane 1) PCRA (Fig.14a. lane 2) and PP2B (Fig.14a. lane 7) were included in the SDS-PAGE gel. These results demonstrated that PP2B bound to both PCRA (Fig.14a. lanes 4-6) and GST alone (Fig.14a. lane 3). Quantification of the protein bands using Image Gauge illustrated that binding of PP2B to PCRA (Fig.14b. NHE1 PP2B) was not significantly greater than to GST alone (Fig.14b. GST PP2B), suggesting that full length PP2B does not bind with the C-terminus of NHE1.

3. *In Vivo* Interactions of NHE1 and Protein Phosphatases

To examine the interactions between NHE1 and protein phosphatases *in vivo* we used immunoprecipitation reactions. Initial immunoprecipitations of NHE1 were executed without pretreatment of cells with cross-linking reagents. Two cell lines were employed in immunoprecipitation of NHE1 studies, the PS127A Chinese hamster lung fibroblast cell line [177] and the AP1-NHE1 Chinese hamster ovary cell line [215]. Both cell lines overexpress human NHE1; however, the NHE1 sequence in AP1-NHE1 cells contains an HA epitope tag [215]. To ensure expression of NHE1, the PS127A cell line required periodic acid selection treatment [227], as previously outlined in the methods section 5.1.

Cell lysates from both cell lines were prepared in advance as described earlier. These were thawed on ice and 100 µl of each lysate was retained as a positive control. Immunoprecipitation of NHE1 was achieved using 30 µl of a rabbit polyclonal, anti-NHE1 antibody [216]. The final immunoprecipitates were separated on a 10% SDS-PAGE gel, followed by transfer to a nitrocellulose membrane. The membrane was subsequently probed with either a mouse monoclonal primary antibody against NHE1 (Chemicon), or a mouse monoclonal primary antibody against the HA epitope tag, which was used exclusively with the AP1-NHE1 immunoprecipitates. In both cases the secondary antibody used in the immunological reaction was goat anti-mouse.

Fig.15a. (IP NHE1) illustrates successfully immunoprecipitated NHE1 from AP1-NHE1 cells. A positive control is illustrated (Ctrl Lysate) using a cell lysate of the same cell line. Similar results are illustrated in the right panel from PS127A lung fibroblasts. They demonstrate an immunoprecipitated NHE1 (Fig.15a. IP NHE1), in

comparison to a positive control using a sample of the PS127A cell lysate (Ctrl Lysate).

3.1. *Immunoblot Analysis Following Immunoprecipitation of NHE1*

To investigate whether PP1 or PP2B could bind to NHE1 in either cell line the nitrocellulose membrane (Fig.15a) was stripped by incubation in an acidic glycine solution pH 2.8 for 30 minutes at room temperature. The stripping solution was washed several times with TBS and water, and the membrane was than immunoblotted with a primary antibody to the phosphatase of interest. The primary antibodies utilized in these experiments were, polyclonal anti-PP1α, monoclonal anti-PP1 or polyclonal anti-PP2B, previously described. We were not able to detect any binding of PP1 nor PP2B to NHE1 in these cells (not shown). This lead us to the approach of treating cells with cross-linker compounds to secure a possible phosphatase and NHE1 interaction, that might not be strong enough to survive the immunoprecipitation protocol.

3.2. *Cross-linking and Immunoprecipitation Analysis of NHE1*

The AP1-NHE1 cell line was exclusively utilized in cross-linking studies followed by immunoprecipitation of NHE1, identical to that previously described. The cells were treated with N-Hydroxysuccinimide-ester cross-linkers DSS (Disuccinimidyl suberate) or DSP [Dithiobis(succinimidylopropionate)] to determine if PP1 or PP2B could be linked to NHE1 by these covalent bond-forming reagents. DSS and DSP are both water insoluble reagents, and consequently were dissolved in

dimethyl sulfoxide (DMSO) immediately before use to eliminate the possibility of hydrolysis. Cultured AP1-NHE1 cells were washed with PBS and incubated in PBS in the presence of 2 mM of cross-linking reagent for 30 minutes at room temperature, after which the reaction was quenched using Tris-HCl at pH 7.0. Cell lysates were prepared and used for immunoprecipitation and immunological analysis as outlined earlier.

Western Blot analysis of immunoprecipitated and cross-linked NHE1 from AP1-NHE1 cells was performed using three distinct antibodies. To detect immunoprecipitated NHE1, a monoclonal anti-NHE1 antibody was used. Immunoblot analysis using this antibody (Fig.15b, IP NHE1 DSS or DSP) revealed a cross-linked NHE1 protein (>203 kDa, top arrow) in addition to NHE1 (~115 kDa, bottom arrow). In all cases the majority of the NHE1 was >203 kDa; however, slightly more NHE1 appeared to be cross-linked in cells treated with DSS (Fig.15b IP NHE1 DSS, top arrow).

To detect possible PP1 binding to NHE1 following immunoprecipitation of NHE1 from cross-linked cells, a monoclonal anti-PP1 antibody was used for immunoblot analysis. A ~ 32 kDa protein band was observed in samples of immunoprecipitated NHE1 from cells cross-linked with DSS or DSP (Fig.16a. IP NHE1 DSS or DSP, arrow). Based on the positive control of purified PP1 ~ 37 kDa (Fig.16a. +Ctrl PP1), and the high specificity of the antibody used, the immunoreactive ~ 32 kDa protein bands were identified as PP1 proteins interacting with NHE1. PP1 was not detected in untreated cell lysates (Fig.16a. +Ctrl Lysate) from which NHE1 was immunoprecipitated.

To detect possible PP2B binding to NHE1 following immunoprecipitation of NHE1 from cross-linked cells, a polyclonal anti-PP2B antibody was utilized in the immunological reaction. PP2B binding was not detected in samples of immunoprecipitated NHE1 from untreated cells (Fig.16b. +Ctrl Lysate) or cross-linked cells (Fig.16b. IP NHE1 DSS or DSP). The recognition of the positive control of PP2B on the immunoblot (Fig.16b. +Ctrl PP2B) confirmed that the immunoblotting reaction was working correctly. Overall, the immunoprecipitation results indicated that NHE1 can be cross-linked to PP1 in living cells.

4. The Effects of Phosphatases on NHE1 Activity in Mammalian Cells

4.1 *NHE1 Activity in Neonatal Rat Cardiomyocytes Treated with Okadaic Acid*

Initial experiments to investigate the effect of phosphatases on NHE1 activity involved the treatment of neonatal rat cardiac myocytes with the phosphatase inhibitor okadaic acid. Okadaic acid inhibits different phosphatases at different concentrations. It inhibits PP2A at nanomolar concentrations, PP1 at micromolar concentrations and it is a weak inhibitor of PP2B [107]. Myocytes were treated with 8 μM okadaic acid in Na^+-containing buffer and allowed to recover from an ammonium chloride induced acid load (40 mM NH_4Cl). The long-term recovery from an acid load was calculated every 5 minutes for 15 minutes. Fig. 17a illustrates that okadaic acid caused only a minor change in pH after 15 minutes. The myocytes treated with okadaic acid were also used to examine steady-state pH. In these experiments the intracellular pH was measured in myocytes treated with 8 μM okadaic acid in Na^+-

containing buffer for 10 minutes but without an acid load. Fig. 17b illustrates that steady-state pH did not change after 10 minutes when the myocytes were treated with okadaic acid. These results did not show any effect of the okadaic acid sensitive phosphatase, PP2A on NHE1 activity. The results suggested that phosphatases more resistant to okadaic acid inhibition may be more important in regulating NHE1 activity cardiomyocytes.

4.2 *NHE1 Activity in Cells Transiently Overexpressing PP1 or PP2B*

Further experiments to test the effect of protein phosphatases on NHE1 activity involved transient transfections of PP1 or PP2B into CHO cells. Fig. 18a (PP1, top arrow) illustrates overexpression of PP1 in CHO cells after 24 hours of the transfection. Endogenous PP1 expression was also detected using the monoclonal anti-PP1 antibody (bottom arrow) in CHO cells transiently transfected with PP1 (PP1) and in CHO cells transfected with an empty vector (Ctrl Empty Vector). A positive control of purified PP1 (+Ctrl PP1) was used to confirm the immunoreactivity of the antibody. The rate of recovery from an ammonium chloride induced acid load was measured as described in the methods section 9.1. Fig. 18b shows that transient overexpression of human PP1γ did not effect the rate of recovery from an ammonium chloride induced acid load (Fig.18b, PP1) compared with cells mock-transfected with an empty vector (Fig.18b, Ctrl Empty Vector). Fig. 19a (PP2B, arrow) shows that PP2B was expressed in CHO cells after 24 hours of the transfection. Similarly, the rate of recovery from an acid load was not significantly different in CHO cells transiently expressing a constitutively active form of PP2B

(Fig.19b, PP2B), compared to cells mock-transfected with an empty vector (Fig.19b. Ctrl Empty Vector).

4.3. *NHE1 Activity in Cells Stably Overexpressing PP1 and I2*

To obtain a higher degree of more consistent phosphatase expression, stable cell lines were made of CHO cells transfected with pDEST40-PP1 or pDEST40-I2 expression plasmids, as previously described in the methods section 7.4. Stable cell lines overexpressing PP2B were not successful despite the 57% transfection efficiency and screening of 30 isolated colonies by Western blotting. The transfection efficiency of cells transfected with pDEST40-PP1 or pDEST40-I2 was 57% and 45% respectfully. Stable expression of V5-epitope tagged PP1 and I2 in CHO cells was obtained and verified using a polyclonal anti-V5 antibody. Two colonies for each cell line (Fig.20) were examined. The PP1 cell line #42 exhibited a lower level of PP1 overexpression (Fig.20 Col#42 PP1) compared with cell line PP1 #15 (Fig.20 Col#15 PP1). Both cell lines overexpressing I2 showed relatively the same level of I2 expression (Fig.20 Col#2, Col#21 I2). Control cells were mock-transfected with an empty vector and showed no expression of V5-tagged PP1 or I2 (Fig.20 Ctrl Empty Vector). These cell lines were used to measure the rate of recovery from an ammonium chloride induced acid load, in the presence or absence of the hormone thrombin. A typical tracing of these experiments is illustrated in Fig.21a,b and Fig.22 summarizes the results. The unstimulated rate of recovery was significantly slower in cells overexpressing PP1 (Fig.22a columns 2,4), when compared with the rate of recovery in control cells mock-transfected with an empty vector (Fig.22a columns

1,3). In contrast, cells overexpressing I2 demonstrated a significantly faster rate of recovery (Fig.22b columns 2,4), compared to age and growth matched control cells (Fig.22b columns 1,3).

In previous findings thrombin has been shown to stimulate the Na^+/H^+ exchanger [56, 225, 226]. In this report these results were reproduced using CHO cells mock-transfected with an empty pDEST40 expression plasmid (Fig.23a,b, columns 1,2). In cells overexpressing PP1 the results were found to be similar. The addition of thrombin during the recovery of cells from an acid challenge, resulted in a higher rate of recovery from an acid load (Fig.23a columns 4,6), compared with unstimulated cells overexpressing PP1 (Fig.23a columns 3,5). The effect of thrombin on NHE activity was not observed in cells overexpressing I2. Thrombin failed to stimulate the NHE (Fig.23b columns 4,6) and the rate of recovery from an acid load was not different from that of unstimulated I2 expressing cells (Fig.23b columns 3,5).

4.4. *Measurement of H^+ Extrusion from Cells Stably Overexpressing PP1 and I2*

To confirm that the changes in recovery from acid loads were due to the activity of the NHE, and not due to changes in cell buffering, we measured the buffering capacity of various cell lines. The calculated buffering capacity [228] of cell lines overexpressing PP1 was 12.44 mM/pH, and of cell lines overexpressing I2 it was 38.75 mM/pH, compared with the buffering capacity of mock-transfected cell lines which was 28.13 mM/pH. The buffering capacity was subsequently utilized to determine the H^+ efflux in cells stably overexpressing PP1 or I2. The average calculated H^+ extrusion rate was significantly decreased in cells overexpressing PP1

(Fig.24a PP1 Cells). Contrasting results were observed in cells overexpressing I2, where the average calculated H^+ efflux rate was greatly increased (Fig.24b I2 Cells).

4.5. *NHE1 Activity Inhibition*

To verify that the activity we determined was due to NHE mechanisms, the rate of recovery from an ammonium chloride induced acid load measured in the presence of HMA (a specific NHE inhibitor). The results obtained with the control and I2 overexpressing cells were representative of pH measurements in other cells. HMA completely abolished the recovery from an acid load in both cell lines (Fig.25 lanes 3,4).

5. NHE1 Expression in Cells Stably Overexpressing PP1 and I2

To determine whether the changes in NHE1 activity that were observed were a result of changes in NHE1 protein expression, Western blot analysis was performed using cell lysates of the cell lines tested in fluorometric experiments, subsequently probed for NHE1 expression with a monoclonal anti-NHE1 antibody. The positive control used was an HA-tagged NHE1 (Fig.26a right arrow), which is slightly larger in size than the untagged NHE1 expressed in normal CHO cells (Fig.26a left arrow). NHE1 protein expression in cells overexpressing PP1 (Fig.26a PP1 cells) was similar to that seen in control cells (Fig.26a Ctrl Empty Vector). Similarly, in cells overexpressing I2, the level of NHE1 protein expression (Fig.27a I2 cells) was almost identical to the level of NHE1 expressed in mock-transfected cells (Fig.27a Ctrl

Empty Vector). There was no significant alteration of NHE1 protein expression in cells overexpressing PP1 or I2.

6. Measuring Phosphorylase Phosphatase and PP1 Activity

The level of phosphorylase phosphatase (PP1/PP2A) activity was examined in heart cell extracts utilized in dephosphorylation studies previously described in the methods section 2.2. To measure the level of phosphorylase phosphatase activity phosphatase assays were done using the phosphorylase *a* substrate, as described in the methods section 8. Heart cell extracts in the presence of okadaic acid were used as the control (Fig. 28a Ctrl) and the level of phosphorylase phosphatase activity in the control was normalized to 100%. Two samples of heart extracts were examined in triplicate assays. Fig. 28a shows that both samples of heart extracts had over 60% of total phosphorylase phosphatase activity. Similar phosphatase assays were also done to test the level of phosphorylase phosphatase activity and PP1 activity in various cell lines. In cell lines overexpressing I2 the total phosphorylase phosphatase activity was lower (Fig.28b columns 3,5) compared with control cells mock-transfected with an empty vector (Fig.28b column 1). Phosphorylase phosphatase activity represents combined PP1 and PP2A activity. The PP1 activity in these cell lines was calculated according to the formulas in Table 10. Similarly, control cells showed a higher level of PP1 activity (Fig.28b column 2) compared with cells overexpressing I2 (Fig.28b columns 4,6). The cell lysates were assayed in triplicate samples. Values obtained among the triplicate samples were within 100-200 counts per minute, which is a small variation and therefore standard errors are too small to be displayed. For reason

unknown at this time, several attempts at phosphatase assays of PP1 activity were not successful in the cell lines overexpressing PP1.

Fig. 6. NHE1 dephosphorylation by PP1.
A: Representative autoradiogram of dephosphorylation of the C-terminal cytoplasmic NHE1 GST-fusion protein (PCRA, arrow). DP PP1/Mn^{2+}, experimental samples treated with 10 μg PP1 plus 5 mM $MnCl_2$.
DP Ctrl, control samples treated the same as experimental samples except without PP1. B: Coomassie blue stained SDS-PAGE gel illustrating the amount of PCRA (arrow) present in each dephosphorylation reaction.
C: Quantitative analysis of the [^{32}P]:protein ratio in the presence (PP1/Mn^{2+}) or absence (Ctrl) of PP1. * means that PP1 significantly dephosphorylated the C-terminus of NHE1, $p < 0.01$. Results are mean ± SE of 6 experiments.

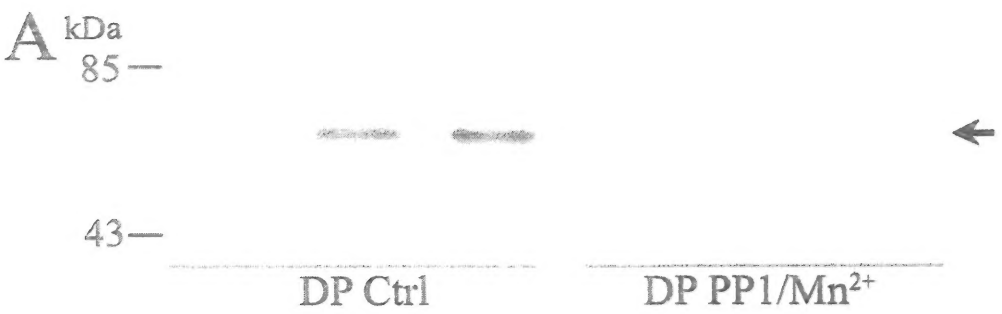
A
kDa
85—
43—
DP Ctrl
DP PP1/Mn2+

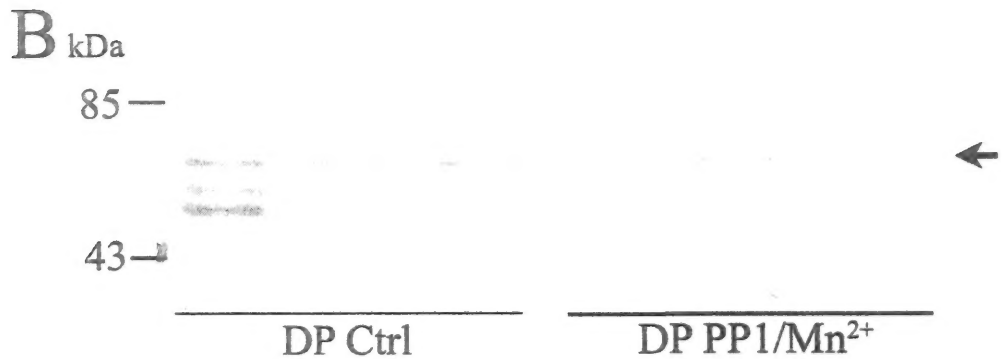
B
kDa
85—
43—
DP Ctrl
DP PP1/Mn2+

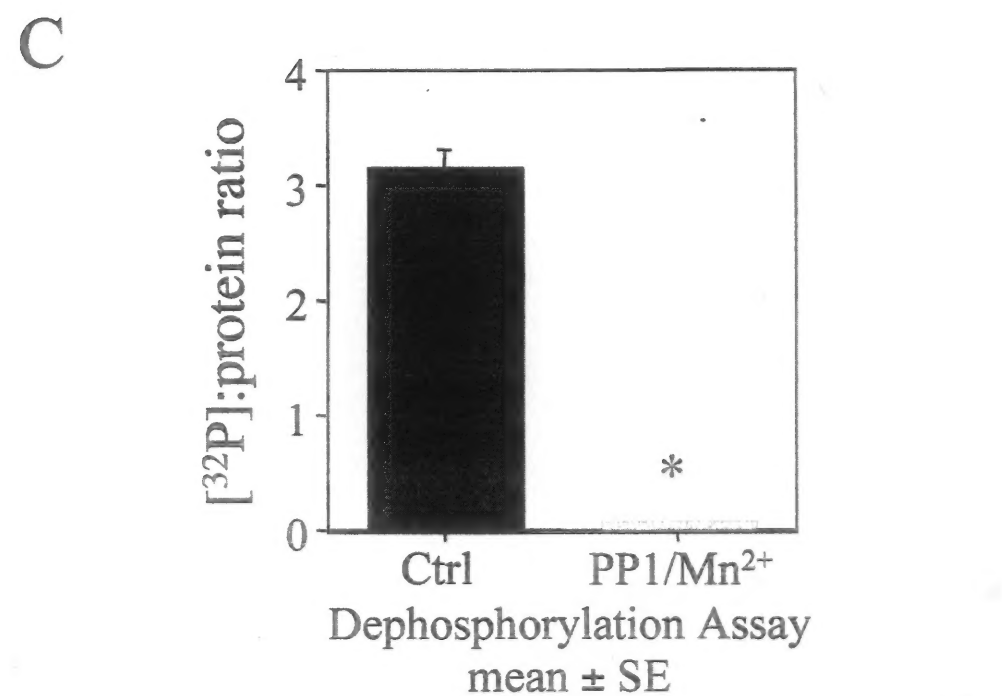
C
[32P]:protein ratio
4
3
2
1
0
*
Ctrl
PP1/Mn2+
Dephosphorylation Assay
mean ± SE

Fig. 7. Dephosphorylation of NHE1 by PP2A in the presence and absence of Mn^{2+}. A: Representative autoradiogram of dephosphorylation of the C-terminal cytoplasmic NHE1 GST-fusion protein (PCRA, arrow) by 10 μg PP2A in the presence or absence of 5 mM Mn^{2+} (DP PP2A $+Mn^{2+}$), (DP PP2A $-Mn^{2+}$). Control dephosphorylation (DP Ctrl) lacked PP2A. Dephosphorylation in the presence of PP1 was used as a positive control (DP PP1) B: Coomassie blue stained SDS-PAGE gel illustrating the amount of PCRA (arrow) present in each dephosphorylation reaction. C: Quantitative analysis of [^{32}P]:protein ratio in the presence (PP2A $+Mn^{2+}$) or absence (PP2A $-Mn^{2+}$) of 5 mM Mn^{2+} and in the absence of PP2A (Ctrl). * means that PP2A$+Mn^{2+}$, PP2A$-Mn^{2+}$ and PP1$+Mn^{2+}$, significantly dephosphorylated the C-terminus of NHE1, $p < 0.05$ for each experiment, results are mean ± SE of 4 experiments. ‡ means that dephosphorylation of NHE1 by PP2A$-Mn^{2+}$ was significantly greater than by PP2A$+Mn^{2+}$, $p < 0.05$, results are mean ± SE of 4 experiments. # means that dephosphorylation of NHE1 by PP1$+Mn^{2+}$ was significantly greater than by PP2A$-Mn^{2+}$, $p < 0.05$, results are mean ±SE of 4 experiments.

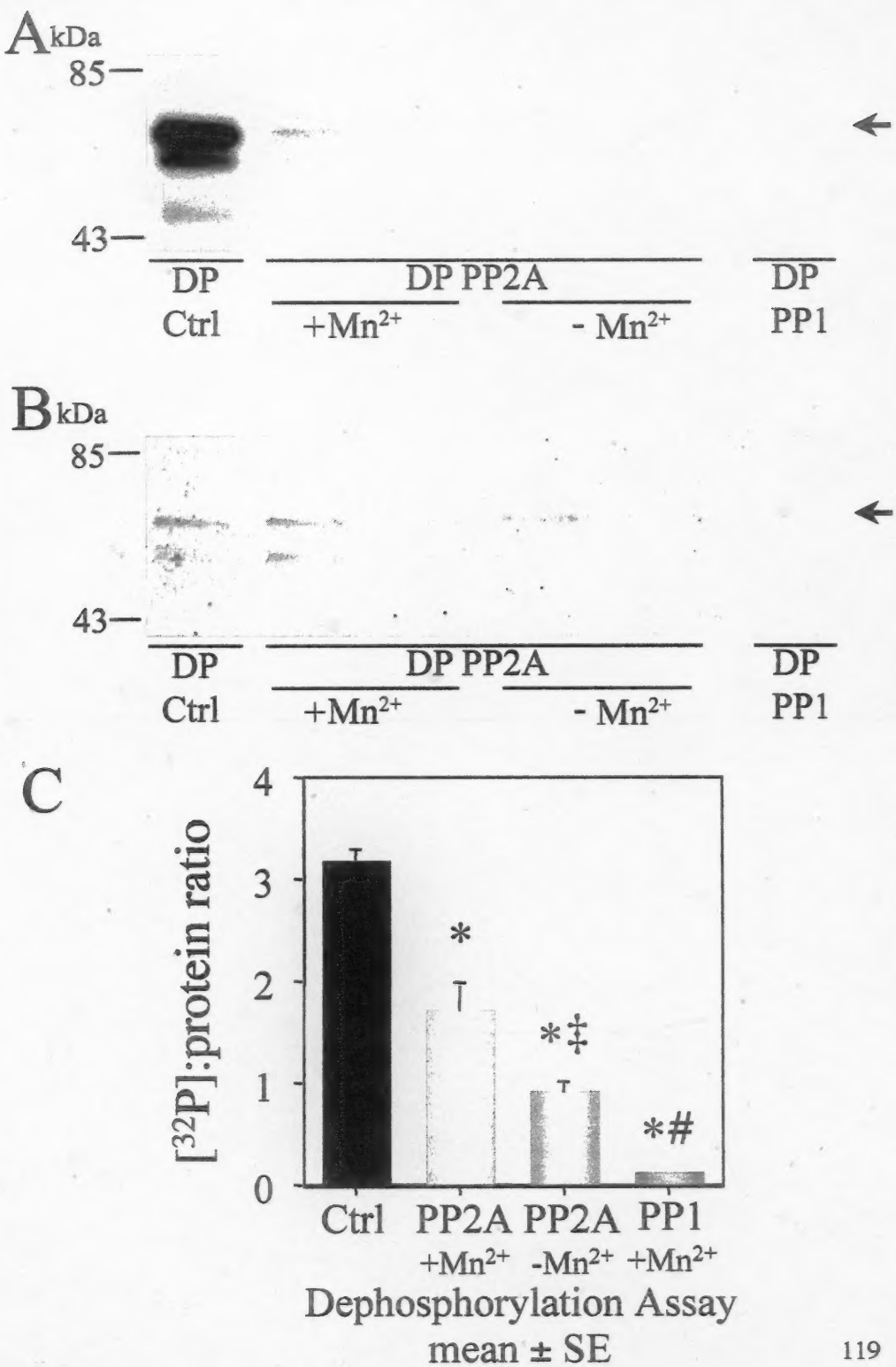
A
kDa
85—
43—
DP
Ctrl
DP PP2A
+Mn2+
- Mn2+
DP
PP1
B
kDa
85—
43—
DP
Ctrl
DP PP2A
+Mn2+
- Mn2+
DP
PP1
C
[32P]:protein ratio
4
3
2
1
0
*
*‡
*#
Ctrl
PP2A +Mn2+
PP2A -Mn2+
PP1 +Mn2+
Dephosphorylation Assay
mean ± SE

Fig. 8. NHE1 dephosphorylation by PP2B.
A: Representative autoradiogram of dephosphorylation of the C-terminal cytoplasmic NHE1 GST-fusion protein (PCRA, arrow) in the presence of 10 μg PP2B, 10 mM calcium and 5 μg calmodulin (DP PP2B/Ca^{2+}/CaM). Control dephosphorylation (DP Ctrl) lacked PP2B. P, phosphorylated PCRA; C, PCRA not phosphorylated. B: Coomassie blue stained SDS-PAGE gel illustrating the amount of PCRA (arrow) present in each dephosphorylation reaction. C: Quantitative analysis of [^{32}P]:protein ratio in the presence of PP2B/Ca^{2+}/CaM and absence of PP2B/Ca^{2+}/CaM (Ctrl). PP2B did not significantly dephosphorylate the C-terminus of NHE1, $p > 0.6$. Results are mean ± SE of 7 experiments.

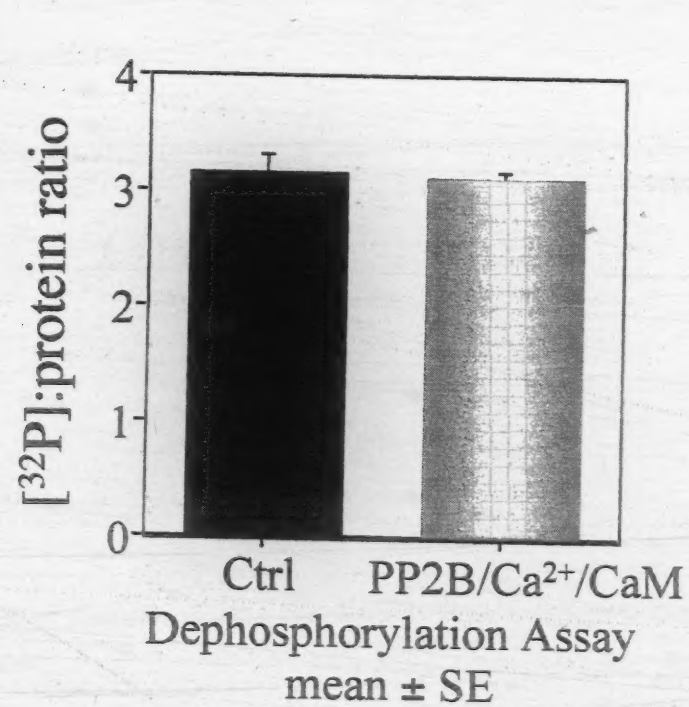

Dephosphorylation Assay
mean ± SE

Fig. 9a,b. NHE1 dephosphorylation by PP1.
A: Representative autoradiogram of dephosphorylation of the C-terminal cytoplasmic NHE1 GST-fusion protein (PCRA, arrow) in the presence of 10 μg PP1 plus 5 mM $MnCl_2$ for 15 minutes (DP PP1/Mn^{2+}). Control dephosphorylation (DP Ctrl) lacked PP1. B: Coomassie blue stained SDS-PAGE gel illustrating the amount of PCRA (arrow) present in each dephosphorylation reaction.

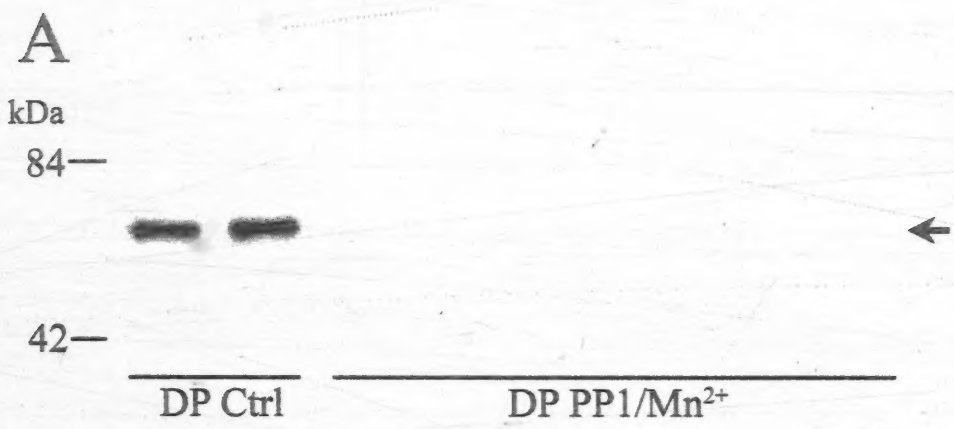
A
kDa
84—
42—
DP Ctrl
DP PP1/Mn2+

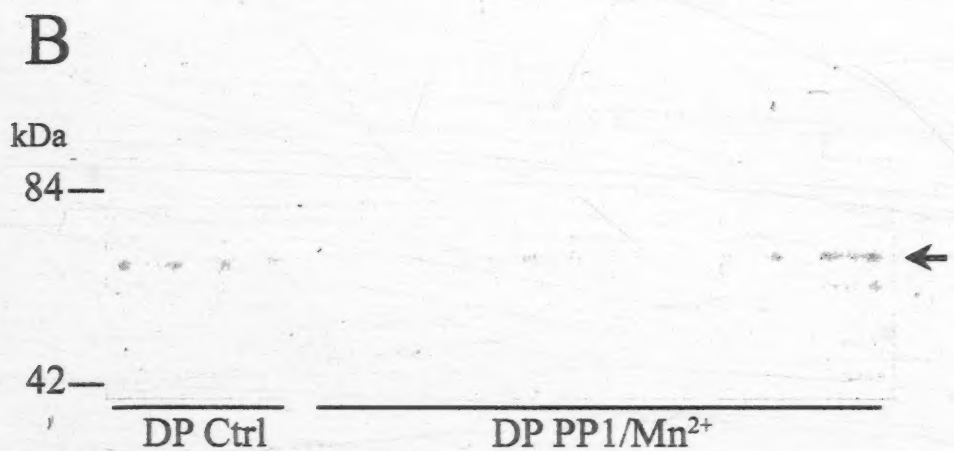
B
kDa
84—
42—
DP Ctrl
DP PP1/Mn2+

Fig. 9c-e. Dephosphorylation of NHE1 by PP1 in the presence of spinophilin. C: Representative autoradiogram of dephosphorylation of the C-terminal cytoplasmic NHE1 GST-fusion protein (PCRA, arrow) in the presence of 10 μg PP1 plus 5 mM $MnCl_2$ + 5 μg spinophilin (DP PP1/Mn^{2+}.Spinophilin) for 15 minutes. Control dephosphorylation (DP Ctrl) lacked PP1+spinophilin. D: Coomassie blue stained SDS-PAGE gel illustrating the amount of PCRA (arrow) present in each dephosphorylation reaction. E: Quantitative analysis of the [^{32}P]:protein ratio in the presence of PP1+spinophilin or absence (control) reactions. PP1 almost completely dephosphorylated NHE1; however the degree of PP1 dephosphorylation was significantly reduced in the presence of spinophilin. Results are mean of ± SE of 6 experiments. * means PP1 significantly dephosphorylated NHE1 in the absence and presence of spinophilin, $p < 0.01$. ‡ means that spinophilin significantly reduced dephosphorylation of NHE1 by PP1, $p < 0.01$.

C

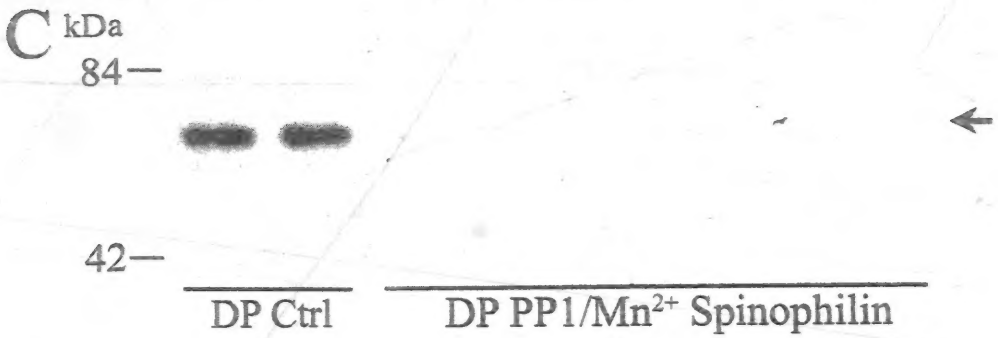

D

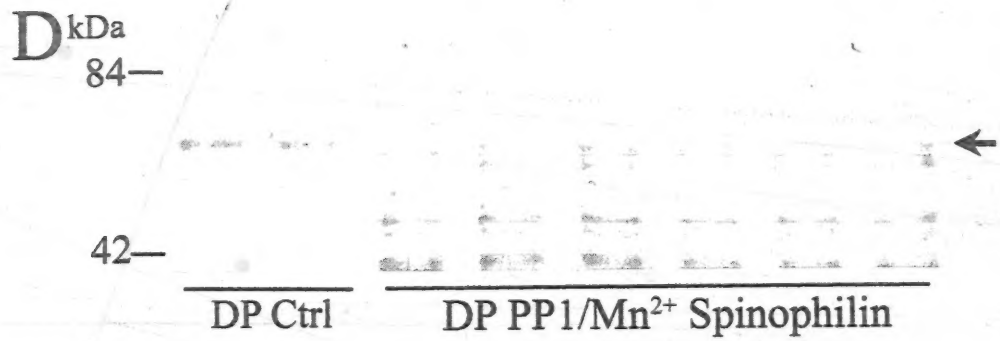

E

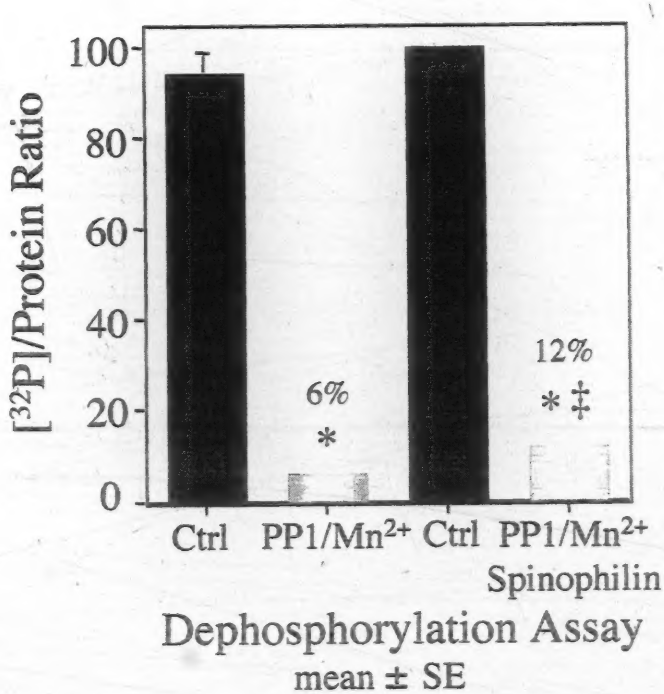

Dephosphorylation Assay

mean ± SE

Fig. 10. NHE1 dephosphorylation by crude heart cell extracts.
A: Representative autoradiogram of dephosphorylation of the C-terminal cytoplasmic NHE1 GST-fusion protein (PCRA, arrow) in the presence of heart cell extracts (DP heart cell extracts). Control dephosphorylations (DP Ctrl) lacked heart extracts. Phosphorylation of PCRA resulted in a strong [^{32}P] signal (P) compared to the unphosphorylated PCRA fusion protein (C). B: Coomassie blue stained SDS-PAGE gel illustrates the amount of PCRA (arrow) present in each dephosphorylation reaction. C: Quantitative analysis of the [^{32}P]:protein ratio in the presence (Heart Cell Extracts) or absence (Ctrl) of heart cell extracts. Heart cell extracts did not significantly dephosphorylate NHE1, $p=1$. Results are mean ± SE of 4 experiments.

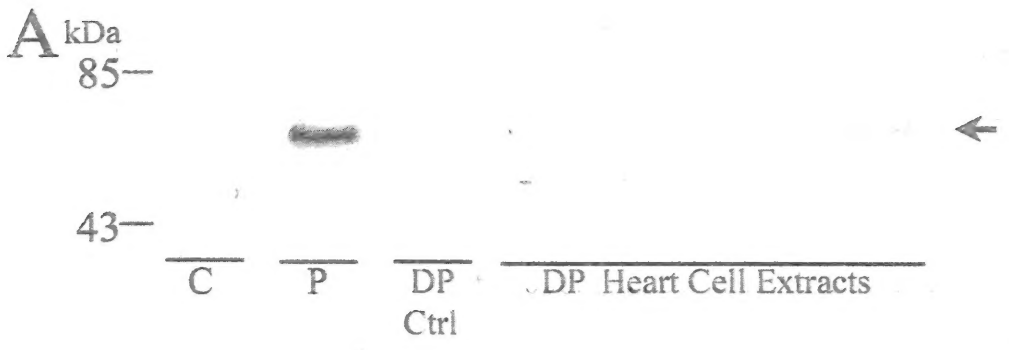
A
kDa
85—
43—
C
P
DP Ctrl
DP Heart Cell Extracts

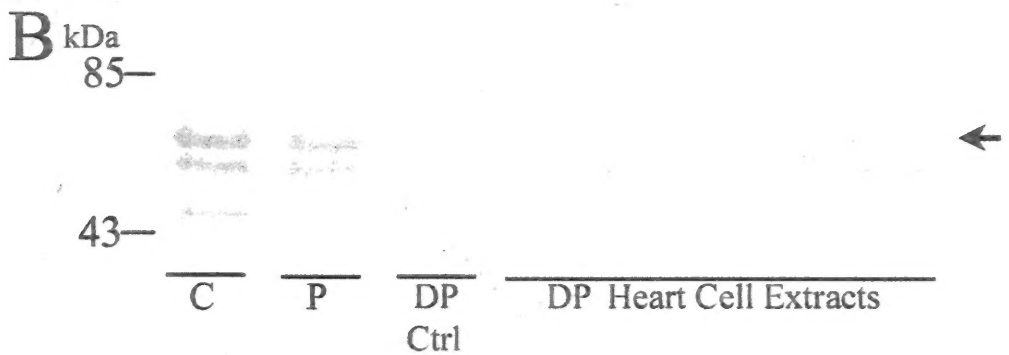
B
kDa
85—
43—
C
P
DP Ctrl
DP Heart Cell Extracts

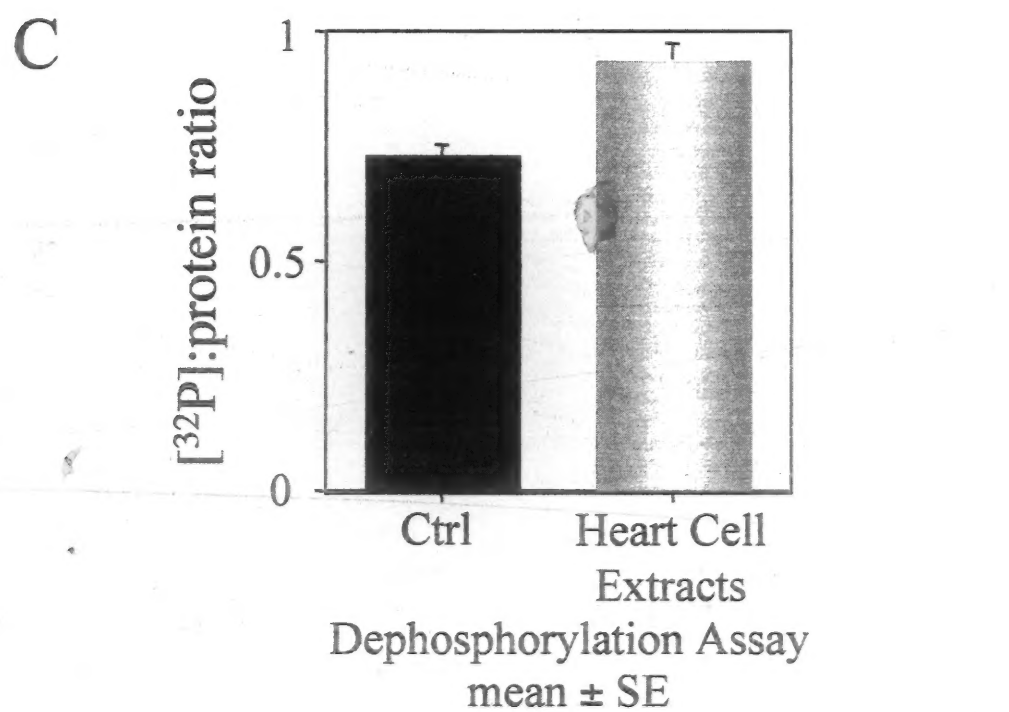
C
[32P]:protein ratio
1
0.5
0
Ctrl
Heart Cell Extracts
Dephosphorylation Assay
mean ± SE

Fig. 11. Western blot analysis of PP1 present in NHE1 GST pull-down assays using a broad range phosphatase antibody.

A: Representative Western blot was probed with a polyclonal anti-PP1 (broad range phosphatase) antibody. The GST protein (lane 1) and C-terminal NHE1 GST-fusion protein PCRA (lane 2) were used alone as negative controls. GST incubated with PP1 was used as a control (lanes 3,4). A positive control of purified PP1 was used to confirm immunoreactivity of the antibody (lane 7). PP1 bound to PCRA, (arrow, lanes 5,6) and to GST alone (arrow, lanes 3,4). B: Quantitative analysis of GST pull-down experiments with PP1 and GST alone (GST PP1) or with PCRA (NHE1 PP1). * means that PP1 binding to PCRA is significantly greater than to GST alone, $p < 0.05$, results are mean ± SE of 4 experiments.

A

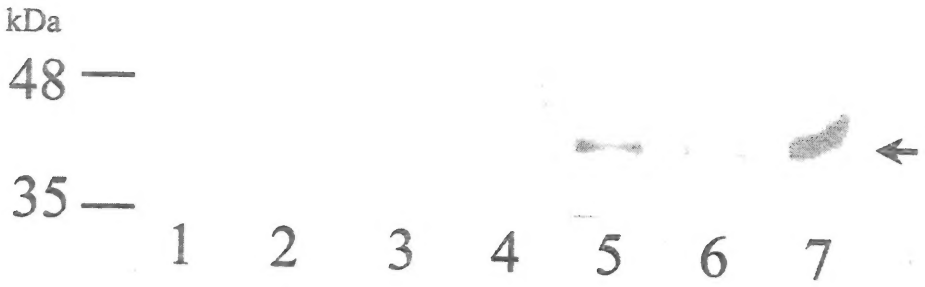
kDa
48
35
1
2
3
4
5
6
7

B

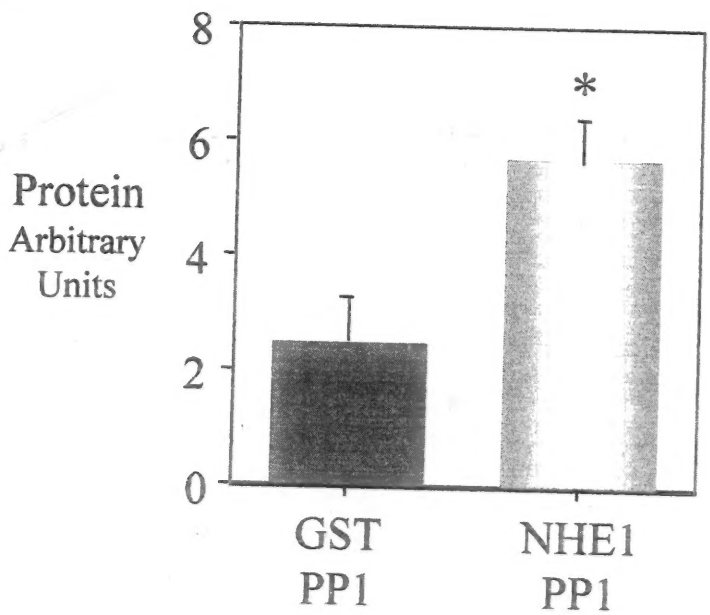
Protein
Arbitrary
Units
8
6
4
2
0
*
GST
PP1
NHE1
PP1

Fig. 12. Western blot analysis of PP2B present in NHE1 GST pull-down assays using a broad range phosphatase antibody.

A: Representative Western blot was probed with a polyclonal anti-PP1 (broad range phosphatase) antibody. GST alone, incubated with PP2B was used as a control (lane 1). A positive control of purified PP2B was used to confirm immunoreactivity of the antibody (lane 5). The C-terminal NHE1 GST-fusion protein PCRA was used alone as a negative control (lane 4). Full length PP2B (61kDa, top arrow) did not bind to GST alone (lane 1) or PCRA (lanes 2,3). A 31kDa fragment present in the PP2B sample (bottom arrow) bound to PCRA (lanes 2,3) but not to GST alone (lane 1). B: Quantitative analysis of GST pull-down experiments with PP2B and GST alone (GST PP2B) or with PCRA (NHE1 PP2B). Only 2 control (GST PP2B) experiments performed. SE is not visible because it is too small to be displayed. Significance is not available due to the low number of control experiments. The dark grey column represents PP2B bound to PCRA. Results are mean ± SE of 3 experiments. C: Representative amino acid sequence of human PP2B. The 31kDa fragment was sequenced and identified as an N-terminal portion of PP2B (bold black sequence).

A

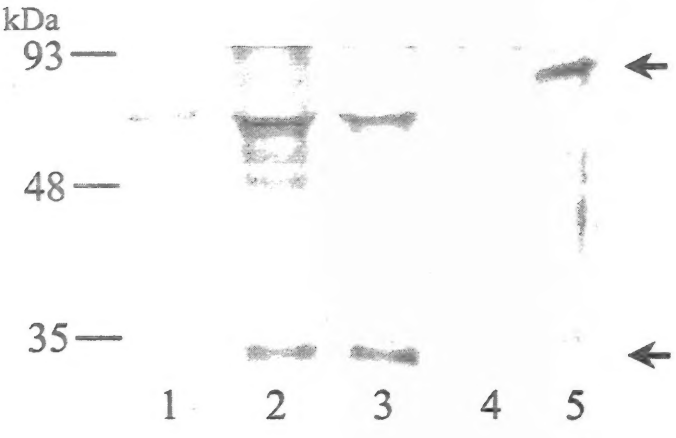

B

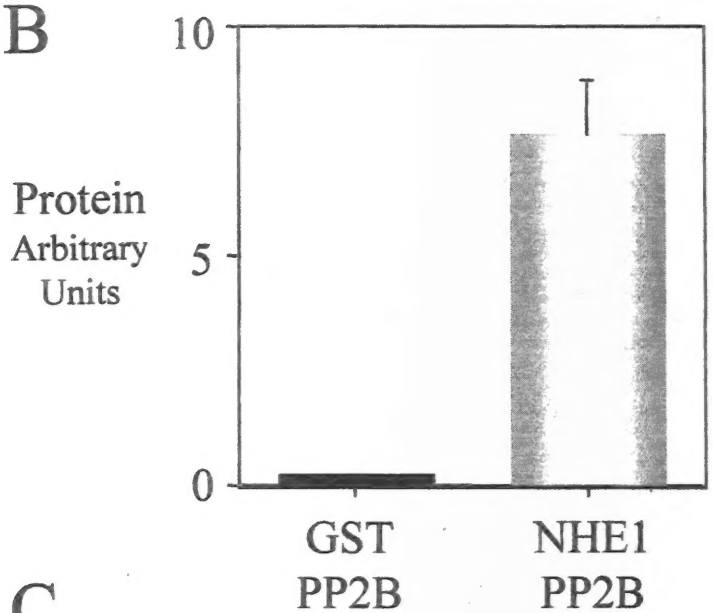

C

```
  1 MSEPKAIDPK LSTTDRVVKA VPFPPSHRLT AKEVFDNDGK PRVDILKAHL
 51 MKEGRLEESV ALRIITEGAS ILRQEKNLLD IDAPVTVCGD IHGQFFDLMK
101 LFEVGGSPAN TRYLFLGDYV DRGYFSIECV LYLWALKILY PKTLFLLRGN
151 HECRHLTEYF TFKQECKIKY SERVYDACMD AFDCLPLAAL MNQQFLCVHG
201 GLSPEINTLD DIRKLDRFKE PPAYGPMCDI LWSDPLEDFG NEKTQEHFTH
251 NTVRGCSYFY SYPAVCDFLQ HNNLLSILRA HEAQDAGYRM YRKSQTTGFP
301 SLITIFSAPN YLDVYNNKAA VLKYENNVMN IRQFNCSPHP YWLPNFMDVF
351 TWSLPFVGEK VTEMLVNVLN ICSDDELGSE EDGFDGATAA ARKEVIRNKI
401 RAIGKMARVF SVLREESESV LTLKGLTPTG MLPSGVLSGG KQTLQSATVE
451 AIEADEAIKG FSPQHKITSF EEAKGLDRIN ERMPPRRDAM PSDANLNSIN
501 KALASETNGT DSNGSNSSNI Q
```

Fig. 13. Western blot analysis of PP1 present in NHE1 GST pull-down assays, using a PP1 specific antibody.

A: Representative Western blot was probed with a monoclonal anti-PP1 antibody. GST incubated with PP1 was used as a control (lanes 3,4). A positive control of purified PP1 was used to confirm immunoreactivity of the antibody (lane 8). The C-terminal NHE1 GST-fusion protein PCRA (lane 2) and GST (lane 1) were used alone, as negative controls. PP1 (arrow) bound to GST alone (lanes 3,4) and to PCRA (lanes 5-7). B: Quantitative analysis of GST pull-down experiments with PP1 and GST alone (GST PP1) or with PCRA (NHE1 PP1). Results are mean ± SE of 3 experiments.

A

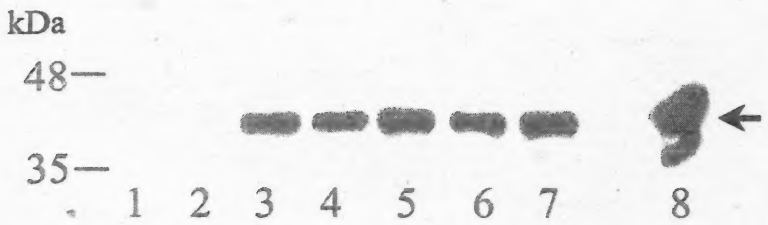
kDa
48—
35—
1 2 3 4 5 6 7 8

B

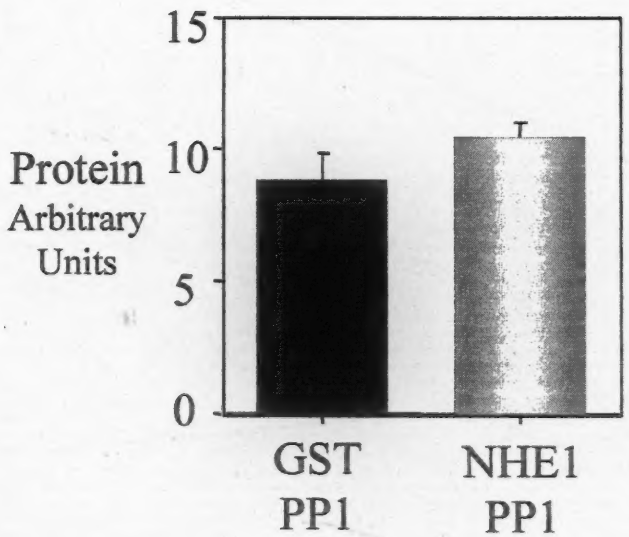
Protein
Arbitrary
Units
15
10
5
0
GST
PP1
NHE1
PP1

Fig. 14. Western blot analysis of PP2B present in NHE1 GST pull-down assays, using a PP2B specific antibody.

A: Representative Western blot was probed with a polyclonal anti-PP2B antibody. GST incubated with PP2B was used as a control (lane 3). A positive control of purified PP2B was used to confirm immunoreactivity of the antibody (lane 7). The C-terminal NHE1 GST-fusion protein PCRA (lane 2) and GST (lane 1) were used alone, as negative controls. Full length PP2B (61kDa, arrow) bound to GST alone (lane 3) and to PCRA (lanes 4-6). B: Quantitative analysis of GST pull-down experiments with PP2B and GST alone (GST PP2B) or with PCRA (NHE1 PP2B). Results for (NHE1 PP2B) are mean ± SE of 3 experiments.

A

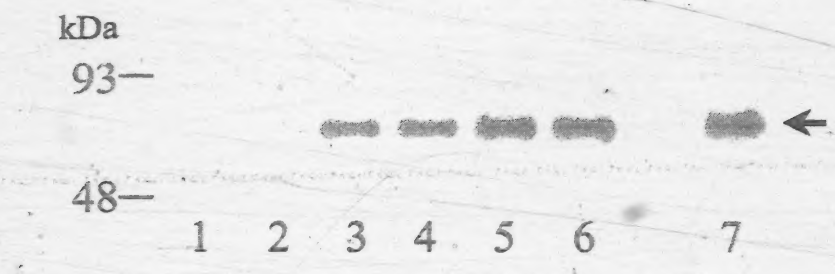
kDa
93—
48—
1 2 3 4 5 6 7

B

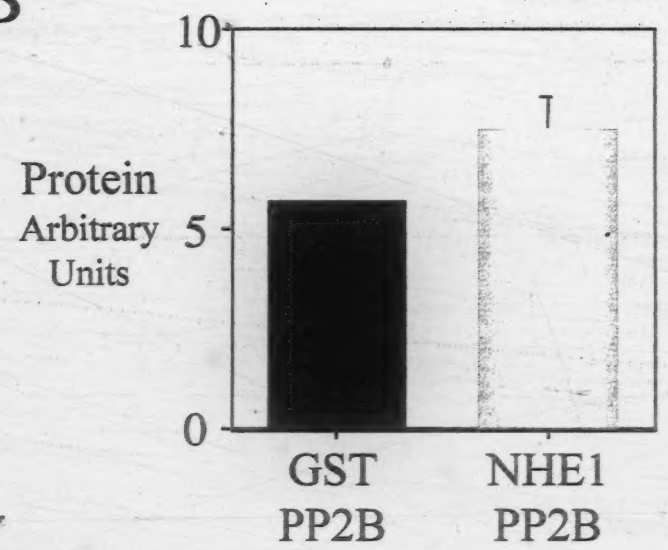
10
5
0
Protein
Arbitrary
Units
GST
PP2B
NHE1
PP2B

Fig. 15. NHE1 immunoprecipitation from AP1-NHE1 and PS127A cells.
A: Representative Western blot of immunoprecipitated (IP) NHE1 (arrow) from AP1-NHE1 and PS127A cell lines. Cell lysates were used as positive controls (Ctrl Lysate) and illustrate NHE1 (arrow) not immunoprecipitated from the AP1-NHE1 and PS127A cell lines. The antibody used for the IP was a polyclonal anti-NHE1 antibody and the antibody used for Western blot analysis was a monoclonal anti-NHE1 antibody (Chemicon). B: Representative Western blot of immunoprecipitated (IP) NHE1 from AP1-NHE1 cells treated with cross-linkers DSS and DSP. The antibodies for IP and for Western blot analysis were as in Fig.12a. Top arrow illustrates cross-linked NHE1; bottom arrow illustrates NHE1 protein of 115 kDa.

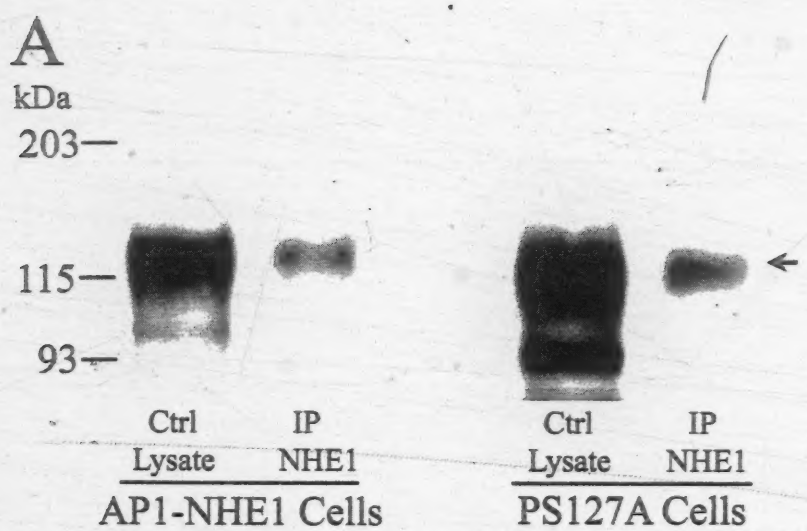
A
kDa
203—
115—
93—
Ctrl Lysate
IP NHE1
Ctrl Lysate
IP NHE1
AP1-NHE1 Cells
PS127A Cells

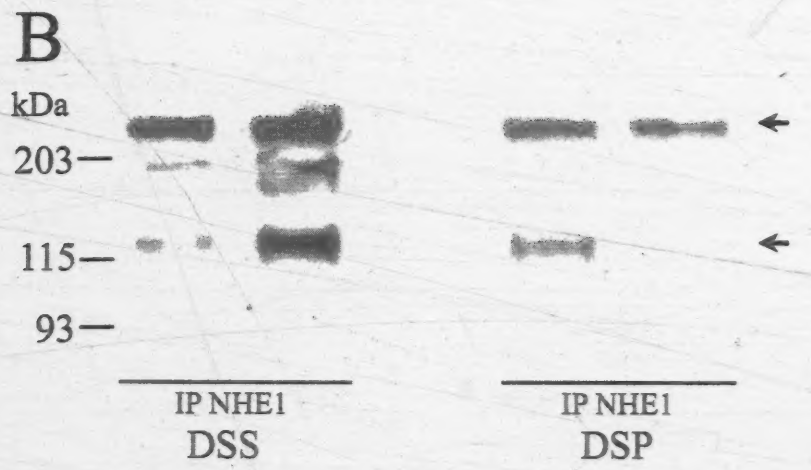
B
kDa
203—
115—
93—
IP NHE1
DSS
IP NHE1
DSP

Fig. 16. Western Blot analysis of phosphatases present in NHE1 immunoprecipitations.

A: After confirming successful immunoprecipitation of NHE1 protein, representative Western blots were stripped and reprobed with a monoclonal anti-PP1 antibody. Untreated cell lysates from the same cells were used as positive controls (+ Ctrl Lysate). A positive control of purified PP1 (+ Ctrl PP1) was used to confirm immunoreactivity of the antibody. PP1 was cross-linked to NHE1 (arrow) in AP1-NHE1 cells (IP NHE1) treated with DSS or DSP. B: Representative Western blot of immunoprecipitated NHE1 (IP NHE1) reprobed with a polyclonal anti-PP2B antibody. Untreated cell lysates from the same cells were used as positive controls (+ Ctrl Lysate). A positive control of purified PP2B (+ Ctrl PP2B) was used to confirm immunoreactivity of the antibody. PP2B was not cross-linked to NHE1 (arrow) in AP1-NHE1 cells (IP NHE1) treated with DSS or DSP.

A

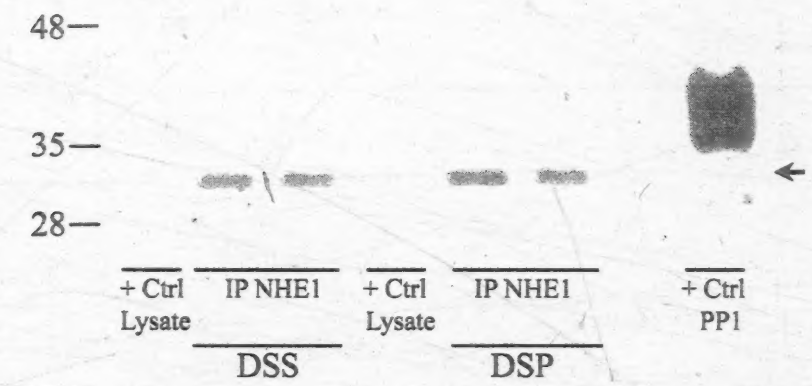
kDa
48—
35—
28—
+ Ctrl Lysate
IP NHE1
+ Ctrl Lysate
IP NHE1
+ Ctrl PP1
DSS
DSP

B

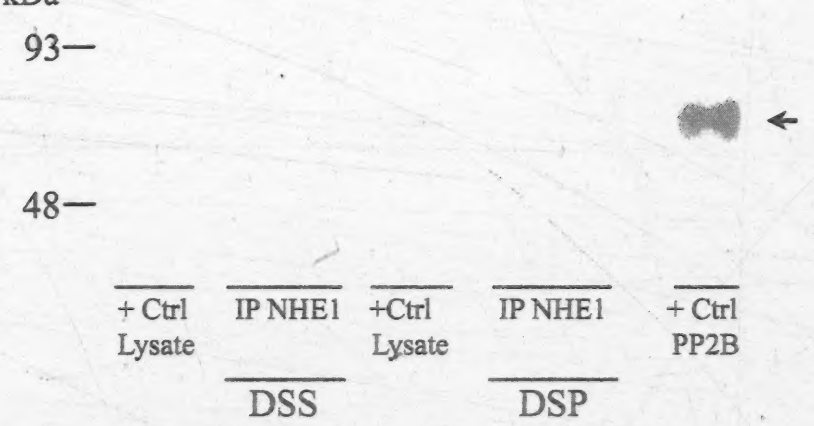
kDa
93—
48—
+ Ctrl Lysate
IP NHE1
+Ctrl Lysate
IP NHE1
+ Ctrl PP2B
DSS
DSP

Fig. 17. NHE1 activity in neonatal rat myocytes treated with phosphatase inhibitor, okadaic acid.

A: To determine if phosphatases regulated NHE1 activity in heart cells, the rate of recovery from an ammonium chloride induced acid load (40mM NH_4Cl) was measured in the presence or absence of 8 μM okadaic acid. Black columns represent control myocytes treated with DMSO. Dark grey columns represent myocytes treated with 8 μM okadaic acid. The change in pH was calculated every 5 minutes for 15 minutes. Results are mean ± SE of 6 experiments. Some SE values are too small to be displayed. B: To determine if phosphatases affected steady state pH, cardiac myocytes were treated with 8 μM okadaic acid in Na^+-containing buffer and the pH was measured (without an acid load) for 10 minutes. Black columns represent control myocytes treated with DMSO. Light grey columns represent myocytes treated with 8 μM okadaic acid. Results are a mean ± SE of 6 experiments; however, the SE is too small to be displayed.

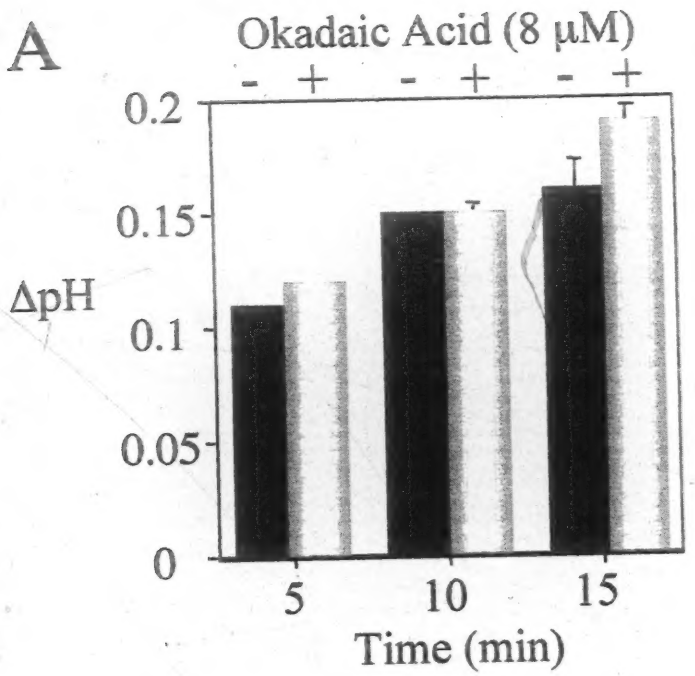
A
Okadaic Acid (8 μM)
- + - + - +
0.2
0.15
ΔpH
0.1
0.05
0
5
10
15
Time (min)

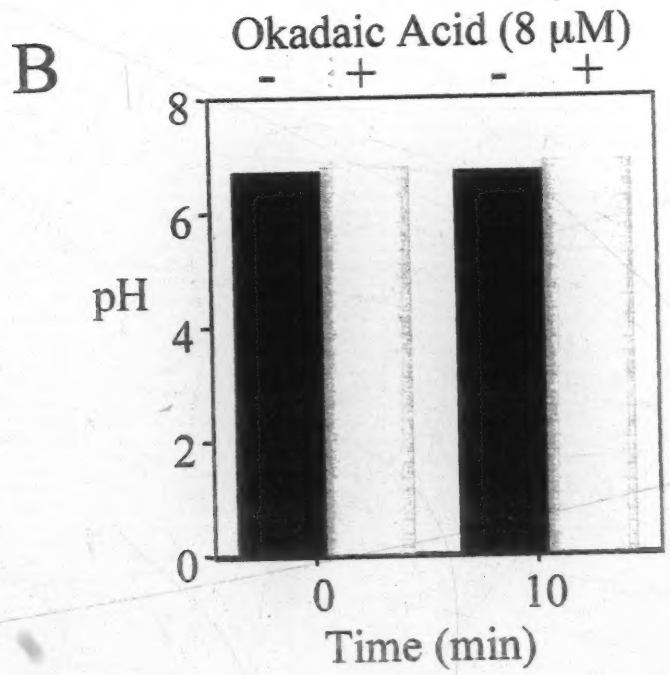
B
Okadaic Acid (8 μM)
- + - +
8
6
pH
4
2
0
0
10
Time (min)

Fig. 18. Western Blot of transient cell lines expressing PP1 and measurement of NHE1 activity.

A: Representative Western blot of CHO cells transiently transfected with the pDEST40-PP1 expression plasmid and probed with a monoclonal anti-PP1 antibody. A positive control of purified PP1 was used to confirm immunoreactivity of the antibody (+ Ctrl PP1, bottom arrow). CHO cells mock-transfected with an empty vector were used as a control (Ctrl Empty Vector). PP1 transiently overexpressed in CHO cells after 24 hours (PP1, top arrow). PP1 endogenous expression in CHO cells (bottom arrow).B: The rate of recovery from an ammonium chloride induced acid load (40mM NH_4Cl) was measured in cells transiently overexpressing PP1. The black column represents control cells (Ctrl Empty Vector), mock-transfected with an empty vector. The light grey column represents cells transiently overexpressing PP1. The rate of recovery was not significantly different in cells overexpressing PP1, $p > 0.4$. The results are mean ± SE of 18 assays.

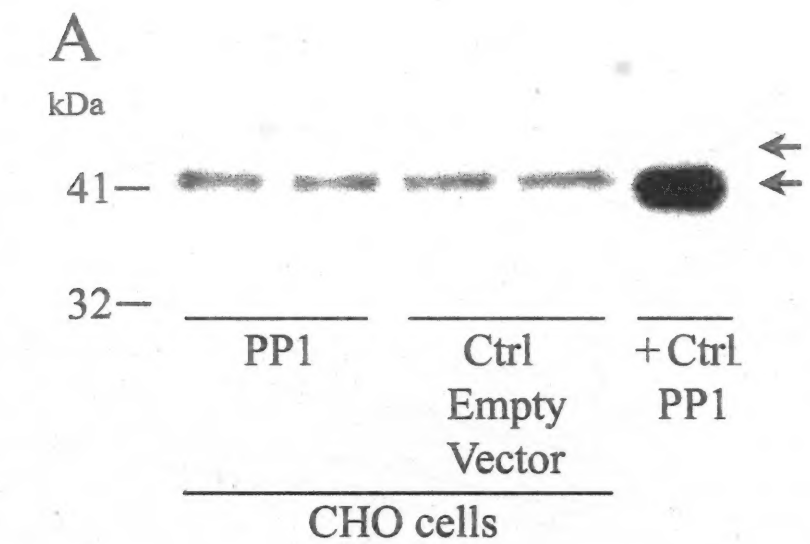
A
kDa
41—
32—
PP1
Ctrl
Empty
Vector
+Ctrl
PP1
CHO cells

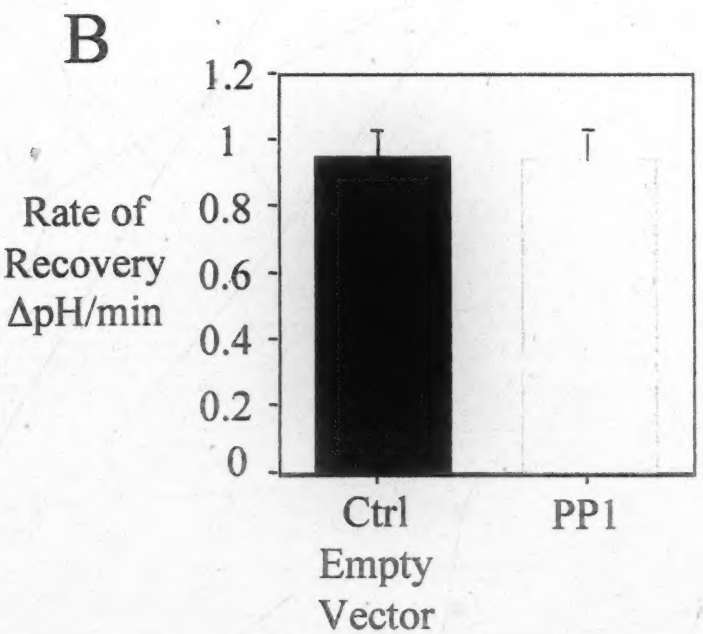
B
Rate of
Recovery
ΔpH/min
1.2
1
0.8
0.6
0.4
0.2
0
Ctrl
Empty
Vector
PP1

Fig. 19. Western Blot of transient cell lines expressing PP2B and measurement of NHE1 activity.

A: Representative Western blot of CHO cells transiently transfected with the pDEST40-PP2B expression plasmid and probed with a polyclonal anti-PP2B antibody. CHO cells mock-transfected with an empty vector were used as a control (Ctrl Empty Vector). PP2B transiently expressed in CHO cells after 24 hours (PP2B, arrow). B: The rate of recovery from an ammonium chloride induced acid load (40mM NH_4Cl) was measured in cells transiently expressing PP2B. The black column represents control cells (Ctrl Empty Vector); mock-transfected with an empty vector. The dark grey column represents cells transiently expressing PP2B. The rate of recovery was not significantly different in cells expressing PP2B, $p > 0.3$. The results are mean ± SE of 24 assays.

A

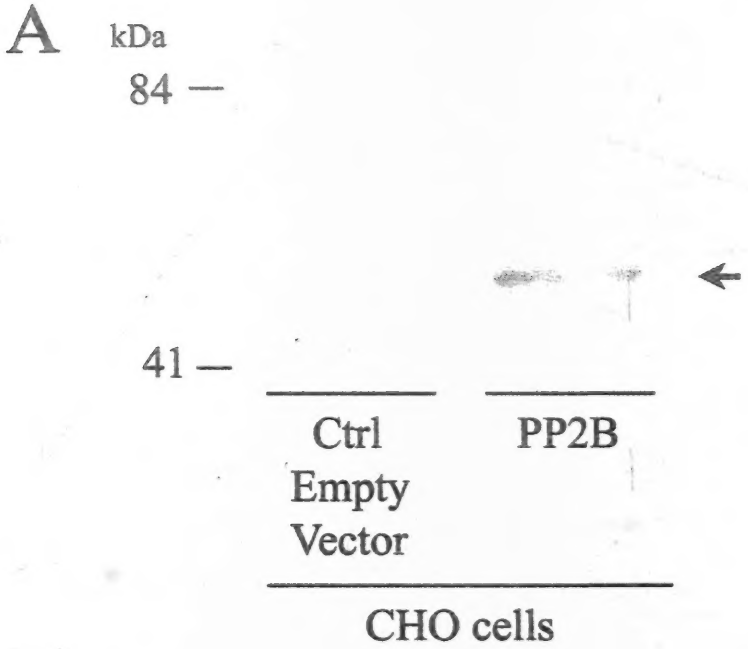
kDa
84 —
41 —
Ctrl
Empty
Vector
PP2B
CHO cells

B

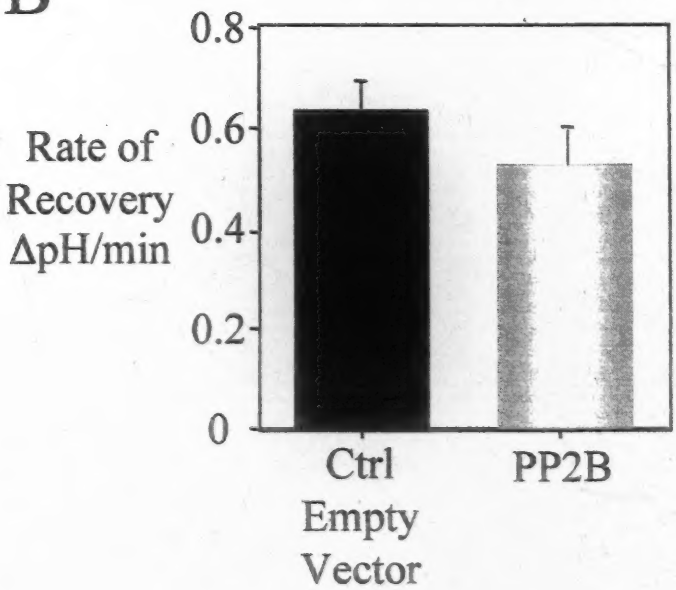
Rate of
Recovery
ΔpH/min
0.8
0.6
0.4
0.2
0
Ctrl
Empty
Vector
PP2B

Fig. 20. Western Blot of stable cell lines expressing PP1 and I2.
Representative Western blot of cell lysates from colonies of PP1 and I2 cells, probed with an anti-V5 antibody. PP1 cell lines #15 and #42 vary in overexpression, while I2 overexpression is identical in cell lines #2 and #21. Ctrl Empty Vector, control cell lines mock-transfected with an empty vector, do not express V5-tagged PP1 or I2.

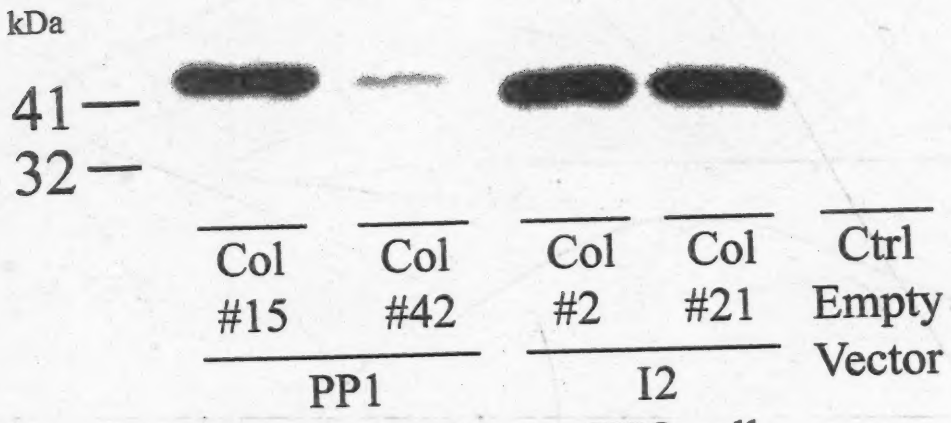

Overexpression in CHO cells

Fig. 21. Typical tracing of NHE1 activity of mammalian cells.
A: Representative tracing of a typical assay measuring the rate of recovery from an acid load in mammalian cells. The acid load was induced using ammonium chloride (40mM NH_4Cl) for 3 minutes followed by Na^+-free buffer. The rate of recovery was measured for 3 minutes in Na^+-containing buffer, followed by a three-point calibration in Nigericin containing solution at pH 8, 7 and 6. B: An enlarged representative tracing of the recovery from an ammonium chloride induced acid load in cells stably expressing I2 (I2 cells) and PP1 (PP1 cells). CHO cells mock-transfected with an empty pDEST40 expression plasmid were used as controls (Ctrl). The rate of recovery was calculated using the first 20 seconds of recovery in Na^+-containing buffer. A specific NHE1 inhibitor, HMA, hexamethylene-amiloride (10μM), was used to illustrate that NHE1 activity was responsible for the recovery from an acid load.

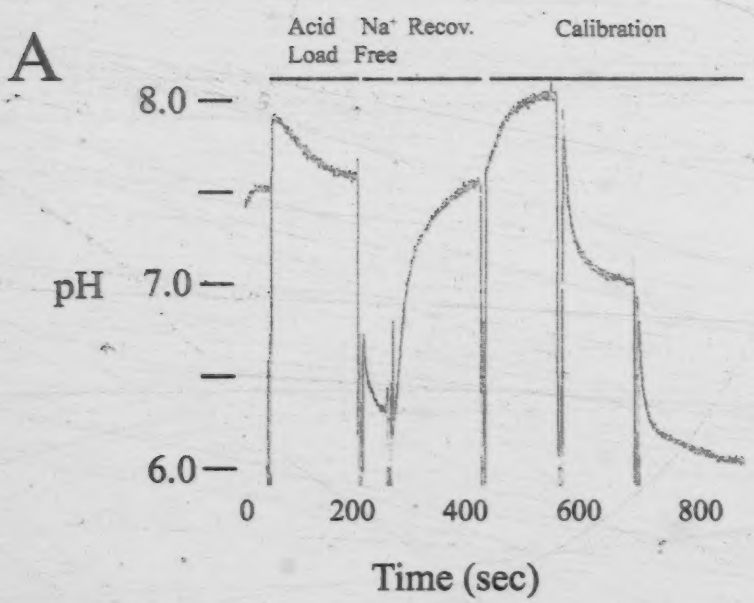
A
Acid Load
Na+ Free
Recov.
Calibration
8.0
pH 7.0
6.0
0
200
400
600
800
Time (sec)

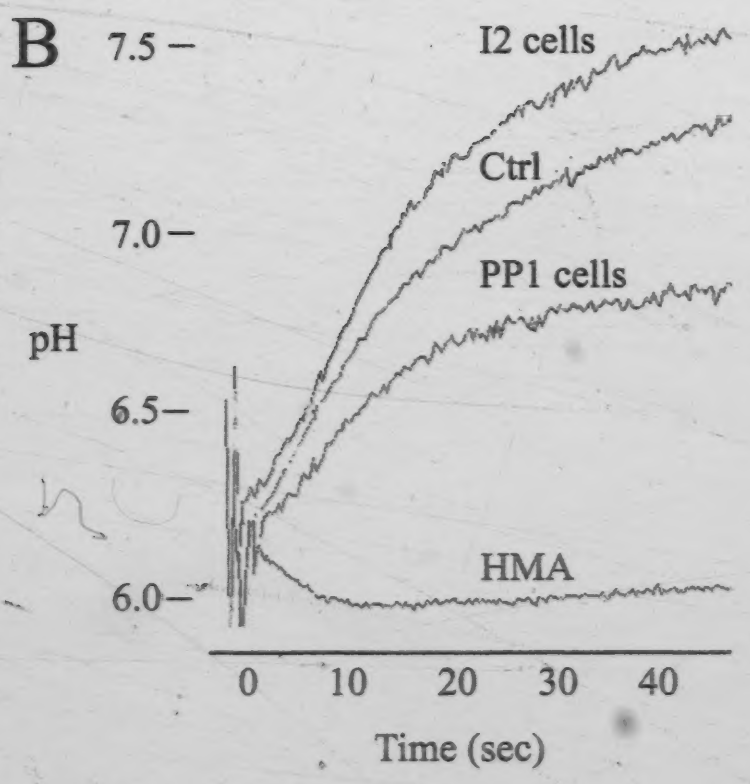
B
7.5
7.0
pH
6.5
6.0
I2 cells
Ctrl
PP1 cells
HMA
0
10
20
30
40
Time (sec)

Fig. 22. NHE1 activity of cells overexpressing PP1 or I2.

A: The rate of recovery from an ammonium chloride induced acid load (40mM NH_4Cl) was measured in cells overexpressing PP1. Black columns (1,3) represent the rate of recovery from an acid load in control cells, mock-transfected with an empty vector. Light grey columns (2,4) represent the rate of recovery of two cell lines overexpressing PP1, #15 and #42. * means that rate of recovery was significantly slower in cells overexpressing PP1 compared to control cells. For cell line PP1#15 $p < 0.05$, results are mean ± SE of 13 experiments. For cell line PP1#42 $p < 0.01$, results are mean ± SE of 8 experiments B: Identical experiments were performed using cells overexpressing I2.

* means that I2 overexpressing cell lines, #2 and #21 (columns 2,4) recovered significantly faster from an acid load compared to control cells (columns 1,3). For cell line I2#2 $p < 0.05$, results are mean ± SE of 8 experiments. For cell line I2#21 $p < 0.01$, results are mean ± SE of 13 experiments.

A

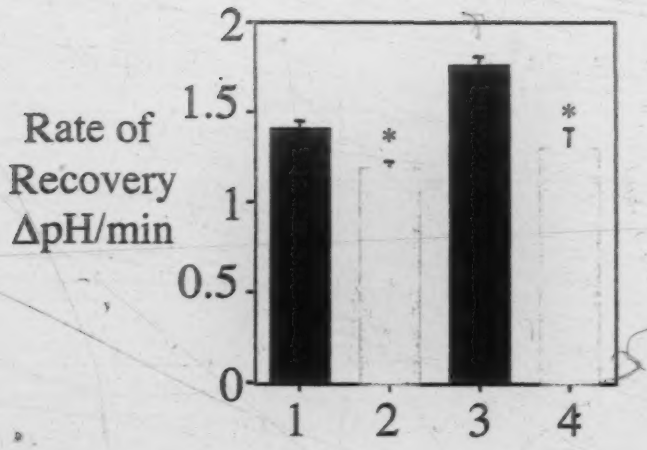
Rate of
Recovery
ΔpH/min
2
1.5
1
0.5
0
1
2
3
4

B

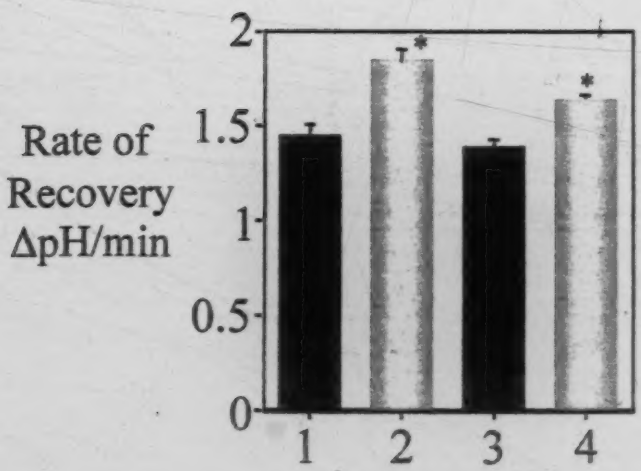
Rate of
Recovery
ΔpH/min
2
1.5
1
0.5
0
1
2
3
4

Fig. 23. NHE1 activity of cells overexpressing PP1 or I2 stimulated with Thrombin. A: The rate of recovery from an ammonium chloride induced acid load (40mM NH_4Cl) was measured in the presence or absence of 2 units/ml thrombin. Results are shown for two colonies overexpressing PP1, #15 and #42 and mock-transfected cells. * means that NHE1 activity was stimulated in cells overexpressing PP1 (columns 4,6) as it was in control cells (column 2). Column 1 represents NHE1 activity in unstimulated control cells. Columns 3 and 5 represent NHE1 activity in two colonies of unstimulated cells overexpressing PP1. For the control cell line $p < 0.01$, results are mean ± SE of 13 experiments. For cell line PP1#15 $p < 0.05$, results are mean ± SE of 13 experiments. For cell line PP1#42 $p < 0.05$, results are mean ± SE of 8 experiments B: Identical experiments were performed using two colonies of cells overexpressing I2, #2 and #21.
* means that in control cells (column 2) mock-transfected with an empty vector NHE1 activity was stimulated by thrombin, compared to unstimulated control cells (column 1), $p < 0.01$, results are mean ± SE of 13 experiments. NHE1 was not stimulated in either colony of I2 overexpressing cells (columns 4,6). Columns 3 and 5 represent NHE1 activity in two colonies of unstimulated cells overexpressing I2. For cell line I2#2 $p > 0.8$, results are mean ± SE of 9 experiments. For cell line I2#21 $p = 1$, results are mean ± SE of 9 experiments.

A

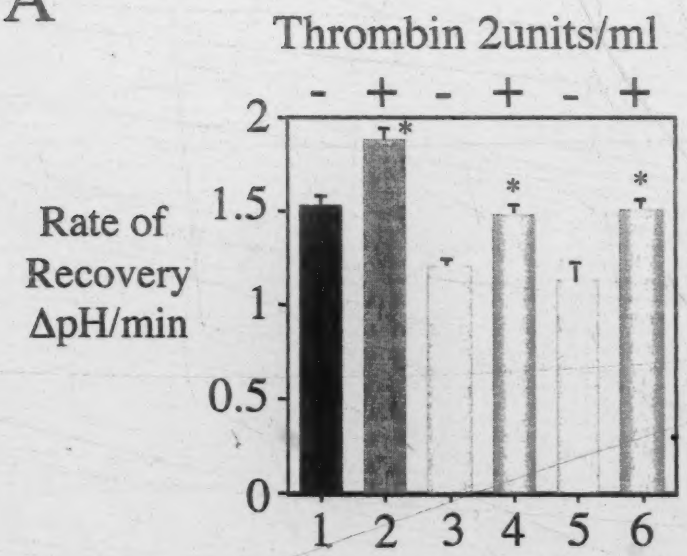
Thrombin 2units/ml
- + - + - +
Rate of Recovery ΔpH/min
2
1.5
1
0.5
0
1 2 3 4 5 6

B

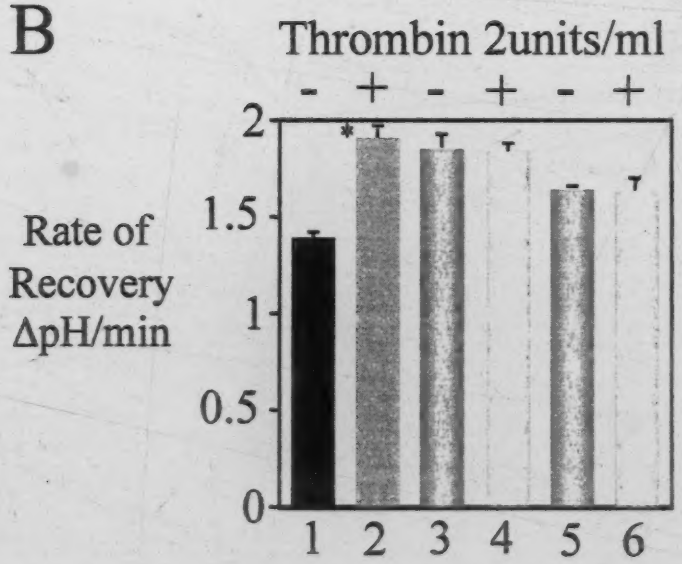
Thrombin 2units/ml
- + - + - +
Rate of Recovery ΔpH/min
2
1.5
1
0.5
0
1 2 3 4 5 6

Fig. 24. H^+ efflux of cells overexpressing PP1 or I2.
A: The buffering capacity of cell lines overexpressing PP1 or I2 was measured as detailed in the methods section 9.3. H^+ effux was calculated: buffering capacity x rate of recovery (ΔpH/min). Cells overexpressing PP1 showed a significantly slower rate of H^+ extrusion (PP1 cells), $p < 0.05$, results are mean ± SE of 8 experiments. B: Identical experiments were performed using cells expressing I2. The results demonstrated that H^+ efflux was much faster in cells overexpressing I2 (I2 cells) in comparison with control cells, $p < 0.01$, results are mean ± SE of 8 experiments.

A

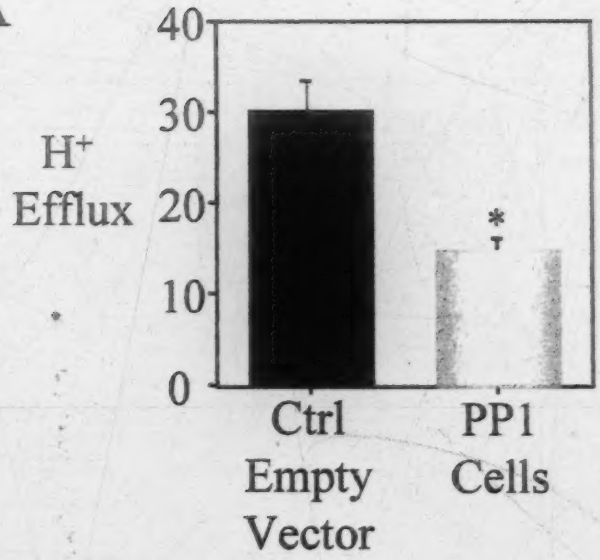
40
30
20
10
0
H+
Efflux
*
Ctrl
Empty
Vector
PP1
Cells

B

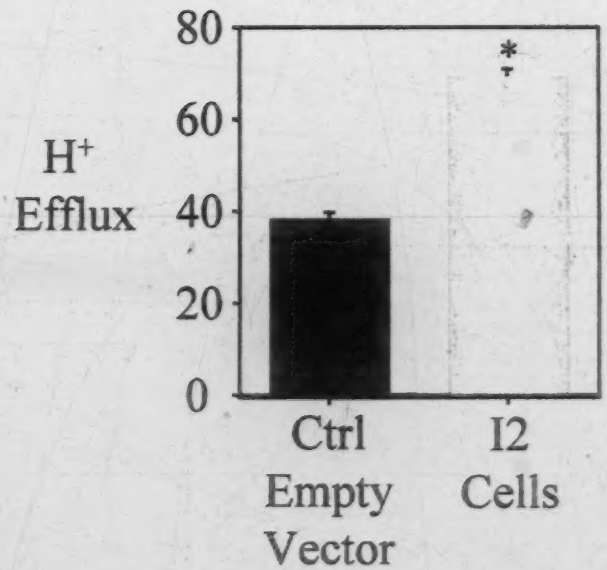
80
60
40
20
0
H+
Efflux
*
Ctrl
Empty
Vector
I2
Cells

Fig. 25. NHE1 activity in the presence of the NHE inhibitor Hexamethylene - Amiloride (HMA)

To confirm that recovery from the ammonium chloride induced acid load was due to NHE activity, the activity was measured in the presence of a specific NHE inhibitor, HMA (10 μM). * represents the higher rate of recovery from an acid load of I2 cells compared to control cells as previously shown in Fig.19. ‡ means the HMA abolished the recovery from an acid load in both cell lines, indicating that the recovery was due to the Na^+/H^+ exchanger activity. For control cell lines (column 3) $p < 0.01$. For the I2 cell lines (column 4) $p < 0.05$. Results are mean ± SE of 3 experiments.

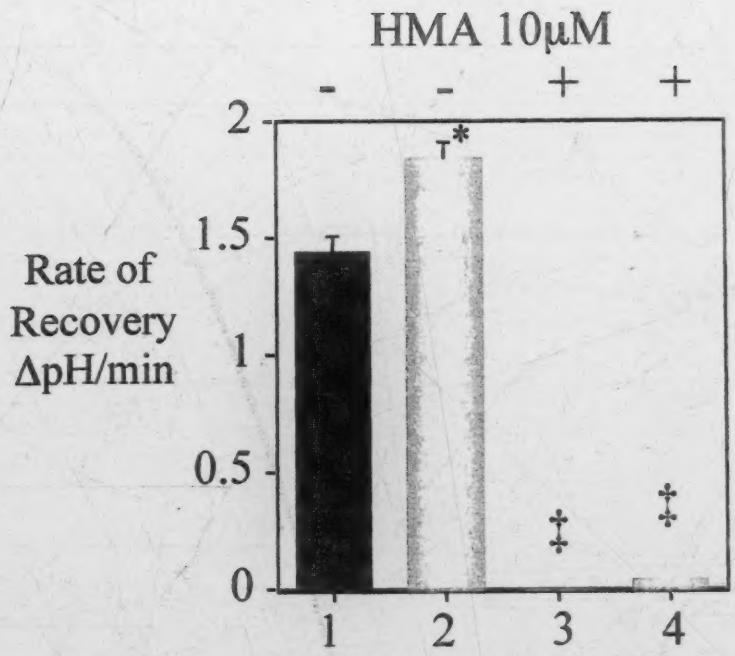
HMA 10μM
- - + +
2
1.5
1
0.5
0
Rate of Recovery ΔpH/min
*
1 2 3 4

Fig. 26. NHE1 protein expression in cell lines expressing PP1.
A: Representative Western blot of cell lysates prepared from control cells (Ctrl Empty Vector) and cells overexpressing PP1 (PP1 Cells). As a positive control a slightly larger HA-tagged NHE1 (+Ctrl NHE1) was used. Right arrow indicates HA-tagged NHE1, left arrow indicates the untagged NHE protein. The membrane was probed with a monoclonal anti-NHE1 antibody. B: Quantitative analysis of NHE1 protein expression in control and PP1 cells.

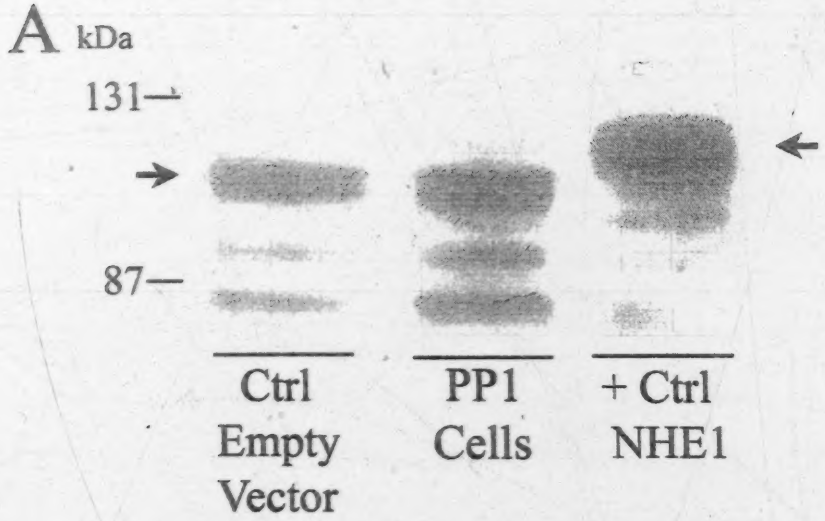
A
kDa
131
87
Ctrl
Empty
Vector
PP1
Cells
+ Ctrl
NHE1

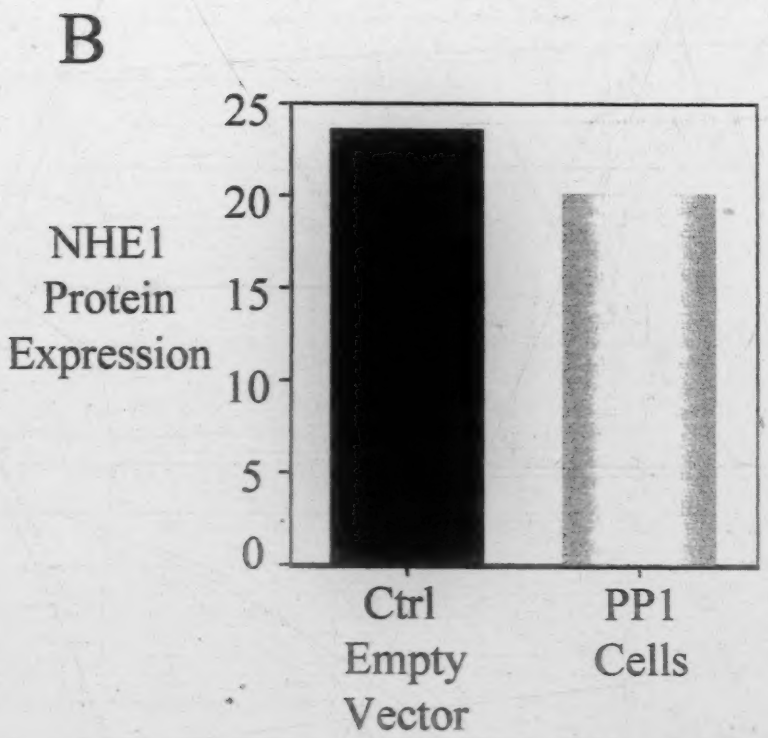
B
NHE1
Protein
Expression
25
20
15
10
5
0
Ctrl
Empty
Vector
PP1
Cells

Fig. 27. NHE1 protein expression in cell lines expressing I2.
A: Representative Western blot of cell lysates prepared from control cells (Ctrl Empty Vector) and cells overexpressing I2 (I2 Cells). As a positive control a slightly larger HA-tagged NHE1 (+Ctrl NHE1) was used. Right arrow indicates HA-tagged NHE1, left arrow indicates the untagged NHE protein. The membrane was probed with a monoclonal anti-NHE1 antibody. B: Quantitative analysis of NHE1 protein expression in control and I2 cell lines.

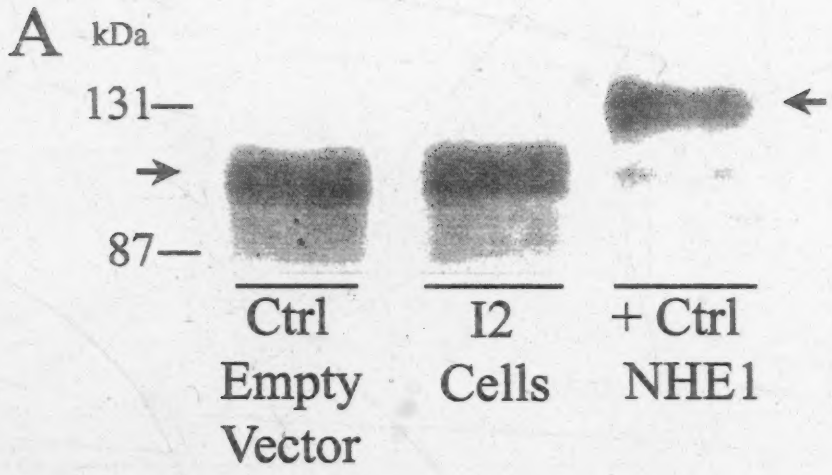
A
kDa
131—
87—
Ctrl
Empty
Vector
I2
Cells
+ Ctrl
NHE1

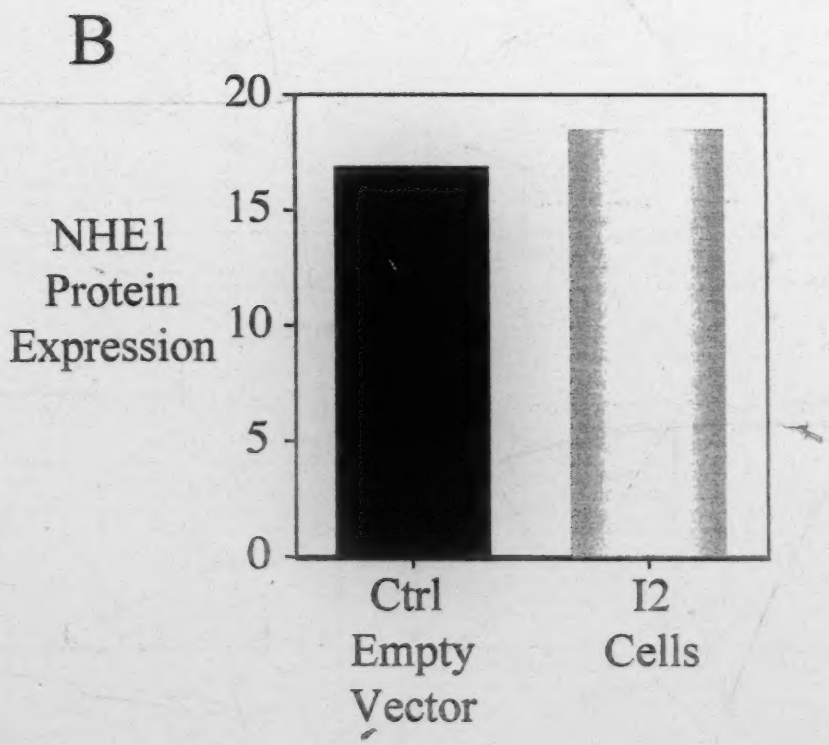
B
NHE1
Protein
Expression
20
15
10
5
0
Ctrl
Empty
Vector
I2
Cells

Fig. 28. Phosphatase activity in heart cell extracts and cells overexpressing I2.

A: Quantitative results of phosphorylase phosphatase activity (PP1/PP2A) in crude heart cell extracts prepared as described in the methods section 3. To determine the total phosphorylase phosphatase activity in the heart extracts the phosphorylase *a* assay was done as described in the methods section 8.1. Ctrl, represents a sample of crude heart cell extracts in the presence of okadaic acid. Two different heart cell extract samples (column 1,2, Heart Cell Extracts) were tested in triplicate. Results are a mean ± SE of 3 samples; however the SE is too small to be visible. B: To determine the total phosphorylase phosphatase activity and PP1 activity in cell lysates, the phosphorylase *a* assay was done as described in the methods section 8.2. Quantitative analysis of the total phosphorylase phosphatase (PP1/PP2A) and PP1 activity in cells overexpressing I2. Black columns (1,3 and 5) represent the total phosphorylase phosphatase activity in cell lysates. Grey columns (2,4 and 6) represent the PP1 activity in cell lysates. Columns 1 and 2 represent control cells mock-transfected with an empty vector. Columns 3-6 represent cell lines overexpressing I2. Percentage (%) values mean the %[^{32}P] released from the substrate (phosphorylase *a*) by PP1/PP2A or by PP1 alone present in cell lysates.

A

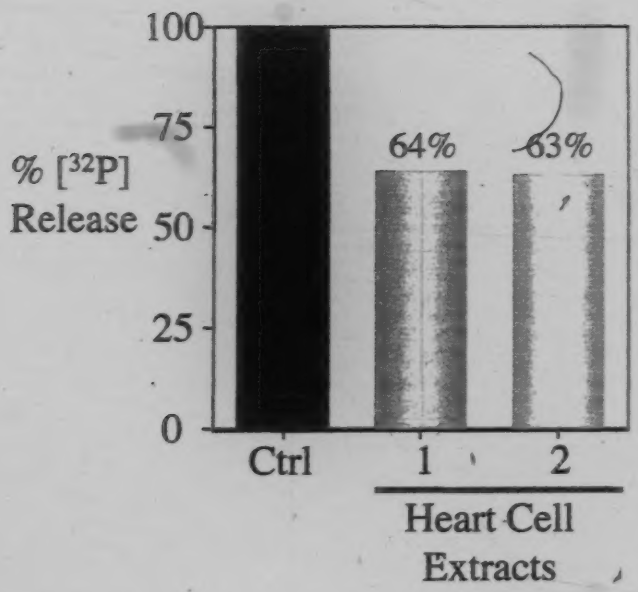
100
75
50
25
0
% [32P] Release
64%
63%
Ctrl
1
2
Heart Cell Extracts

B

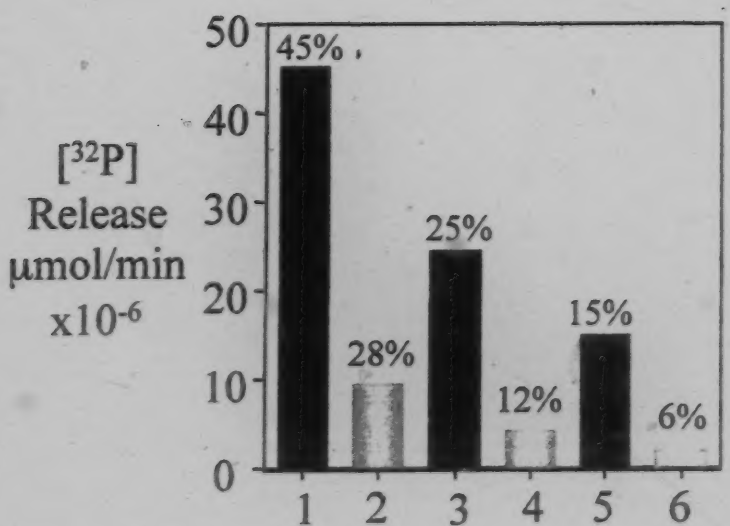
50
40
30
20
10
0
[32P] Release µmol/min x10-6
45%
28%
25%
12%
15%
6%
1
2
3
4
5
6

Chapter IV

E: Discussion

F: Summary and General Conclusions

G: Future Experiments

E. Discussion

1. *Summary of NHE1 Regulation*

NHE1 is a plasma membrane glycoprotein essential for maintaining pH homeostasis in cells. It is also a key protein involved in cell volume regulation, fluid secretion, salt and water absorption across epithelia [13, 14] cell growth [15] differentiation [18] and cell motility [21]. NHE1 is regulated by numerous factors including: intracellular acidification [35]; cytosolic Ca^{2+}, calmodulin [37]; calcineurin homologous proteins (CHP1, CHP2) [42, 44]; tescalcin [46]; carbonic anhydrase II [47]; PIP_2 and cellular ATP [49]; various hormones and growth factors [52, 54, 56, 57]. Phosphorylation and numerous kinases play a key role in NHE1 regulation [23, 70, 76, 78-80, 92, 99]; however, mechanisms of dephosphorylation have not been well elucidated. This report demonstrates significant evidence that a key phosphatase involved in the regulation of NHE1 is protein phosphatase-1 (PP1).

2. *Dephosphorylation of NHE1*

In vitro dephosphorylation studies of a NHE1, C-terminal, GST fusion protein, composed of the distal 178 amino acids (PCRA), provided evidence of PP1 having the ability to completely dephosphorylate the cytoplasmic tail of NHE1 (Fig.6). These results were consistent with earlier studies briefly demonstrating that the phosphatase inhibitor, okadaic acid can prevent dephosphorylation of NHE1 [71]. Another study showed evidence that 14-3-3 proteins, which are important determinants of exchanger activation by serum, protect NHE1 from dephosphorylation [177]. In our study, the ability of PP1 to dephosphorylate NHE1

was also examined in the presence of a regulatory subunit, spinophilin, previously shown to target PP1 to the cytoskeleton and the plasma membrane [100, 130]. In the presence of spinophilin the degree to which PP1 could dephosphorylate NHE1 was reduced by 6%. It has been suggested that spinophilin can bind and move intracellular signaling molecules, such as PP1, into close proximity of membrane bound receptors [130]. Therefore it is possible that the decrease in the degree of dephosphorylation of NHE1 by PP1 is due to PP1 being sequestered by spinophilin.

In our study, dephosphorylation of NHE1 by purified PP2A and PP2B was also examined. PP2A was able to dephosphorylate NHE1; however not to the same degree as PP1 (Fig.7). These experiments also demonstrated that PP2A dephosphorylated NHE1 to a greater extent in the absence of Mn^{2+}. In contrast to PP1 and PP2A, PP2B (calcineurin) did not reverse the phosphorylation of NHE1 *in vitro* (Fig.8). Calcineurin is composed of four distinct functional domains including: PP2B-A, the catalytic subunit; a regulatory PP2B-B binding domain; a CaM binding region and an auto-inhibitory domain. PP2B activity is stimulated by Ca^{2+} binding to the PP2B-B subunit and by Ca^{2+}-induced binding of CaM to PP2B-A [229]. In our experiments we investigated dephosphorylation of NHE1 by the catalytic subunit, PP2B-A in the presence of Ca^{2+} and CaM but in the absence of PP2B-B. It has been shown that the binding of PP2B-B with PP2B-A plays an important role in activating the catalytic subunit [230]. Therefore it is possible that the inability of PP2B-A to dephosphorylate NHE1 was due to a decreased level of activity of the catalytic subunit in the absence of PP2B-B.

In the mammalian heart, more than 90% of the protein phosphatase activity is comprised of PP1 and PP2A [231, 232]. The expression of PP1 and PP2A isoforms varies with myocardial regions, where the ventricles contain higher PP1 and PP2A levels compared to the atria [233]. These observations led us to investigate the ability of protein phosphatases present in crude, ventricular, rat heart cell extracts, to dephosphorylate NHE1. The heart cell extracts were prepared from adult rat hearts and phosphatase activity measurements indicated that the total PP1 and PP2A activity in the extracts was over 60% (Fig.28a); however, the heart extracts did not dephosphorylate NHE1 (Fig.10). We did not measure PP1 activity alone in the heart extracts. Early studies have shown that PP1 expression is low in the rat heart and skeletal muscle [234]. In addition, PP1 activity is unstable and difficult to detect in heart cell extracts (Personal Communication, Dr. C. Holmes). Therefore, it is possible that the combined PP1 and PP2A activity in crude heart cell extracts was insufficient to dephosphorylate NHE1. It is also possible that our heart cell extracts did not contain active PP1.

3. *NHE1 Interactions with PP1 or PP2B*

The Na^+/H^+ exchanger GST fusion protein was used to investigate physical interactions between the cytoplasmic C-terminus of NHE1 and phosphatases. GST pull-down experiments involved the incubation of PCRA with PP1 or PP2B. These experiments were analyzed by Western blots probed with a broad range anti-phosphatase antibody (Fig.11 and Fig.12) and antibodies exhibiting high specificity for PP1 (Fig.13) or PP2B (Fig.14). The incubations of PCRA with PP1 (37 kDa) that

were analyzed with a broad range phosphatase antibody, demonstrated PP1 binding to the C-terminus of NHE1 (Fig.11). These results were not observed when the same experiments were analyzed with an anti-PP1 antibody specific for PP1 (Fig.13).

In GST pull-down experiments involving PP2B, the full length PP2B (60 kDa) protein showed binding to GST and not the C-terminus of NHE1. Surprising results were obtained using one particular sample of PP2B, obtained from the lab of Dr. Charles Holmes. This PP2B sample contained a small fragment ~31 kDa (Fig.12a lane 5, bottom arrow) identified by mass spectrometry as a short N-terminal sequence of PP2B (Fig.12c). Western blot analysis of PCRA-PP2B GST pull-down experiments with a broad specificity anti-phosphatase antibody revealed significant binding of the ~31 kDa PP2B sequence with NHE1 (Fig.12a-b). The truncated fragment was not observed in other samples of purified PP2B. It was lost during the purification procedure of other PP2B preparations. This limited further investigations involving the truncated PP2B fragment. Based on the size and amino acid sequenced data (Fig.12c) the ~31 kDa fragment of PP2B would be a constitutively active form of PP2B, with a truncation of its CaM and autoinhibitory domains in the C-terminus [235]. The binding to NHE1 could potentially regulate the exchanger through a mechanism different from dephosphorylation.

It has been shown that calcineurin can bind to other membrane proteins such as the IP_3 receptor [159] and the ryanodine receptor (RyR) [160, 235]. In the case of the RyR the FK506 binding proteins, FKBP12 and FKBP12.6 were shown to anchor calcineurin in a calcium dependent manner. The FKBP12.6 selectively binds the cardiac-RyR where as both isoforms can bind to the skeletal-RyR [235]. The

calcineurin inhibitors, FK506 and rapamycin, cause the dissociation of FKBP12 or FKBP12.6 from the RyR. *In vitro*, this dissociation causes an increase in Ca^{2+} release from Ca^{2+}-channels in the presence of agonists. In cardiomyocytes, this dissociation causes an increase in Ca^{2+} spikes compared with cells untreated with FK506 [235]. The calcineurin inhibitor CsA did not cause FKBP12/calcineurin to dissociate from the RyR and did not affect Ca^{2+} release from Ca^{2+} channels. These findings suggest that the Ca^{2+}-release channel activity is regulated by calcineurin bound to the RyR and not by unbound calcineurin [235]. They demonstrate that calcineurin can regulate membrane proteins by phosphorylation independent mechanisms.

In vitro assays demonstrated a weak interaction between NHE1 and PP1. In one case (Fig.11) PP1 appeared to react with NHE1 while in another (Fig.13) the interaction was not detected. The major binding motif of PP1 is RVxF. This sequence is absent from the NHE1 sequence. Despite the importance of the RVxF motif some proteins are known to interact with PP1 through different sites [100]. Together with the dephosphorylation of NHE1 by PP1 experiments, the GST pull-down assays involving PP1 suggest that a low affinity interaction between the two proteins is possible. Low affinity binding between proteins is difficult to detect by GST pull-down or immunoprecipitation techniques. Low affinity interactions can still be studied by trapping proteins with homobifunctional cross-linkers [236], such as DSS or DSP. Physical interactions between NHE1 and PP1 or PP2B were investigated by immunoprecipitating NHE1 from cells pretreated with DSS or DSP. Subsequently the immunoprecipitated NHE1 samples were analyzed by Western blot analysis using anti-PP1 or anti-PP2B antibodies. The results demonstrated that PP1 can be cross-

linked to NHE1 in living cells (Fig16.a), suggesting that the C-terminus of NHE1 has a low affinity for PP1 binding. This protocol failed to detect any interaction between the full length PP2B protein and NHE1 (Fig16.b), suggesting that PP2B may not bind to the cytoplasmic tail of NHE1 directly.

As previously described, NHE1 can be regulated by the cAMP/PKA pathway [94, 95, 97, 98, 237]. PKA is composed of R, regulatory, and C, catalytic subunits, which interact to form different PKA isoforms. The R subunits of PKA are involved in interactions with A kinase anchor proteins (AKAPs), which immobilize PKA at specific intracellular locations [238]. The 78 kDa AKAP identified as ezrin [239] has been shown interact with NHE3 *via* NHERF (Na^+/H^+ exchanger regulatory factor). This complex was demonstrated to be essential for cAMP-mediated phosphorylation of NHE3 and the inhibition of Na^+/H^+ exchange [240]. Macromolecular complexes involving kinases, protein phosphatases and AKAPs have been shown to regulate other ion channels. These include the L-type Ca^{2+} channel [241], specific K^+ channels [242] the cardiac RyR [243, 244] and the Na^+/Ca^{2+} exchanger, NCX1 [245]. Our results demonstrated that PP1 interacts with NHE1. The interaction appears to be weak and it is more apparent in the presence of immobilizing, cross-linking reagents. It is possible that AKAPs may assist in the interaction between PP1 and NHE1 *in vivo*. This might lead to a tighter association between PP1 and NHE1. Further experiments are necessary to explore this possibility.

In addition, our results showed that a fragment of the PP2B catalytic subunit associates with NHE1. Although we were unable to show any interaction between NHE1 and the entire catalytic subunit of PP2B, again it is possible that an association

may occur in the presence of an AKAP. Several AKAPs have been shown to recruit PP2B and regulate its association with target proteins [238, 246]. Further experiments could also explore the possible interaction between NHE1, PP2B and AKAPs.

4. *NHE1 Activity in the Presence of a Phosphatase Inhibitor, Okadaic Acid*

The involvement of phosphatases in NHE1 regulation *in vivo* was examined using the phosphatase inhibitor okadaic acid. Okadaic acid is a naturally occurring toxin that has been found to inhibit PP1 and PP2A activity [166]. PP1, PP2A and PP2B differ in sensitivity towards okadaic acid. PP2A is most sensitive and it is inhibited by okadaic acid with nanomolar concentrations, while PP1 is inhibited with micromolar concentrations of the toxin [107]. Okadaic acid is not a strong inhibitor of PP2B [107]. The effect of okadaic acid on the activity of NHE1 was investigated in neonatal rat cardiomyocytes. The rate of recovery from an ammonium chloride induced acid load and steady state pH were measured in myocytes treated with 8 μM okadaic acid (Fig.17). Okadaic acid at 8 μM was expected to inhibit PP2A activity. Inhibition of PP2A activity did not affect NHE1 activity in these experiments. This lead us to believe that phosphatases exhibiting a greater resistance to okadaic acid, such as PP1 and PP2B, may be more involved in the regulation of NHE1 *in vivo*. Therefore, further investigations of NHE1 regulation involving PP2A were not attempted. In addition, it was expected that treatment of cardiomyocytes with 8 μM okadaic acid would also affect PP1 activity; however, significant effects on the rate of recovery from an ammonium chloride induced acid load or steady state pH were not observed.

In other studies, okadaic acid has been shown to increase the phosphorylation and activity of the NHE in numerous cell types including: platelets, rat thymic lymphocytes, human bladder carcinoma cells and Chinese hamster lung fibroblasts [71, 72, 168, 169]. Stimulation of NHE1 by okadaic acid has also been demonstrated in human red blood cells [171] and human blood lymphycytes [170]. Our results suggest that PP1 may not be as important in NHE1 regulation in cardiomyocytes as it is in other cell types.

5. *NHE1 Activity in Cell Lines Transiently Expressing PP1 or PP2B.*

Chinese hamster ovary cells transiently expressing PP1 or PP2B were used to further examine the involvement of PP1 and PP2B in NHE1 regulation *in vivo*. The rate of recovery from an ammonium chloride induced acid load was measured in these cell lines. Transient overexpression of PP1 did not affect NHE1 activity. Western blot analysis of PP1 expression using a highly specific anti-PP1 antibody showed that after 24 hours, the level of PP1 overexpressed is low (Fig.18a, top arrow). The endogenous PP1 expression in CHO cells is high (Fig.18a bottom arrow) and after 24 hours not enough PP1 is produced in these cells to affect the activity of NHE1. Similar results were obtained with cells transiently expressing PP2B. The expression of PP2B did not affect the rate of recovery from an acid load in CHO cells (Fig.19b). It is also important to mention that PP2B was only expressed transiently in CHO cells. Stable expression was not obtained despite the 57% transfection efficiency and screening of numerous isolated colonies by Western blot analysis, suggesting that PP2B may be lethal and can only be overexpressed transiently.

6. *The Effects of PP1 on NHE1 Activity*

The effects of PP1 on NHE1 *in vivo* were examined using three stable CHO cell lines. One stable cell line was developed to overexpress PP1 and the second to overexpress I2. The control cell line was mock-transfected with an empty vector. I2 is a protein inhibitor of PP1 inactivating its activity at a 2 nM [135], therefore the cell lines expressing I2 were expected to exhibit lower PP1 activity compared with control cells. The expression of V5-tagged PP1 and I2 was confirmed by Western blot analysis using an anti-V5 antibody. Two stable cell lines overexpressing PP1, #15 and #42 were used to investigate the effect of PP1 overexpression on NHE1 activity. The level of PP1 expression in the PP1 #42 cell line was markedly lower (Fig.20 Col#42) compared with the PP1 #15 cell line; however this colony was still used in fluorometric studies. Two stable cell lines overexpressing I2, #2 and #21 were used to investigate the effect of PP1 inhibition on NHE1 activity. The expression level of I2 in both cell lines was almost identical (Fig.20). Initial experiments with the stable cell lines examined the rate of recovery from an ammonium chloride induced acid load (Fig.21). Unstimulated rate of recovery from an acid load was significantly lower in cells overexpressing PP1 compared with control cells mock-transfected with an empty vector (Fig.22a). In contrast, cells expressing I2 demonstrated a much faster rate of recovery from an acid load (Fig.22b). The rate of recovery from an ammonium chloride induced acid load was also measured in the presence of thrombin. Upon the addition of thrombin hormone, previously known to stimulate NHE1 [59], cells overexpressing PP1 showed similar results seen in normal cells, being significantly stimulated by the agonist (Fig.23a columns 4,6). No effect was

observed in cells overexpressing I2. Thrombin did not stimulate NHE1 in these cell lines (Fig.23b columns 4,6). These results suggest that inhibition of PP1 in CHO cells causes NHE1 to be hyperactive, and cannot be more stimulated by thrombin.

To determine that the results seen in the rate of recovery from acid load experiments were not due to the buffering of cells, the buffering capacity of the cell lines was measured and used to calculate the true movement of H^+ from the cells. Overexpression of PP1 caused a decrease in H^+ efflux (Fig.24a). The opposite effect was observed in cells overexpressing I2. The H^+ efflux in cells overexpressing I2 was almost two fold compared to control cells (Fig.24b). To confirm that the results obtained were due to the Na^+/H^+ exchanger, the rate of recovery from an acid load was measured in the presence of HMA (10 μM), a specific inhibitor of NHE1. In the presence of HMA the recovery from an acid load was abolished in these cell lines (Fig.25). These experiments confirm that our results obtained from pH_i measurements are due to the changes in NHE1 activity and not due to the buffering capacity of the cells.

Furthermore, we investigated whether the changes in intracellular pH were due to changes in NHE1 protein expression. Western blot analysis using an antibody against NHE1 was done to examine the level of NHE1 protein expression in cell lines overexpressing PP1 or I2 and in control cell lines mock-transfected with an empty vector. An equal amount of total protein was analyzed in each cell line. The results demonstrated that the level of NHE1 protein expression in PP1 (Fig.26) and I2 (Fig.27) cell lines was similar to the level of NHE1 protein expressed in control cells.

It is believed that the level of NHE1 expression is not altered in cells overexpressing PP1 or I2.

Phosphatase assays of lysates from cells overexpressing I2 demonstrated that the PP1 activity and the total phosphorylase phosphatase (PP1/PP2A) activity are reduced in these cell lines. In the I2 #2 cell line only 6% PP1 activity was measured, while the I2 #21 cell line demonstrated 12% PP1 activity. The PP1 activity of these cell lines was compared with control cells, which exhibited 28% PP1 activity (Fig.28b).

F. Summary and General Conclusions

In this study we examined which protein phosphatases are involved in regulation of the NHE1 isoform of the Na^+/H^+ exchanger. *In vitro* dephosphorylation of NHE1 by PP1, PP2A and PP2B was initially investigated. NHE1 dephosphorylation was examined using a C-terminal GST fusion protein of NHE1, composed of the distal 178 amino acids (PCRA), purified protein phosphatases and heart cell extracts. Our results showed that:

1) PP1 completely dephosphorylates NHE1.
2) PP2A significantly dephosphorylates NHE1.
3) PP2B does not dephosphorylate NHE1.
4) Crude heart cell extracts, exhibiting over 60% phosphorylase phosphatase (PP1/PP2A) activity, do not dephosphorylate NHE1.

Interactions between NHE1 and PP1 or PP2B were examined *in vitro* and *in vivo*. GST pull-down experiments and immunoprecipitation of NHE1 studies were used to investigate physical interactions of the cytoplasmic tail of NHE1 with PP1 and PP2B. The following conclusions were reached:

1) PP1 interacts with the C-terminus of NHE1 *in vitro*; however the interaction is weak.
2) NHE1 can be cross-linked to PP1 in CHO cells, suggesting that NHE1 is associated with PP1 *in vivo* with a low affinity.
3) The cytoplasmic tail of NHE1 does not bind full length PP2B *in vivo* or *in vitro*.
4) The C-terminus of NHE1 binds an N-terminal fragment of the PP2B catalytic subunit.

The role of phosphatases in NHE1 regulation is supported by a few published studies. The phosphatase inhibitor, okadaic acid, increases NHE1 activity and phosphorylation in platelets, rat thymic lymphocytes, human bladder carcinoma cells Chinese hamster lung fibroblasts, human red blood cells and human blood lymphocytes [71, 72, 169, 171, 247]. The phosphatase inhibitor, calyculin A can also activate NHE1 in Ehrlich ascites tumor cells [172]. Mutation studies of serine 703 to alanine in NHE1 have demonstrated the loss of serum stimulation of NHE1 [79]. Serine 703 has also been shown to bind the phosphoserine binding protein, 14-3-3, preventing *in vitro* dephosphorylation of NHE1 by PP1 [177]. These studies suggest that PP1 is a good candidate for regulating NHE1 activity.

In this project the effect of okadaic acid on NHE1 activity was also investigated using neonatal rat cardiomyocytes.

1) Okadaic acid [248] did not affect the change in pH over 15 minutes
2) Okadaic acid treatment did not alter the steady state pH in myocytes over 10 minutes.

These results suggest that PP2A is an unlikely candidate involved in NHE1 activity regulation in cardiomyocytes. Phosphatases that exhibit a greater resistance to okadaic acid inhibition may be the important phosphatases in NHE1 regulation.

This is the first report investigating the effects of PP1 on NHE1 *in vivo*. These effects have been characterized by:

1) Measuring the rate of recovery from an ammonium chloride induced acid load in:
    a. CHO cells transiently overexpressing PP1.
    b. Cell lines stably overexpressing PP1
    c. Cell lines stably expressing I2
    d. CHO cells containing PP1 or I2 and treated with thrombin.
2) Measuring buffering capacity and H^+ efflux of stable cell lines expressing PP1 and I2
3) Western blot analysis of NHE1 protein expression in cell lines stably expressing PP1 and I2

Together these results have demonstrated that PP1 regulates NHE1 activity *in vivo*. PP1 overexpression and inhibition in cells directly affects NHE1 activity in the following manner:

1) Transient overexpression of PP1 in CHO cells does not affect the rate of recovery from an ammonium chloride induced acid load
2) Stable overexpression of PP1 causes a decrease in the rate of recovery from an ammonium chloride induced acid load. These cell lines retain the ability of thrombin to stimulate NHE1.
3) Inhibition of PP1 activity (confirmed by phosphatase assays) in cell lines stably expressing I2, causes an increase in the rate of recovery from an ammonium chloride induced acid load. Thrombin is unable to stimulate NHE1 in cells overexpressing I2.
4) The rate of H^+ efflux is reduced in cells stably overexpressing PP1 and increased two fold in cells stably expressing I2.
5) The rate of recovery from an acid load in both stable cell lines is abolished by HMA, indicating that the effects observed are a function of NHE1 activity.
6) Stable overexpression of PP1 or I2 does not affect the protein expression of NHE1.

This report strongly demonstrates that PP1 is a key regulating phosphatase of NHE1 *in vitro* and *in vivo*. The involvement of other phosphatase proteins in NHE1 regulation cannot be conclusively ruled out at this time. Further experiments investigating the role of other phosphatases in NHE regulation are necessary to

elucidate the mechanisms of phosphorylation reversal in these exchangers, a process that is currently not well understood.

G. Future Experiments

The findings of this study are accompanied by new questions:

1) Do effects of PP1 on NHE1 differ in ischemia/reperfusion?
    a. Investigation of NHE1 activity in ischemic myocytes may provide insight to this question.
2) Is the monomeric ser/thr protein phosphatase, PP2C, involved in NHE1 regulation by dephosphorylation?
    a. *In vitro* dephosphorylation experiments of NHE1 by PP2C would begin to answer this question.
    b. Measurements of NHE1 activity in cells treated with a PP2C specific inhibitor would give further insight to the indirect effects of PP2C on NHE1 *in vivo*.
    c. Development of stable cell lines overexpressing PP2C would be useful to show direct effects of PP2C on NHE1 *in vivo*.
3) How does regulation of the NHE by PP1 vary between tissues?
    a. Measurements of NHE activity in various cell types would be useful to determine the effects of PP1 on NHE in different tissues. Some of the cell types that could be used in these experiments are: human leukemic HL60 cells, P19 mouse embryonal carcinoma cells differentiated into

neuronal cells, L6 rat skeletal muscle cells differentiated into myotubule cells, and vascular smooth muscle cells.

4) Are macromolecular complexes involving AKAPs and protein phosphatases involved in NHE1 regulation?

   a. Immunoblotting of immunoprecipitated NHE1 with antibodies against specific AKAPs would help identify possible AKAPs linking NHE1 with PP1 or PP2B. Some of the AKAPs that could be investigated include: AKAP220, which has been shown to interact with different PP1 isoforms and regulate PP1 and PKA association [249]. AKAP79/150/250, have been shown to recruit PP2B into macromolecular complexes [238, 246]. In addition, AKAP78 (Ezrin) and AKAP15/18 could be examined as these have been co-localized with plasma membrane channels [240] [241, 242, 244, 245].

Chapter V

H: References

H: References

1 Spitzer, K. V.-J., R. (2003) Regulation of the Intracellular pH in Mammalian Cells. *In* The Sodium-Hydrogen Exchanger: From Molecule to its Role in Disease. Karmazyn M., Avkiran M. and Fliegel L., Eds., Kuwer Academic Publishers, Dordrecht, pp.1-15.

2 Orlowski, J. (1999) Na^+/H^+ exchangers. Molecular diversity and relevance to heart. Ann N Y Acad Sci. **874**, 346-53

3 Baetz, D., Haworth, R. S., Avkiran, M. and Feuvray, D. (2002) The ERK pathway regulates Na(+)-HCO(3)(-) cotransport activity in adult rat cardiomyocytes. Am J Physiol Heart Circ Physiol. **283**, H2102-9

4 Le Prigent, K., Lagadic-Gossmann, D., Mongodin, E. and Feuvray, D. (1997) HCO3(-)-dependent alkalinizing transporter in adult rat ventricular myocytes: characterization and modulation. Am J Physiol. **273**, H2596-603

5 Baird, N. R., Orlowski, J., Szabo, E. Z., Zaun, H. C., Schultheis, P. J., Menon, A. G. and Shull, G. E. (1999) Molecular cloning, genomic organization, and functional expression of Na^+/H^+ exchanger isoform 5 (NHE5) from human brain. J Biol Chem. **274**, 4377-82

6 Numata, M., Petrecca, K., Lake, N. and Orlowski, J. (1998) Identification of a mitochondrial Na^+/H^+ exchanger. J Biol Chem. **273**, 6951-9

7 Numata, M. and Orlowski, J. (2001) Molecular cloning and characterization of a novel $(Na^+,K^+)/H^+$ exchanger localized to the trans-Golgi network. J Biol Chem. **276**, 17387-94

8 Goyal, S., Vanden Heuvel, G. and Aronson, P. S. (2003) Renal expression of novel Na^+/H^+ exchanger isoform NHE8. Am J Physiol Renal Physiol. **284**, F467-73

9 Brett, C. L., Wei, Y., Donowitz, M. and Rao, R. (2002) Human Na(+)/H(+) exchanger isoform 6 is found in recycling endosomes of cells, not in mitochondria. Am J Physiol Cell Physiol. **282**, C1031-41

10 Szabo, E. Z., Numata, M., Shull, G. E. and Orlowski, J. (2000) Kinetic and pharmacological properties of human brain Na(+)/H(+) exchanger isoform 5 stably expressed in Chinese hamster ovary cells. J Biol Chem. **275**, 6302-7

11 Nass, R. and Rao, R. (1998) Novel localization of a Na^+/H^+ exchanger in a late endosomal compartment of yeast. Implications for vacuole biogenesis. J Biol Chem. **273**, 21054-60

12 Orlowski, J. a. G., S. (2003) Molecular and Functional Diversity of Mammalian Na^+/H^+ Exchangers. *In* The Sodium-Hydrogen Exchanger: From Molecule to its Role in Disease. Karmazyn M., Avkiran M. and Fliegel L., Eds., Kluwer Academic Publishers, Dordrecht, pp. 17-34.

13 Orlowski, J. and Grinstein, S. (1997) Na^+/H^+ exchangers of mammalian cells. J Biol Chem. **272**, 22373-6

14 Wakabayashi, S., Shigekawa, M. and Pouyssegur, J. (1997) Molecular physiology of vertebrate Na^+/H^+ exchangers. Physiol Rev. **77**, 51-74

15 Pouyssegur, J., Sardet, C., Franchi, A., L'Allemain, G. and Paris, S. (1984) A specific mutation abolishing Na^+/H^+ antiport activity in hamster fibroblasts precludes growth at neutral and acidic pH. Proc Natl Acad Sci U S A. **81**, 4833-7

16 Delvaux, M., Bastie, M. J., Chentoufi, J., Cragoe, E. J., Jr., Vaysse, N. and Ribet, A. (1990) Amiloride and analogues inhibit $Na(^+)$-H^+ exchange and cell proliferation in AR42J pancreatic cell line. Am J Physiol. **259**, G842-9

17 Kapus, A., Grinstein, S., Wasan, S., Kandasamy, R. and Orlowski, J. (1994) Functional characterization of three isoforms of the Na^+/H^+ exchanger stably expressed in Chinese hamster ovary cells. ATP dependence, osmotic sensitivity, and role in cell proliferation. J Biol Chem. **269**, 23544-52

18 Wang, H., Singh, D. and Fliegel, L. (1997) The Na^+/H^+ antiporter potentiates growth and retinoic acid-induced differentiation of P19 embryonal carcinoma cells. J Biol Chem. **272**, 26545-9

19 Rieder, C. V. and Fliegel, L. (2002) Developmental regulation of $Na(^+)/H(^+)$ exchanger expression in fetal and neonatal mice. Am J Physiol Heart Circ Physiol. **283**, H273-83

20 Bussolino, F., Wang, J. M., Turrini, F., Alessi, D., Ghigo, D., Costamagna, C., Pescarmona, G., Mantovani, A. and Bosia, A. (1989) Stimulation of the Na^+/H^+ exchanger in human endothelial cells activated by granulocyte- and granulocyte-macrophage-colony-stimulating factor. Evidence for a role in proliferation and migration. J Biol Chem. **264**, 18284-7

21 Putney, L. K., Denker, S. P. and Barber, D. L. (2002) The changing face of the Na^+/H^+ exchanger, NHE1: structure, regulation, and cellular actions. Annu Rev Pharmacol Toxicol. **42**, 527-52

22 Denker, S. P. and Barber, D. L. (2002) Cell migration requires both ion translocation and cytoskeletal anchoring by the Na-H exchanger NHE1. J Cell Biol. **159**, 1087-96

23 Yan, W., Nehrke, K., Choi, J. and Barber, D. L. (2001) The Nck-interacting kinase (NIK) phosphorylates the Na^+-H^+ exchanger NHE1 and regulates NHE1 activation by platelet-derived growth factor. J Biol Chem. **276**, 31349-56

24 Kinsella, J. L., Heller, P. and Froehlich, J. P. (1998) Na^+/H^+ exchanger: proton modifier site regulation of activity. Biochem Cell Biol. **76**, 743-9

25 Orlowski, J. a. S., G. (1996) Characteristics of the Plasma Membrane Na^+/H^+ Exchanger Family. *In* The Na^+/H^+ Exchanger. Fliegel L, Ed., R.G.Landes Company, Texas, pp.123-148.

26 Khadilkar, A., Iannuzzi, P. and Orlowski, J. (2001) Identification of sites in the second exomembrane loop and ninth transmembrane helix of the mammalian Na^+/H^+ exchanger important for drug recognition and cation translocation. J Biol Chem. **276**, 43792-800

27 Wakabayashi, S., Pang, T., Su, X. and Shigekawa, M. (2000) A novel topology model of the human $Na(^+)/H(^+)$ exchanger isoform 1. J Biol Chem. **275**, 7942-9

28 Wakabayashi, S., Fafournoux, P., Sardet, C. and Pouyssegur, J. (1992) The Na^+/H^+ antiporter cytoplasmic domain mediates growth factor signals and controls "$H(^+)$-sensing". Proc Natl Acad Sci U S A. **89**, 2424-8

29 Counillon, L., Franchi, A. and Pouyssegur, J. (1993) A point mutation of the Na^+/H^+ exchanger gene (NHE1) and amplification of the mutated allele confer amiloride resistance upon chronic acidosis. Proc Natl Acad Sci U S A. **90**, 4508-12

30 Counillon, L., Noel, J., Reithmeier, R. A. and Pouyssegur, J. (1997) Random mutagenesis reveals a novel site involved in inhibitor interaction within the fourth transmembrane segment of the Na^+/H^+ exchanger-1. Biochemistry. **36**, 2951-9

31 Touret, N., Poujeol, P. and Counillon, L. (2001) Second-site revertants of a low-sodium-affinity mutant of the Na^+/H^+ exchanger reveal the participation of TM4 into a highly constrained sodium-binding site. Biochemistry. **40**, 5095-101

32 Fliegel, L., Dyck, J. R., Wang, H., Fong, C. and Haworth, R. S. (1993) Cloning and analysis of the human myocardial Na^+/H^+ exchanger. Mol Cell Biochem. **125**, 137-43

33 Karmazyn, M., Gan, X. T., Humphreys, R. A., Yoshida, H. and Kusumoto, K. (1999) The myocardial $Na(^+)$-$H(^+)$ exchange: structure, regulation, and its role in heart disease. Circ Res. **85**, 777-86

34 Kobayashi, Y., Pang, T., Iwamoto, T., Wakabayashi, S. and Shigekawa, M. (2000) Lithium activates mammalian Na^+/H^+ exchangers: isoform specificity and inhibition by genistein. Pflugers Arch. **439**, 455-62

35 Aronson, P. S., Nee, J. and Suhm, M. A. (1982) Modifier role of internal H^+ in activating the Na^+-H^+ exchanger in renal microvillus membrane vesicles. Nature. **299**, 161-3

36 Wakabayashi, S., Pang, T., Hisamitsu, T. and Shigekawa, M. (2003) Two Fundamental Regulatory Factors of the Na^+/H^+ Exchangers *The Proton and CHP. In* The Sodium-Hydrogen Exchanger: From Molecule to its Role in Disease. Karmazyn M., Avkiran M. and Fliegel L., Eds., Kluwer Academic Publishers, pp. 35-49.

37 Bertrand, B., Wakabayashi, S., Ikeda, T., Pouyssegur, J. and Shigekawa, M. (1994) The Na^+/H^+ exchanger isoform 1 (NHE1) is a novel member of the calmodulin-binding proteins. Identification and characterization of calmodulin-binding sites. J Biol Chem. **269**, 13703-9

38 Wakabayashi, S., Bertrand, B., Ikeda, T., Pouyssegur, J. and Shigekawa, M. (1994) Mutation of calmodulin-binding site renders the Na^+/H^+ exchanger (NHE1) highly $H(^+)$-sensitive and Ca2+ regulation-defective. J Biol Chem. **269**, 13710-5

39 Ikeda, T., Schmitt, B., Pouyssegur, J., Wakabayashi, S. and Shigekawa, M. (1997) Identification of cytoplasmic subdomains that control pH-sensing of the Na^+/H^+ exchanger (NHE1): pH-maintenance, ATP-sensitive, and flexible loop domains. J Biochem (Tokyo). **121**, 295-303

40 Wakabayashi, S., Hisamitsu, T., Pang, T. and Shigekawa, M. (2003) Mutations of Arg440 and Gly455/Gly456 oppositely change pH sensing of Na^+/H^+ exchanger 1. J Biol Chem. **278**, 11828-35

41 Maune, J. F., Klee, C. B. and Beckingham, K. (1992) Ca2+ binding and conformational change in two series of point mutations to the individual $Ca(2^+)$-binding sites of calmodulin. J Biol Chem. **267**, 5286-95

42 Pang, T., Su, X., Wakabayashi, S. and Shigekawa, M. (2001) Calcineurin homologous protein as an essential cofactor for Na^+/H^+ exchangers. J Biol Chem. **276**, 17367-72

43 Lin, X. and Barber, D. L. (1996) A calcineurin homologous protein inhibits GTPase-stimulated Na-H exchange. Proc Natl Acad Sci U S A. **93**, 12631-6

44 Pang, T., Wakabayashi, S. and Shigekawa, M. (2002) Expression of calcineurin B homologous protein 2 protects serum deprivation-induced cell death by serum-independent activation of Na^+/H^+ exchanger. J Biol Chem. **277**, 43771-7

45 Mailander, J., Muller-Esterl, W. and Dedio, J. (2001) Human homolog of mouse tescalcin associates with $Na(^+)/H(^+)$ exchanger type-1. FEBS Lett. **507**, 331-5

46 Li, X., Liu, Y., Kay, C. M., Muller-Esterl, W. and Fliegel, L. (2003) The Na^+/H^+ exchanger cytoplasmic tail: structure, function, and interactions with tescalcin. Biochemistry. **42**, 7448-56

47 Li, X., Alvarez, B., Casey, J. R., Reithmeier, R. A. and Fliegel, L. (2002) Carbonic anhydrase II binds to and enhances activity of the Na^+/H^+ exchanger. J Biol Chem. **277**, 36085-91

48 Vuillemin, M. and Pexieder, T. (1997) Carbonic anhydrase II expression pattern in mouse embryonic and fetal heart. Anat Embryol (Berl). **195**, 267-77

49 Aharonovitz, O., Zaun, H. C., Balla, T., York, J. D., Orlowski, J. and Grinstein, S. (2000) Intracellular pH regulation by $Na(^+)/H(^+)$ exchange requires phosphatidylinositol 4,5-bisphosphate. J Cell Biol. **150**, 213-24

50 Hilgemann, D. W. and Ball, R. (1996) Regulation of cardiac Na^+,Ca2+ exchange and KATP potassium channels by PIP2. Science. **273**, 956-9

51 Baukrowitz, T., Schulte, U., Oliver, D., Herlitze, S., Krauter, T., Tucker, S. J., Ruppersberg, J. P. and Fakler, B. (1998) PIP2 and PIP as determinants for ATP inhibition of KATP channels. Science. **282**, 1141-4

52 Ebata, S., Muto, S., Okada, K., Nemoto, J., Amemiya, M., Saito, T. and Asano, Y. (1999) Aldosterone activates Na^+/H^+ exchange in vascular smooth muscle cells by nongenomic and genomic mechanisms. Kidney Int. **56**, 1400-12

53 Wolska, B. M., Averyhart-Fullard, V., Omachi, A., Stojanovic, M. O., Kallen, R. G. and Solaro, R. J. (1997) Changes in thyroid state affect pHi and Nai$^+$ homeostasis in rat ventricular myocytes. J Mol Cell Cardiol. **29**, 2653-63

54 Li, X., Misik, A. J., Rieder, C. V., Solaro, R. J., Lowen, A. and Fliegel, L. (2002) Thyroid hormone receptor alpha 1 regulates expression of the Na^+/H^+ exchanger (NHE1). J Biol Chem. **277**, 28656-62

55 Strazzabosco, M., Poci, C., Spirli, C., Zsembery, A., Granato, A., Massimino, M. L. and Crepaldi, G. (1995) Intracellular pH regulation in Hep G2 cells: effects of epidermal growth factor, transforming growth factor-alpha, and insulinlike growth factor-II on Na^+/H^+ exchange activity. Hepatology. **22**, 588-97

56 Fliegel, L. (1999) Functional and cellular regulation of the myocardial Na^+/H^+ exchanger. J Thromb Thrombolysis. **8**, 9-14

57 Avkiran, M. and Yokoyama, H. (2000) Adenosine A(1) receptor stimulation inhibits alpha(1)-adrenergic activation of the cardiac sarcolemmal $Na(^+)/H(^+)$ exchanger. Br J Pharmacol. **131**, 659-62

58 Coughlin, S. R. (1999) How the protease thrombin talks to cells. Proc Natl Acad Sci U S A. **96**, 11023-7

59 Yasutake, M., Haworth, R. S., King, A. and Avkiran, M. (1996) Thrombin activates the sarcolemmal $Na(^+)$-H^+ exchanger. Evidence for a receptor-mediated mechanism involving protein kinase C. Circ Res. **79**, 705-15

60 Ishihara, H., Connolly, A. J., Zeng, D., Kahn, M. L., Zheng, Y. W., Timmons, C., Tram, T. and Coughlin, S. R. (1997) Protease-activated receptor 3 is a second thrombin receptor in humans. Nature. **386**, 502-6

61 Sabri, A., Muske, G., Zhang, H., Pak, E., Darrow, A., Andrade-Gordon, P. and Steinberg, S. F. (2000) Signaling properties and functions of two distinct cardiomyocyte protease-activated receptors. Circ Res. **86**, 1054-61

62 Krapf, R., Pearce, D., Lynch, C., Xi, X. P., Reudelhuber, T. L., Pouyssegur, J. and Rector, F. C., Jr. (1991) Expression of rat renal Na/H antiporter mRNA levels in response to respiratory and metabolic acidosis. J Clin Invest. **87**, 747-51

63 Kinsella, J., Cujdik, T. and Sacktor, B. (1984) Na^+-H^+ exchange in isolated renal brush-border membrane vesicles in response to metabolic acidosis. Kinetic effects. J Biol Chem. **259**, 13224-7

64 Moe, O. W., Miller, R. T., Horie, S., Cano, A., Preisig, P. A. and Alpern, R. J. (1991) Differential regulation of Na/H antiporter by acid in renal epithelial cells and fibroblasts. J Clin Invest. **88**, 1703-8

65 Fliegel, L., Haworth, R. S. and Dyck, J. R. (1993) Characterization of the placental brush border membrane Na^+/H^+ exchanger: identification of thiol-dependent transitions in apparent molecular size. Biochem J. **289 (Pt 1)**, 101-7

66 Dyck, J. R., Maddaford, T. G., Pierce, G. N. and Fliegel, L. (1995) Induction of expression of the sodium-hydrogen exchanger in rat myocardium. Cardiovasc Res. **29**, 203-8

67 Gan, X. T., Chakrabarti, S. and Karmazyn, M. (1999) Modulation of Na^+/H^+ exchange isoform 1 mRNA expression in isolated rat hearts. Am J Physiol. **277**, H993-8

68 Counillon, L. and Pouyssegur, J. (2000) The expanding family of eucaryotic $Na(^+)/H(^+)$ exchangers. J Biol Chem. **275**, 1-4

69 Sardet, C., Counillon, L., Franchi, A. and Pouyssegur, J. (1990) Growth factors induce phosphorylation of the Na^+/H^+ antiporter, glycoprotein of 110 kD. Science. **247**, 723-6

70 Wang, H., Silva, N. L., Lucchesi, P. A., Haworth, R., Wang, K., Michalak, M., Pelech, S. and Fliegel, L. (1997) Phosphorylation and regulation of the Na^+/H^+ exchanger through mitogen-activated protein kinase. Biochemistry. **36**, 9151-8

71 Sardet, C., Fafournoux, P. and Pouyssegur, J. (1991) Alpha-thrombin, epidermal growth factor, and okadaic acid activate the Na^+/H^+ exchanger, NHE-1, by phosphorylating a set of common sites. J Biol Chem. **266**, 19166-71

72 Bianchini, L., Woodside, M., Sardet, C., Pouyssegur, J., Takai, A. and Grinstein, S. (1991) Okadaic acid, a phosphatase inhibitor, induces activation and phosphorylation of the Na^+/H^+ antiport. J Biol Chem. **266**, 15406-13

73 Moor, A. N. and Fliegel, L. (1999) Protein kinase-mediated regulation of the $Na(^+)/H(^+)$ exchanger in the rat myocardium by mitogen-activated protein kinase-dependent pathways. J Biol Chem. **274**, 22985-92

74 Wakabayashi, S., Bertrand, B., Shigekawa, M., Fafournoux, P. and Pouyssegur, J. (1994) Growth factor activation and "$H(^+)$-sensing" of the Na^+/H^+ exchanger isoform 1 (NHE1). Evidence for an additional mechanism not requiring direct phosphorylation. J Biol Chem. **269**, 5583-8

75 Berk, B. C. (1996) Regulation of the Na^+/H^+ Exchanger in Vascular Smooth Muscle. *In* The Na^+/H^+ Exchanger. Fliegel L, Ed., R.G.Landes Company, Texas, pp. 47-67.

76 Bianchini, L., L'Allemain, G. and Pouyssegur, J. (1997) The p42/p44 mitogen-activated protein kinase cascade is determinant in mediating activation of the Na^+/H^+ exchanger (NHE1 isoform) in response to growth factors. J Biol Chem. **272**, 271-9

77 Fliegel, L., Walsh, M. P., Singh, D., Wong, C. and Barr, A. (1992) Phosphorylation of the C-terminal domain of the Na^+/H^+ exchanger by Ca2+/calmodulin-dependent protein kinase II. Biochem J. **282 (Pt 1)**, 139-45

78 Tominaga, T., Ishizaki, T., Narumiya, S. and Barber, D. L. (1998) p160ROCK mediates RhoA activation of Na-H exchange. Embo J. **17**, 4712-22

79 Takahashi, E., Abe, J., Gallis, B., Aebersold, R., Spring, D. J., Krebs, E. G. and Berk, B. C. (1999) p90(RSK) is a serum-stimulated Na^+/H^+ exchanger isoform-1 kinase. Regulatory phosphorylation of serine 703 of Na^+/H^+ exchanger isoform-1. J Biol Chem. **274**, 20206-14

80 Khaled, A. R., Moor, A. N., Li, A., Kim, K., Ferris, D. K., Muegge, K., Fisher, R. J., Fliegel, L. and Durum, S. K. (2001) Trophic factor withdrawal: p38 mitogen-activated protein kinase activates NHE1, which induces intracellular alkalinization. Mol Cell Biol. **21**, 7545-57

81 Moor, A. N., Gan, X. T., Karmazyn, M. and Fliegel, L. (2001) Activation of Na^+/H^+ exchanger-directed protein kinases in the ischemic and ischemic-reperfused rat myocardium. J Biol Chem. **276**, 16113-22

82 Haworth, R. S., McCann, C., Snabaitis, A. K., Roberts, N. A. and Avkiran, M. (2003) Stimulation of the plasma membrane Na^+/H^+ exchanger NHE1 by sustained intracellular acidosis: Evidence for a novel mechanism mediated by the ERK pathway. J Biol Chem

83 Smith, J. A., Poteet-Smith, C. E., Malarkey, K. and Sturgill, T. W. (1999) Identification of an extracellular signal-regulated kinase (ERK) docking site in ribosomal S6 kinase, a sequence critical for activation by ERK in vivo. J Biol Chem. **274**, 2893-8

84 Davis, R. J. (1993) The mitogen-activated protein kinase signal transduction pathway. J Biol Chem. **268**, 14553-6

85 Takahashi, E., Abe, J. and Berk, B. C. (1997) Angiotensin II stimulates p90rsk in vascular smooth muscle cells. A potential $Na^{(+)}$-H^{+} exchanger kinase. Circ Res. **81**, 268-73

86 Snabaitis, A. K., Yokoyama, H. and Avkiran, M. (2000) Roles of mitogen-activated protein kinases and protein kinase C in alpha(1A)-adrenoceptor-mediated stimulation of the sarcolemmal $Na^{(+)}$-$H^{(+)}$ exchanger. Circ Res. **86**, 214-20

87 Zugaza, J. L., Sinnett-Smith, J., Van Lint, J. and Rozengurt, E. (1996) Protein kinase D (PKD) activation in intact cells through a protein kinase C-dependent signal transduction pathway. Embo J. **15**, 6220-30

88 Valverde, A. M., Sinnett-Smith, J., Van Lint, J. and Rozengurt, E. (1994) Molecular cloning and characterization of protein kinase D: a target for diacylglycerol and phorbol esters with a distinctive catalytic domain. Proc Natl Acad Sci U S A. **91**, 8572-6

89 Van Lint, J. V., Sinnett-Smith, J. and Rozengurt, E. (1995) Expression and characterization of PKD, a phorbol ester and diacylglycerol-stimulated serine protein kinase. J Biol Chem. **270**, 1455-61

90 Haworth, R. S., Sinnett-Smith, J., Rozengurt, E. and Avkiran, M. (1999) Protein kinase D inhibits plasma membrane $Na^{(+)}/H^{(+)}$ exchanger activity. Am J Physiol. **277**, C1202-9

91 Luo, Z. D., Wang, Y., Werlen, G., Camp, S., Chien, K. R. and Taylor, P. (1999) Calcineurin enhances acetylcholinesterase mRNA stability during C2-C12 muscle cell differentiation. Mol Pharmacol. **56**, 886-94

92 Borgese, F., Sardet, C., Cappadoro, M., Pouyssegur, J. and Motais, R. (1992) Cloning and expression of a cAMP-activated Na^{+}/H^{+} exchanger: evidence that the cytoplasmic domain mediates hormonal regulation. Proc Natl Acad Sci U S A. **89**, 6765-9

93 Levine, S. A., Montrose, M. H., Tse, C. M. and Donowitz, M. (1993) Kinetics and regulation of three cloned mammalian Na^{+}/H^{+} exchangers stably expressed in a fibroblast cell line. J Biol Chem. **268**, 25527-35

94 Helmle-Kolb, C., Counillon, L., Roux, D., Pouyssegur, J., Mrkic, B. and Murer, H. (1993) Na/H exchange activities in NHE1-transfected OK-cells: cell polarity and regulation. Pflugers Arch. **425**, 34-40

95 Kong, S. K., Choy, Y. M., Fung, K. P. and Lee, C. Y. (1989) cAMP activates Na^{+}/H^{+} antiporter in murine macrophages. Biochem Biophys Res Commun. **165**, 131-7

96 Moule, S. K. and McGivan, J. D. (1990) Regulation of the plasma membrane potential in hepatocytes--mechanism and physiological significance. Biochim Biophys Acta. **1031**, 383-97

97 Gupta, A., Schwiening, C. J. and Boron, W. F. (1994) Effects of CGRP, forskolin, PMA, and ionomycin on pHi dependence of Na-H exchange in UMR-106 cells. Am J Physiol. **266**, C1088-92

98 Kandasamy, R. A., Yu, F. H., Harris, R., Boucher, A., Hanrahan, J. W. and Orlowski, J. (1995) Plasma membrane Na^+/H^+ exchanger isoforms (NHE-1, -2, and -3) are differentially responsive to second messenger agonists of the protein kinase A and C pathways. J Biol Chem. **270**, 29209-16

99 Moor, A. N., Murtazina, R. and Fliegel, L. (2000) Calcium and osmotic regulation of the Na^+/H^+ exchanger in neonatal ventricular myocytes. J Mol Cell Cardiol. **32**, 925-36

100 Cohen, P. T. (2002) Protein phosphatase 1--targeted in many directions. J Cell Sci. **115**, 241-56

101 Morrison, D. K., Murakami, M. S. and Cleghon, V. (2000) Protein kinases and phosphatases in the Drosophila genome. J Cell Biol. **150**, F57-62

102 Herzig, S. and Neumann, J. (2000) Effects of serine/threonine protein phosphatases on ion channels in excitable membranes. Physiol Rev. **80**, 173-210

103 Mumby, M. C. and Walter, G. (1993) Protein serine/threonine phosphatases: structure, regulation, and functions in cell growth. Physiol Rev. **73**, 673-99

104 Barford, D., Das, A. K. and Egloff, M. P. (1998) The structure and mechanism of protein phosphatases: insights into catalysis and regulation. Annu Rev Biophys Biomol Struct. **27**, 133-64

105 Barton, G. J., Cohen, P. T. and Barford, D. (1994) Conservation analysis and structure prediction of the protein serine/threonine phosphatases. Sequence similarity with diadenosine tetraphosphatase from Escherichia coli suggests homology to the protein phosphatases. Eur J Biochem. **220**, 225-37

106 Berndt, N., Campbell, D. G., Caudwell, F. B., Cohen, P., da Cruz e Silva, E. F., da Cruz e Silva, O. B. and Cohen, P. T. (1987) Isolation and sequence analysis of a cDNA clone encoding a type-1 protein phosphatase catalytic subunit: homology with protein phosphatase 2A. FEBS Lett. **223**, 340-6

107 Cohen, P. and Cohen, P. T. (1989) Protein phosphatases come of age. J Biol Chem. **264**, 21435-8

108 Bollen, M., DePaoli-Roach, A. A. and Stalmans, W. (1994) Native cytosolic protein phosphatase-1 (PP-1S) containing modulator (inhibitor-2) is an active enzyme. FEBS Lett. **344**, 196-200

109 Shenolikar, S. (1994) Protein serine/threonine phosphatases--new avenues for cell regulation. Annu Rev Cell Biol. **10**, 55-86

110 Dombradi, V., Axton, J. M., Brewis, N. D., da Cruz e Silva, E. F., Alphey, L. and Cohen, P. T. (1990) Drosophila contains three genes that encode distinct isoforms of protein phosphatase 1. Eur J Biochem. **194**, 739-45

111 Sasaki, K., Shima, H., Kitagawa, Y., Irino, S., Sugimura, T. and Nagao, M. (1990) Identification of members of the protein phosphatase 1 gene family in the rat and enhanced expression of protein phosphatase 1 alpha gene in rat hepatocellular carcinomas. Jpn J Cancer Res. **81**, 1272-80

112 Durfee, T., Becherer, K., Chen, P. L., Yeh, S. H., Yang, Y., Kilburn, A. E., Lee, W. H. and Elledge, S. J. (1993) The retinoblastoma protein associates with the protein phosphatase type 1 catalytic subunit. Genes Dev. **7**, 555-69

113 Yoshida, K., Watanabe, M., Kato, H., Dutta, A. and Sugano, S. (1999) BH-protocadherin-c, a member of the cadherin superfamily, interacts with protein phosphatase 1 alpha through its intracellular domain. FEBS Lett. **460**, 93-8

114 Watanabe, T., Huang, H. B., Horiuchi, A., da Cruze Silva, E. F., Hsieh-Wilson, L., Allen, P. B., Shenolikar, S., Greengard, P. and Nairn, A. C. (2001) Protein phosphatase 1 regulation by inhibitors and targeting subunits. Proc Natl Acad Sci U S A. **98**, 3080-5

115 Doherty, M. J., Moorhead, G., Morrice, N., Cohen, P. and Cohen, P. T. (1995) Amino acid sequence and expression of the hepatic glycogen-binding (GL)-subunit of protein phosphatase-1. FEBS Lett. **375**, 294-8

116 Egloff, M. P., Johnson, D. F., Moorhead, G., Cohen, P. T., Cohen, P. and Barford, D. (1997) Structural basis for the recognition of regulatory subunits by the catalytic subunit of protein phosphatase 1. Embo J. **16**, 1876-87

117 Hsieh-Wilson, L. C., Allen, P. B., Watanabe, T., Nairn, A. C. and Greengard, P. (1999) Characterization of the neuronal targeting protein spinophilin and its interactions with protein phosphatase-1. Biochemistry. **38**, 4365-73

118 Trinkle-Mulcahy, L., Ajuh, P., Prescott, A., Claverie-Martin, F., Cohen, S., Lamond, A. I. and Cohen, P. (1999) Nuclear organisation of NIPP1, a regulatory subunit of protein phosphatase 1 that associates with pre-mRNA splicing factors. J Cell Sci. **112 (Pt 2)**, 157-68

119 Beullens, M., Van Eynde, A., Vulsteke, V., Connor, J., Shenolikar, S., Stalmans, W. and Bollen, M. (1999) Molecular determinants of nuclear protein phosphatase-1 regulation by NIPP-1. J Biol Chem. **274**, 14053-61

120 Helps, N. R., Luo, X., Barker, H. M. and Cohen, P. T. (2000) NIMA-related kinase 2 (Nek2), a cell-cycle-regulated protein kinase localized to centrosomes, is complexed to protein phosphatase 1. Biochem J. **349**, 509-18

121 Schillace, R. V., Voltz, J. W., Sim, A. T., Shenolikar, S. and Scott, J. D. (2001) Multiple interactions within the AKAP220 signaling complex contribute to protein phosphatase 1 regulation. J Biol Chem. **276**, 12128-34

122 Egloff, M. P., Cohen, P. T., Reinemer, P. and Barford, D. (1995) Crystal structure of the catalytic subunit of human protein phosphatase 1 and its complex with tungstate. J Mol Biol. **254**, 942-59

123 MacKintosh, R. W., Dalby, K. N., Campbell, D. G., Cohen, P. T., Cohen, P. and MacKintosh, C. (1995) The cyanobacterial toxin microcystin binds covalently to cysteine-273 on protein phosphatase 1. FEBS Lett. **371**, 236-40

124 Zhang, J., Zhang, Z., Brew, K. and Lee, E. Y. (1996) Mutational analysis of the catalytic subunit of muscle protein phosphatase-1. Biochemistry. **35**, 6276-82

125 Connor, J. H., Quan, H. N., Ramaswamy, N. T., Zhang, L., Barik, S., Zheng, J., Cannon, J. F., Lee, E. Y. and Shenolikar, S. (1998) Inhibitor-1 interaction domain that mediates the inhibition of protein phosphatase-1. J Biol Chem. **273**, 27716-24

126 Maynes, J. T., Bateman, K. S., Cherney, M. M., Das, A. K., Luu, H. A., Holmes, C. F. and James, M. N. (2001) Crystal structure of the tumor-promoter okadaic acid bound to protein phosphatase-1. J Biol Chem. **276**, 44078-82

127 Connor, J. H., Kleeman, T., Barik, S., Honkanen, R. E. and Shenolikar, S. (1999) Importance of the beta12-beta13 loop in protein phosphatase-1 catalytic subunit for inhibition by toxins and mammalian protein inhibitors. J Biol Chem. **274**, 22366-72

128 Satoh, A., Nakanishi, H., Obaishi, H., Wada, M., Takahashi, K., Satoh, K., Hirao, K., Nishioka, H., Hata, Y., Mizoguchi, A. and Takai, Y. (1998) Neurabin-II/spinophilin. An actin filament-binding protein with one pdz domain localized at cadherin-based cell-cell adhesion sites. J Biol Chem. **273**, 3470-5

129 Allen, P. B., Ouimet, C. C. and Greengard, P. (1997) Spinophilin, a novel protein phosphatase 1 binding protein localized to dendritic spines. Proc Natl Acad Sci U S A. **94**, 9956-61

130 Smith, F. D., Oxford, G. S. and Milgram, S. L. (1999) Association of the D2 dopamine receptor third cytoplasmic loop with spinophilin, a protein phosphatase-1-interacting protein. J Biol Chem. **274**, 19894-900

131 Yang, J., Hurley, T. D. and DePaoli-Roach, A. A. (2000) Interaction of inhibitor-2 with the catalytic subunit of type 1 protein phosphatase. Identification of a sequence analogous to the consensus type 1 protein phosphatase-binding motif. J Biol Chem. **275**, 22635-44

132 Bennett, D., Szoor, B. and Alphey, L. (1999) The chaperone-like properties of mammalian inhibitor-2 are conserved in a Drosophila homologue. Biochemistry. **38**, 16276-82

133 Cohen, P. T., Schelling, D. L., da Cruz e Silva, O. B., Barker, H. M. and Cohen, P. (1989) The major type-1 protein phosphatase catalytic subunits are the same gene products in rabbit skeletal muscle and rabbit liver. Biochim Biophys Acta. **1008**, 135-8

134 Bollen, M. and Stalmans, W. (1992) The structure, role, and regulation of type 1 protein phosphatases. Crit Rev Biochem Mol Biol. **27**, 227-81

135 Alessi, D. R., Street, A. J., Cohen, P. and Cohen, P. T. (1993) Inhibitor-2 functions like a chaperone to fold three expressed isoforms of mammalian protein phosphatase-1 into a conformation with the specificity and regulatory properties of the native enzyme. Eur J Biochem. **213**, 1055-66

136 MacKintosh, C., Garton, A. J., McDonnell, A., Barford, D., Cohen, P. T., Tonks, N. K. and Cohen, P. (1996) Further evidence that inhibitor-2 acts like a chaperone to fold PP1 into its native conformation. FEBS Lett. **397**, 235-8

137 Wang, Q. M., Park, I. K., Fiol, C. J., Roach, P. J. and DePaoli-Roach, A. A. (1994) Isoform differences in substrate recognition by glycogen synthase kinases 3 alpha and 3 beta in the phosphorylation of phosphatase inhibitor 2. Biochemistry. **33**, 143-7

138 Park, I. K. and DePaoli-Roach, A. A. (1994) Domains of phosphatase inhibitor-2 involved in the control of the ATP-Mg-dependent protein phosphatase. J Biol Chem. **269**, 28919-28

139 Connor, J. H., Frederick, D., Huang, H., Yang, J., Helps, N. R., Cohen, P. T., Nairn, A. C., DePaoli-Roach, A., Tatchell, K. and Shenolikar, S. (2000) Cellular mechanisms regulating protein phosphatase-1. A key functional interaction between inhibitor-2 and the type 1 protein phosphatase catalytic subunit. J Biol Chem. **275**, 18670-5

140 Cardenas, M. E., Muir, R. S., Breuder, T. and Heitman, J. (1995) Targets of immunophilin-immunosuppressant complexes are distinct highly conserved regions of calcineurin A. Embo J. **14**, 2772-83

141 Evans, D. R. and Simon, J. A. (2001) The predicted beta12-beta13 loop is important for inhibition of PP2Acalpha by the antitumor drug fostriecin. FEBS Lett. **498**, 110-5

142 Janssens, V. and Goris, J. (2001) Protein phosphatase 2A: a highly regulated family of serine/threonine phosphatases implicated in cell growth and signalling. Biochem J. **353**, 417-39

143 Khew-Goodall, Y., Mayer, R. E., Maurer, F., Stone, S. R. and Hemmings, B. A. (1991) Structure and transcriptional regulation of protein phosphatase 2A catalytic subunit genes. Biochemistry. **30**, 89-97

144 Ruediger, R., Hentz, M., Fait, J., Mumby, M. and Walter, G. (1994) Molecular model of the A subunit of protein phosphatase 2A: interaction with other subunits and tumor antigens. J Virol. **68**, 123-9

145 Chen, J., Parsons, S. and Brautigan, D. L. (1994) Tyrosine phosphorylation of protein phosphatase 2A in response to growth stimulation and v-src transformation of fibroblasts. J Biol Chem. **269**, 7957-62

146 Lee, J. and Stock, J. (1993) Protein phosphatase 2A catalytic subunit is methyl-esterified at its carboxyl terminus by a novel methyltransferase. J Biol Chem. **268**, 19192-5

147 Xie, H. and Clarke, S. (1994) Protein phosphatase 2A is reversibly modified by methyl esterification at its C-terminal leucine residue in bovine brain. J Biol Chem. **269**, 1981-4

148 Ruvolo, P. P. (2001) Ceramide regulates cellular homeostasis via diverse stress signaling pathways. Leukemia. **15**, 1153-60

149 Ruvolo, P. P., Deng, X., Ito, T., Carr, B. K. and May, W. S. (1999) Ceramide induces Bcl2 dephosphorylation via a mechanism involving mitochondrial PP2A. J Biol Chem. **274**, 20296-300

150 Katayose, Y., Li, M., Al-Murrani, S. W., Shenolikar, S. and Damuni, Z. (2000) Protein phosphatase 2A inhibitors, I(1)(PP2A) and I(2)(PP2A), associate with and modify the substrate specificity of protein phosphatase 1. J Biol Chem. **275**, 9209-14

151 Feng, B. and Stemmer, P. M. (2001) Ca2+ binding site 2 in calcineurin-B modulates calmodulin-dependent calcineurin phosphatase activity. Biochemistry. **40**, 8808-14

152 Klee, C. B., Ren, H. and Wang, X. (1998) Regulation of the calmodulin-stimulated protein phosphatase, calcineurin. J Biol Chem. **273**, 13367-70

153 Rothermel, B. A., Vega, R. B. and Williams, R. S. (2003) The role of modulatory calcineurin-interacting proteins in calcineurin signaling. Trends Cardiovasc Med. **13**, 15-21

154 Gorlach, J., Fox, D. S., Cutler, N. S., Cox, G. M., Perfect, J. R. and Heitman, J. (2000) Identification and characterization of a highly conserved calcineurin binding protein, CBP1/calcipressin, in Cryptococcus neoformans. Embo J. **19**, 3618-29

155 Rao, A., Luo, C. and Hogan, P. G. (1997) Transcription factors of the NFAT family: regulation and function. Annu Rev Immunol. **15**, 707-47

156 Vega, R. B., Yang, J., Rothermel, B. A., Bassel-Duby, R. and Williams, R. S. (2002) Multiple domains of MCIP1 contribute to inhibition of calcineurin activity. J Biol Chem. **277**, 30401-7

157 Lin, X., Sikkink, R. A., Rusnak, F. and Barber, D. L. (1999) Inhibition of calcineurin phosphatase activity by a calcineurin B homologous protein. J Biol Chem. **274**, 36125-31

158 Miskin, J. E., Abrams, C. C., Goatley, L. C. and Dixon, L. K. (1998) A viral mechanism for inhibition of the cellular phosphatase calcineurin. Science. **281**, 562-5

159 Cameron, A. M., Steiner, J. P., Roskams, A. J., Ali, S. M., Ronnett, G. V. and Snyder, S. H. (1995) Calcineurin associated with the inositol 1,4,5-trisphosphate receptor-FKBP12 complex modulates Ca2+ flux. Cell. **83**, 463-72

160 Lam, E., Martin, M. M., Timerman, A. P., Sabers, C., Fleischer, S., Lukas, T., Abraham, R. T., O'Keefe, S. J., O'Neill, E. A. and Wiederrecht, G. J. (1995) A novel FK506 binding protein can mediate the immunosuppressive effects of FK506 and is associated with the cardiac ryanodine receptor. J Biol Chem. **270**, 26511-22

161 Huai, Q., Kim, H. Y., Liu, Y., Zhao, Y., Mondragon, A., Liu, J. O. and Ke, H. (2002) Crystal structure of calcineurin-cyclophilin-cyclosporin shows common but distinct recognition of immunophilin-drug complexes. Proc Natl Acad Sci U S A. **99**, 12037-42

162 Kingsbury, T. J. and Cunningham, K. W. (2000) A conserved family of calcineurin regulators. Genes Dev. **14**, 1595-604

163 Crabtree, G. R. (2001) Calcium, calcineurin, and the control of transcription. J Biol Chem. **276**, 2313-6

164 Rusnak, F. and Mertz, P. (2000) Calcineurin: form and function. Physiol Rev. **80**, 1483-521

165 Olson, E. N. and Williams, R. S. (2000) Remodeling muscles with calcineurin. Bioessays. **22**, 510-9

166 Takai, A., Bialojan, C., Troschka, M. and Ruegg, J. C. (1987) Smooth muscle myosin phosphatase inhibition and force enhancement by black sponge toxin. FEBS Lett. **217**, 81-4

167 Cohen, P. T., Brewis, N. D., Hughes, V. and Mann, D. J. (1990) Protein serine/threonine phosphatases; an expanding family. FEBS Lett. **268**, 355-9

168 Livne, A. A., Aharonovitz, O., Fridman, H., Tsukitani, Y. and Markus, S. (1991) Modulation of Na^+/H^+ exchange and intracellular pH by protein kinase C and protein phosphatase in blood platelets. Biochim Biophys Acta. **1068**, 161-6

169 Livne, A. A., Sardet, C. and Pouyssegur, J. (1991) The Na^+/H^+ exchanger is phosphorylated in human platelets in response to activating agents. FEBS Lett. **284**, 219-22

170 de La Rosa, A., Vilarino, N., Vieytes, R. and Botana, M. (2002) Okadaic acid, a protein phosphatase inhibitor, stimulates the activity of Na^+/H^+ and Na^+-independent Cl-/HCO3- exchangers in human lymphocytes. Naunyn Schmiedebergs Arch Pharmacol. **365**, 74-81

171 Sartori, M., Ceolotto, G. and Semplicini, A. (1999) MAPKinase and regulation of the sodium-proton exchanger in human red blood cell. Biochim Biophys Acta. **1421**, 140-8

172 Pederson, S. F., Varming, C., Christensen, S. T. and Hoffmann, E. K. (2002) Mechanisms of activation of NHE by cell shrinkage and by calyculin A in Ehrlich ascites tumor cells. J Membr Biol. **189**, 67-81

173 Guizouarn, H., Borgese, F., Pellissier, B., Garcia-Romeu, F. and Motais, R. (1995) Regulation of Na^+/H^+ exchange activity by recruitment of new Na^+/H^+ antiporters: effect of calyculin A. Am J Physiol. **268**, C434-41

174 Guizouarn, H., Harvey, B. J., Borgese, F., Gabillat, N., Garcia-Romeu, F. and Motais, R. (1993) Volume-activated Cl(-)-independent and Cl(-)-dependent K^+ pathways in trout red blood cells. J Physiol. **462**, 609-26

175 Malapert, M., Guizouarn, H., Fievet, B., Jahns, R., Garcia-Romeu, F., Motais, R. and Borgese, F. (1997) Regulation of Na^+/H^+ antiporter in trout red blood cells. J Exp Biol. **200 (Pt 2)**, 353-60

176 Muslin, A. J., Tanner, J. W., Allen, P. M. and Shaw, A. S. (1996) Interaction of 14-3-3 with signaling proteins is mediated by the recognition of phosphoserine. Cell. **84**, 889-97

177 Lehoux, S., Abe, J., Florian, J. A. and Berk, B. C. (2001) 14-3-3 Binding to Na^+/H^+ exchanger isoform-1 is associated with serum-dependent activation of Na^+/H^+ exchange. J Biol Chem. **276**, 15794-800

178 Adler, A. I. (2003) Managing diabetes: what to do about cardiovascular disease. Diabetes Res Clin Pract. **61**, S3-8

179 Baker, K. M., Booz, G. W. and Dostal, D. E. (1992) Cardiac actions of angiotensin II: Role of an intracardiac renin-angiotensin system. Annu Rev Physiol. **54**, 227-41

180 Simpson, P. (1983) Norepinephrine-stimulated hypertrophy of cultured rat myocardial cells is an alpha 1 adrenergic response. J Clin Invest. **72**, 732-8

181 Yamazaki, T., Komuro, I., Kudoh, S., Zou, Y., Nagai, R., Aikawa, R., Uozumi, H. and Yazaki, Y. (1998) Role of ion channels and exchangers in mechanical stretch-induced cardiomyocyte hypertrophy. Circ Res. **82**, 430-7

182 Yamazaki, T., Komuro, I., Kudoh, S., Zou, Y., Shiojima, I., Mizuno, T., Takano, H., Hiroi, Y., Ueki, K., Tobe, K. and et al. (1995) Mechanical stress activates protein kinase cascade of phosphorylation in neonatal rat cardiac myocytes. J Clin Invest. **96**, 438-46

183 Yamazaki, T., Tobe, K., Hoh, E., Maemura, K., Kaida, T., Komuro, I., Tamemoto, H., Kadowaki, T., Nagai, R. and Yazaki, Y. (1993) Mechanical loading activates mitogen-activated protein kinase and S6 peptide kinase in cultured rat cardiac myocytes. J Biol Chem. **268**, 12069-76

184 Kusumoto, K., Haist, J. V. and Karmazyn, M. (2001) $Na^{(+)}/H^{(+)}$ exchange inhibition reduces hypertrophy and heart failure after myocardial infarction in rats. Am J Physiol Heart Circ Physiol. **280**, H738-45

185 Gu, J. W., Anand, V., Shek, E. W., Moore, M. C., Brady, A. L., Kelly, W. C. and Adair, T. H. (1998) Sodium induces hypertrophy of cultured myocardial myoblasts and vascular smooth muscle cells. Hypertension. **31**, 1083-7

186 Hayasaki-Kajiwara, Y., Kitano, Y., Iwasaki, T., Shimamura, T., Naya, N., Iwaki, K. and Nakajima, M. (1999) $Na^{(+)}$influx via $Na^{(+)}/H^{(+)}$exchange activates protein kinase C isozymes delta and epsilon in cultured neonatal rat cardiac myocytes. J Mol Cell Cardiol. **31**, 1559-72

187 Avkiran, M. (2003) Basic biology and pharmacology of the cardiac sarcolemmal sodium/hydrogen exchanger. J Card Surg. **18 Suppl 1**, 3-12

188 Avkiran, M. (1999) Protection of the myocardium during ischemia and reperfusion : $Na^{(+)}/H^{(+)}$ exchange inhibition versus ischemic preconditioning. Circulation. **100**, 2469-72

189 Karmazyn, M. (1998) The myocardial sodium-hydrogen exchanger (NHE) and its role in mediating ischemic and reperfusion injury. Keio J Med. **47**, 65-72

190 Murphy, E., Perlman, M., London, R. E. and Steenbergen, C. (1991) Amiloride delays the ischemia-induced rise in cytosolic free calcium. Circ Res. **68**, 1250-8

191 Myers, M. L., Mathur, S., Li, G. H. and Karmazyn, M. (1995) Sodium-hydrogen exchange inhibitors improve postischemic recovery of function in the perfused rabbit heart. Cardiovasc Res. **29**, 209-14

192 Scholz, W., Albus, U., Counillon, L., Gogelein, H., Lang, H. J., Linz, W., Weichert, A. and Scholkens, B. A. (1995) Protective effects of HOE642, a selective sodium-hydrogen exchange subtype 1 inhibitor, on cardiac ischaemia and reperfusion. Cardiovasc Res. **29**, 260-8

193 Karmazyn, M. (1999) The role of the myocardial sodium-hydrogen exchanger in mediating ischemic and reperfusion injury. From amiloride to cariporide. Ann N Y Acad Sci. **874**, 326-34

194 Stromer, H., de Groot, M. C., Horn, M., Faul, C., Leupold, A., Morgan, J. P., Scholz, W. and Neubauer, S. (2000) $Na^{(+)}/H^{(+)}$ exchange inhibition with HOE642 improves postischemic recovery due to attenuation of $Ca(2^{+})$ overload and prolonged acidosis on reperfusion. Circulation. **101**, 2749-55

195 Xue, Y. X., Aye, N. N. and Hashimoto, K. (1996) Antiarrhythmic effects of HOE642, a novel $Na^{(+)}$-H^{+} exchange inhibitor, on ventricular arrhythmias in animal hearts. Eur J Pharmacol. **317**, 309-16

196 Klein, H. H., Pich, S., Bohle, R. M., Lindert-Heimberg, S. and Nebendahl, K. (2000) $Na^{(+)}/H^{(+)}$ exchange inhibitor cariporide attenuates cell injury predominantly during ischemia and not at onset of reperfusion in porcine hearts with low residual blood flow. Circulation. **102**, 1977-82

197 Orlov, S. N., Adragna, N. C., Adarichev, V. A. and Hamet, P. (1999) Genetic and biochemical determinants of abnormal monovalent ion transport in primary hypertension. Am J Physiol. **276**, C511-36

198 Orlov, S. N., Aksentsev, S. L., Pokudin, N. I., Tremblay, J. and Hamet, P. (1998) Na^{+}/H^{+} exchange in vascular smooth muscle cells is controlled by GTP-binding proteins. Hypertension. **31**, 259-65

199 Siczkowski, M., Davies, J. E. and Ng, L. L. (1995) $Na^{(+)}$-H^{+} exchanger isoform 1 phosphorylation in normal Wistar-Kyoto and spontaneously hypertensive rats. Circ Res. **76**, 825-31

200 Phan, V. N., Kusuhara, M., Lucchesi, P. A. and Berk, B. C. (1997) A 90-kD $Na^{(+)}$-H^{+} exchanger kinase has increased activity in spontaneously hypertensive rat vascular smooth muscle cells. Hypertension. **29**, 1265-72

201 Kuro-o, M., Hanaoka, K., Hiroi, Y., Noguchi, T., Fujimori, Y., Takewaki, S., Hayasaka, M., Katoh, H., Miyagishi, A., Nagai, R. and et al. (1995) Salt-sensitive hypertension in transgenic mice overexpressing $Na^{(+)}$-proton exchanger. Circ Res. **76**, 148-53

202 Colman, P. G., Thomas, D. W., Zimmet, P. Z., Welborn, T. A., Garcia-Webb, P. and Moore, M. P. (1999) New classification and criteria for diagnosis of diabetes mellitus. The Australasian Working Party on Diagnostic Criteria for Diabetes Mellitus. N Z Med J. **112**, 139-41

203 Alberti, K. G. (2001) Treating type 2 diabetes--today's targets, tomorrow's goals. Diabetes Obes Metab. **3 Suppl 1**, S3-10

204 Siffert, W., Siffert, G., Scheid, P. and Akkerman, J. W. (1989) Activation of Na^+/H^+ exchange and Ca2+ mobilization start simultaneously in thrombin-stimulated platelets. Evidence that platelet shape change disturbs early rises of BCECF fluorescence which causes an underestimation of actual cytosolic alkalinization. Biochem J. **258**, 521-7

205 Williams, B. and Howard, R. L. (1994) Glucose-induced changes in Na^+/H^+ antiport activity and gene expression in cultured vascular smooth muscle cells. Role of protein kinase C. J Clin Invest. **93**, 2623-31

206 Jandeleit-Dahm, K., Hannan, K. M., Farrelly, C. A., Allen, T. J., Rumble, J. R., Gilbert, R. E., Cooper, M. E. and Little, P. J. (2000) Diabetes-induced vascular hypertrophy is accompanied by activation of $Na(^+)$-$H(^+)$ exchange and prevented by $Na(^+)$-$H(^+)$ exchange inhibition. Circ Res. **87**, 1133-40

207 el-Seifi, S., Freiberg, J. M., Kinsella, J., Cheng, L. and Sacktor, B. (1987) Na^+-H^+ exchange and Na^+-dependent transport systems in streptozotocin diabetic rat kidneys. Am J Physiol. **252**, R40-7

208 Cooper, M. E., Rumble, J., Komers, R., Du, H. C., Jandeleit, K. and Chou, S. T. (1994) Diabetes-associated mesenteric vascular hypertrophy is attenuated by angiotensin-converting enzyme inhibition. Diabetes. **43**, 1221-8

209 Reshkin, S. J., Bellizzi, A., Caldeira, S., Albarani, V., Malanchi, I., Poignee, M., Alunni-Fabbroni, M., Casavola, V. and Tommasino, M. (2000) Na^+/H^+ exchanger-dependent intracellular alkalinization is an early event in malignant transformation and plays an essential role in the development of subsequent transformation-associated phenotypes. Faseb J. **14**, 2185-97

210 Rotin, D., Steele-Norwood, D., Grinstein, S. and Tannock, I. (1989) Requirement of the Na^+/H^+ exchanger for tumor growth. Cancer Res. **49**, 205-11

211 Reshkin, S. J., Bellizzi, A., Cardone, R. A., Tommasino, M., Casavola, V. and Paradiso, A. (2003) Paclitaxel Induces Apoptosis via Protein Kinase A- and p38 Mitogen-activated Protein-dependent Inhibition of the $Na^{(+)}/H^{(+)}$ Exchanger (NHE) NHE Isoform 1 in Human Breast Cancer Cells. Clin Cancer Res. **9**, 2366-73

212 MacKeigan, J. P., Collins, T. S. and Ting, J. P. (2000) MEK inhibition enhances paclitaxel-induced tumor apoptosis. J Biol Chem. **275**, 38953-6

213 Bacus, S. S., Gudkov, A. V., Lowe, M., Lyass, L., Yung, Y., Komarov, A. P., Keyomarsi, K., Yarden, Y. and Seger, R. (2001) Taxol-induced apoptosis depends on MAP kinase pathways (ERK and p38) and is independent of p53. Oncogene. **20**, 147-55

214 Shtil, A. A., Mandlekar, S., Yu, R., Walter, R. J., Hagen, K., Tan, T. H., Roninson, I. B. and Kong, A. N. (1999) Differential regulation of mitogen-activated protein kinases by microtubule-binding agents in human breast cancer cells. Oncogene. **18**, 377-84

215 Wang, H., Singh, D. and Fliegel, L. (1998) Functional role of cysteine residues in the Na^+/H^+ exchanger effects of mutation of cysteine residues on targeting and activity of the Na^+/H^+ exchanger. Arch Biochem Biophys. **358**, 116-24

216 Haworth, R. S., Frohlich, O. and Fliegel, L. (1993) Multiple carbohydrate moieties on the Na^+/H^+ exchanger. Biochem J. **289 (Pt 3)**, 637-40

217 Craig, M., Luu, H. A., McCready, T. L., Williams, D., Andersen, R. J. and Holmes, C. F. (1996) Molecular mechanisms underlying he interaction of motuporin and microcystins with type-1 and type-2A protein phosphatases. Biochem Cell Biol. **74**, 569-78

218 Wei, Q. and Lee, E. Y. (1997) Expression and reconstitution of calcineurin A and B subunits. Biochem Mol Biol Int. **41**, 169-77

219 Holmes, C. F. (1991) Liquid chromatography-linked protein phosphatase bioassay; a highly sensitive marine bioscreen for okadaic acid and related diarrhetic shellfish toxins. Toxicon. **29**, 469-77

220 Helps, N. R., Street, A. J., Elledge, S. J. and Cohen, P. T. (1994) Cloning of the complete coding region for human protein phosphatase inhibitor 2 using the two hybrid system and expression of inhibitor 2 in E. coli. FEBS Lett. **340**, 93-8

221 Endo, S., Connor, J. H., Forney, B., Zhang, L., Ingebritsen, T. S., Lee, E. Y. and Shenolikar, S. (1997) Conversion of protein phosphatase 1 catalytic subunit to a $Mn(2^+)$-dependent enzyme impairs its regulation by inhibitor 1. Biochemistry. **36**, 6986-92

222 Michalak, M., Fliegel, L. and Wlasichuk, K. (1990) Isolation and characterization of calcium binding glycoproteins of cardiac sarcolemmal vesicles. J Biol Chem. **265**, 5869-74

223 Hecker, K. H. and Roux, K. H. (1996) High and low annealing temperatures increase both specificity and yield in touchdown and stepdown PCR. Biotechniques. **20**, 478-85

224 Tung, H. Y., Alemany, S. and Cohen, P. (1985) The protein phosphatases involved in cellular regulation. 2. Purification, subunit structure and properties of protein phosphatases-2A0, 2A1, and 2A2 from rabbit skeletal muscle. Eur J Biochem. **148**, 253-63

225 Zavoico, G. B. and Cragoe, E. J., Jr. (1988) Ca2+ mobilization can occur independent of acceleration of Na^+/H^+ exchange in thrombin-stimulated human platelets. J Biol Chem. **263**, 9635-9

226 Rosskopf, D. (1999) Sodium-hydrogen exchange and platelet function. J Thromb Thrombolysis. **8**, 15-24

227 Franchi, A., Cragoe, E., Jr. and Pouyssegur, J. (1986) Isolation and properties of fibroblast mutants overexpressing an altered Na^+/H^+ antiporter. J Biol Chem. **261**, 14614-20

228 Silva, N. L., Wang, H., Harris, C. V., Singh, D. and Fliegel, L. (1997) Characterization of the Na^+/H^+ exchanger in human choriocarcinoma (BeWo) cells. Pflugers Arch. **433**, 792-802

229 Qin, Y. L., Yu, D. Y. and Wei, Q. (2003) Function and structure of recombinant single chain calcineurin. Biochem Biophys Res Commun. **308**, 87-93

230 Milan, D., Griffith, J., Su, M., Price, E. R. and McKeon, F. (1994) The latch region of calcineurin B is involved in both immunosuppressant-immunophilin complex docking and phosphatase activation. Cell. **79**, 437-47

231 Cohen, P. (1989) The structure and regulation of protein phosphatases. Annu Rev Biochem. **58**, 453-508

232 MacDougall, L. K., Jones, L. R. and Cohen, P. (1991) Identification of the major protein phosphatases in mammalian cardiac muscle which dephosphorylate phospholamban. Eur J Biochem. **196**, 725-34

233 Luss, H., Klein-Wiele, O., Boknik, P., Herzig, S., Knapp, J., Linck, B., Muller, F. U., Scheld, H. H., Schmid, C., Schmitz, W. and Neumann, J. (2000) Regional expression of protein phosphatase type 1 and 2A catalytic subunit isoforms in the human heart. J Mol Cell Cardiol. **32**, 2349-59

234 Shima, H., Hatano, Y., Chun, Y. S., Sugimura, T., Zhang, Z., Lee, E. Y. and Nagao, M. (1993) Identification of PP1 catalytic subunit isotypes PP1 gamma 1, PP1 delta and PP1 alpha in various rat tissues. Biochem Biophys Res Commun. **192**, 1289-96

235 Bandyopadhyay, A., Shin, D. W., Ahn, J. O. and Kim, D. H. (2000) Calcineurin regulates ryanodine receptor/Ca(2^+)-release channels in rat heart. Biochem J. **352 Pt 1**, 61-70

236 Jethmalani, S. M. and Henle, K. J. (1998) Calreticulin associates with stress proteins: implications for chaperone function during heat stress. J Cell Biochem. **69**, 30-43

237 Moule, S. K. and McGivan, J. D. (1990) Epidermal growth factor and cyclic AMP stimulate Na^+/H^+ exchange in isolated rat hepatocytes. Eur J Biochem. **187**, 677-82

238 Feliciello, A., Gottesman, M. E. and Avvedimento, E. V. (2001) The biological functions of A-kinase anchor proteins. J Mol Biol. **308**, 99-114

239 Dransfield, D. T., Bradford, A. J., Smith, J., Martin, M., Roy, C., Mangeat, P. H. and Goldenring, J. R. (1997) Ezrin is a cyclic AMP-dependent protein kinase anchoring protein. Embo J. **16**, 35-43

240 Weinman, E. J., Steplock, D., Donowitz, M. and Shenolikar, S. (2000) NHERF associations with sodium-hydrogen exchanger isoform 3 (NHE3) and ezrin are essential for cAMP-mediated phosphorylation and inhibition of NHE3. Biochemistry. **39**, 6123-9

241 Davare, M. A., Avdonin, V., Hall, D. D., Peden, E. M., Burette, A., Weinberg, R. J., Horne, M. C., Hoshi, T. and Hell, J. W. (2001) A beta2 adrenergic receptor signaling complex assembled with the Ca2+ channel Cav1.2. Science. **293**, 98-101

242 Marx, S. O., Kurokawa, J., Reiken, S., Motoike, H., D'Armiento, J., Marks, A. R. and Kass, R. S. (2002) Requirement of a macromolecular signaling complex for beta adrenergic receptor modulation of the KCNQ1-KCNE1 potassium channel. Science. **295**, 496-9

243 Marks, A. R., Marx, S. O. and Reiken, S. (2002) Regulation of ryanodine receptors via macromolecular complexes: a novel role for leucine/isoleucine zippers. Trends Cardiovasc Med. **12**, 166-70

244 Marx, S. O., Reiken, S., Hisamatsu, Y., Jayaraman, T., Burkhoff, D., Rosemblit, N. and Marks, A. R. (2000) PKA phosphorylation dissociates FKBP12.6 from the calcium release channel (ryanodine receptor): defective regulation in failing hearts. Cell. **101**, 365-76

245 Schulze, D. H., Muqhal, M., Lederer, W. J. and Ruknudin, A. M. (2003) Sodium/calcium exchanger (NCX1) macromolecular complex. J Biol Chem. **278**, 28849-55

246 Shih, M., Lin, F., Scott, J. D., Wang, H. Y. and Malbon, C. C. (1999) Dynamic complexes of beta2-adrenergic receptors with protein kinases and phosphatases and the role of gravin. J Biol Chem. **274**, 1588-95

247 Chu, J., Chu, S. and Montrose, M. H. (2002) Apical Na^+/H^+ exchange near the base of mouse colonic crypts. Am J Physiol Cell Physiol. **283**, C358-72

248 Cantin, B., Giannetti, N., Parekh, H., Panchal, S. N., Kwok, B. W., Najem, R., Woodman, K., Hunt, S. A. and Valantine, H. A. (2002) Mycophenolic acid concentrations in long-term heart transplant patients: relationship with calcineurin antagonists and acute rejection. Clin Transplant. **16**, 196-201

249 Schillace, R. V. and Scott, J. D. (1999) Association of the type 1 protein phosphatase PP1 with the A-kinase anchoring protein AKAP220. Curr Biol. **9**, 321-4